



---

Publicly Accessible Penn Dissertations

---


Spring 5-17-2010

# The C1 Domain in Cancer Signaling Molecules: Regulation by Lipids and Protein-Protein Interactions

Hongbin Wang

University of Pennsylvania, hongbin@mail.med.upenn.edu

Follow this and additional works at: <http://repository.upenn.edu/edissertations>

 Part of the [Pharmacology, Toxicology and Environmental Health Commons](#)

---

## Recommended Citation

Wang, Hongbin, "The C1 Domain in Cancer Signaling Molecules: Regulation by Lipids and Protein-Protein Interactions" (2010).  
*Publicly Accessible Penn Dissertations*. 141.  
<http://repository.upenn.edu/edissertations/141>

This paper is posted at ScholarlyCommons. <http://repository.upenn.edu/edissertations/141>  
For more information, please contact [libraryrepository@pobox.upenn.edu](mailto:libraryrepository@pobox.upenn.edu).

---

# The C1 Domain in Cancer Signaling Molecules: Regulation by Lipids and Protein-Protein Interactions

## **Abstract**

Cysteine-rich (C1) domains, present in PKC isozymes, Chimaerins, RasGRPs, PKDs, Munc13s, DGKs, and MRCKs, can bind the diacylglycerol (DAG) second messenger. In the present thesis research, I demonstrated that p23/Tmp21 acts as a C1-domain docking protein that mediates perinuclear translocation of beta2-chimaerin. Glu227 and Leu248 in the beta2-chimaerin C1-domain are crucial for binding p23/Tmp21 and perinuclear targeting. Isolated C1-domains from individual PKC isozymes or RasGRP1 differentially interact with p23/Tmp21. PKCepsilon interacts with p23/Tmp21 specifically via its C1b domain, however this association is lost in response to phorbol esters. These results demonstrate that p23/Tmp21 acts as an anchor that distinctively modulates compartmentalization of C1-domain-containing proteins, and it plays an essential role in beta2-chimaerin re-localization to the perinuclear region in response to phorbol esters. It has been established that apoptosis induced by phorbol esters in LNCaP cells is primarily mediated by the novel PKCdelta. I demonstrated that depletion of p23/Tmp21 significantly potentiates phorbol 12-myristate 13-acetate (PMA)-induced apoptosis in LNCaP cells. Remarkably, the effect was mediated by PKCdelta as revealed by the fact that PKCdelta RNAi depletion or PKC inhibitor GF 109203X can rescue the potentiating effect of p23/Tmp21 depletion. Immunoprecipitation and confocal microscopy analysis demonstrated that PKCdelta and p23/Tmp21 formed a complex in LNCaP cells. Disruption of PKCdelta-p23/Tmp21 association by depletion of p23/Tmp21 accelerates PMA-induced PKCdelta plasma membrane translocation and the activation of its downstream effector ROCK and JNK. Moreover, I demonstrated that depletion of p23/Tmp21 potentiates doxorubicin-mediated apoptosis of LNCaP cells. This work provided the first evidence that p23/Tmp21 negatively regulates PKCdelta-mediated apoptosis in LNCaP cells in response to PMA and doxorubicin. In addition, I demonstrated that the PKC inhibitor GF 109203X significantly radiosensitizes PC3 androgen-independent prostate cancer cells. Depletion of PKCepsilon but not PKCalpha and PKCdelta by shRNA, significantly radiosensitizes PC3 cells. Confocal images demonstrated that gamma-irradiation-induced PKCepsilon membrane translocation was impaired by the EGFR inhibitor AG1478, the PLCgamma1 inhibitor U73122, or the ROS scavenger N-acetyl-cysteine (NAC). The results revealed a potential role for DAG and C1-domain containing protein in the control of ionizing irradiation induced cell death/survival and also suggested that inhibition of PKCepsilon may be a useful therapeutic approach to radiosensitize prostate cancer cells. Taken together, in this work I present several novel findings that highlight the relevance of C1-domain containing proteins in cancer.

## **Degree Type**

Dissertation

## **Degree Name**

Doctor of Philosophy (PhD)

## **First Advisor**

Marcelo G. Kazanietz

---

**Keywords**

Signal transduction, Cysteine-rich (C1) domains, Beta2-chimaerin, Novel protein kinase C isozymes, p23/Tmp21, Ionizing radiation

**Subject Categories**

Pharmacology, Toxicology and Environmental Health


**THE C1 DOMAIN IN CANCER SIGNALING MOLECULES:  
REGULATION BY LIPIDS AND PROTEIN-PROTEIN INTERACTIONS**

**HONGBIN WANG**

**A DISSERTATION  
In  
Pharmacological Sciences**

**Presented to the Faculties of the University of Pennsylvania  
In Partial Fulfillment of the Requirements for the  
Degree of Doctor of Philosophy**

**2010**



---

**Marcelo G. Kazanietz, Ph.D.  
Supervisor of Dissertation**



---

**Vladimir R. Muzykantov, M.D., Ph.D.  
Graduate Group Chairman**

**Dissertation Committee:**

**Judy L. Meinkoth, Ph.D. (Chairperson)  
Ann R. Kennedy, D.Sc.  
Costas Koumenis, Ph.D.  
Xiaolu Yang, Ph.D.**

## **DEDICATION**

This dissertation is dedicated to my wife Xia, my son Kevin and my daughter Anita who have supported and inspired me all the way since the beginning of my Ph.D. studies. Thanks for your understanding, patience, and love.

Also to my parents, my brothers, and my parents-in-laws who are in China for always letting me know how proud you are of me.

Finally, this dissertation is dedicated to those who believe in the richness of learning.

## **ACKNOWLEDGEMENTS**

I would like to take the opportunity to express sincere appreciation to my dissertation advisor Dr. Marcelo G. Kazanietz for his guidance, sage advice, insightful criticisms, and encouragement.

I also like to thank Dr. Meinkoth, Dr. Kennedy, Dr. Koumenis and Dr. Yang for willing to be my dissertation committee members and their valuable suggestions and comments.

I am also very grateful for the support by radiation oncology NIH training grant (T32-CA-09677) during my Ph.D. study.

Lastly, but not the least, I am thankful to all colleagues and friends who made my stay at the University of Pennsylvania a memorable and valuable experience.

## **ABSTRACT**

### **THE C1 DOMAIN IN CANCER SIGNALING MOLECULES: REGULATION BY LIPIDS AND PROTEIN-PROTEIN INTERACTIONS**

HONGBIN WANG

Marcelo G. Kazanietz. Ph.D.

Cysteine-rich (C1) domains, present in PKC isozymes, Chimaerins (a family of small RacGTPase activating proteins), RasGRPs (a family of guanine nucleotide exchange factor for Ras/Rap1), PKDs (the serine/threonine kinase protein kinase D), Munc13s (the mammalian unc13), DGKs (the DAG kinases  $\beta$  and  $\gamma$ ), and MRCKs (the serine/threonine kinase myotonic dystrophy kinase-related Cdc42-binding kinase), can bind the diacylglycerol (DAG) second messenger. In the present thesis research, I demonstrated that p23/Tmp21 acts as a C1 domain docking protein that mediates perinuclear translocation of  $\beta$ 2-chimaerin. Glu227 and Leu248 in the  $\beta$ 2-chimaerin C1 domain are crucial for binding p23/Tmp21 and perinuclear targeting. Isolated C1 domains from individual PKC isozymes or RasGRP1 differentially interact with p23/Tmp21. PKC $\epsilon$  interacts with p23/Tmp21 specifically via its C1b domain, however this association is lost in response to phorbol esters. These results demonstrate that p23/Tmp21 acts as an anchor that distinctively modulates compartmentalization of C1 domain-containing proteins, and it plays an essential role in  $\beta$ 2-chimaerin re-localization to the perinuclear region in response to phorbol esters. It has been established that apoptosis induced by phorbol esters in LNCaP cells is primarily mediated by the novel PKC $\delta$ . I demonstrated that depletion of

p23/Tmp21 significantly potentiates phorbol 12-myristate 13-acetate (PMA)-induced apoptosis in LNCaP cells. Remarkably, the effect was mediated by PKC $\delta$  as revealed by the fact that PKC $\delta$  RNAi depletion or PKC inhibitor GF 109203X can rescue the potentiating effect of p23/Tmp21 depletion. Immunoprecipitation and confocal microscopy analysis demonstrated that PKC $\delta$  and p23/Tmp21 formed a complex in LNCaP cells. Disruption of PKC $\delta$ -p23/Tmp21 association by depletion of p23/Tmp21 accelerates PMA-induced PKC $\delta$  plasma membrane translocation and the activation of its downstream effector ROCK and JNK. Moreover, I demonstrated that depletion of p23/Tmp21 potentiates doxorubicin-mediated apoptosis of LNCaP cells. This work provided the first evidence that p23/Tmp21 negatively regulates PKC $\delta$ -mediated apoptosis in LNCaP cells in response to PMA and doxorubicin. In addition, I demonstrated that the PKC inhibitor GF 109203X significantly radiosensitizes PC3 androgen-independent prostate cancer cells. Depletion of PKC $\epsilon$  but not PKC $\alpha$  and PKC $\delta$  by shRNA, significantly radiosensitizes PC3 cells. Confocal images demonstrated that  $\gamma$ -irradiation-induced PKC $\epsilon$  membrane translocation was impaired by the EGFR inhibitor AG1478, the PLC $\gamma$ 1 inhibitor U73122, or the ROS scavenger N-acetyl-cysteine (NAC). The results revealed a potential role for DAG and C1 domain-containing protein in the control of ionizing irradiation induced cell death/survival and also suggested that inhibition of PKC $\epsilon$  may be a useful therapeutic approach to radiosensitize prostate cancer cells.

Taken together, in this work I present several novel findings that highlight the relevance of C1 domain-containing proteins in cancer.



## Table of Contents

Title Page.....	i
Dedication.....	ii
Acknowledgements.....	iii
Abstract.....	iv
Table of Contents.....	vi
List of Tables.....	vii
List of Figures.....	vii
Chapter 1: General Introduction.....	1
Chapter 2: Introduction.....	34
Results.....	37
Discussion.....	65
Materials and Methods.....	72
Chapter 3: Introduction.....	82
Results.....	84
Discussion.....	97
Materials and Methods.....	100
Chapter 4: Introduction.....	105
Results.....	107
Discussion.....	120
Materials and Methods.....	123
Chapter 5: Final Remarks.....	126
Bibliography.....	134

## **List of Tables**

<b>Table 2.1</b> -Primers used to generate constructs.....	79
<b>Table 4.1</b> -Sequences of MISSION <sup>®</sup> shRNA lentiviral transduction particles used to generate PKC $\alpha$ , PKC $\delta$ , or PKC $\epsilon$ stably depleted PC3 cell lines.....	125

## **List of Figures**

### **Chapter 1**

<b>Figure 1.1</b> -Main pathways that lead to the production of DAG.....	3
<b>Figure 1.2</b> - Structures of phorbol 12-myristate 13-acetate (PMA) and DAG .....	5
<b>Figure 1.3</b> -The family of PKC isozymes .....	7
<b>Figure 1.4</b> -Novel phorbol ester/DAG receptors.....	13
<b>Figure 1.5</b> -Structures of cysteine-rich (C1) domains from PKC $\delta$ and $\beta$ 2-chimaerin .....	15
<b>Figure 1.6</b> -Switches between Rac-GDP and Rac-GTP.....	19
<b>Figure 1.7</b> -Time-lapse images of GFP- $\beta$ 2-chimaerin (wt) or GFP- $\beta$ 2-chimaerin (C246A) localization after PMA treatment.....	21
<b>Figure 1.8</b> -Crystal structure of $\beta$ 2-chimaerin.....	24
<b>Figure 1.9</b> -Model of activation and regulation of $\beta$ 2-chimaerin upon growth factor stimulation.....	29

### **Chapter 2**

<b>Figure 2.1</b> -Differential interaction of C1 domains with p23/Tmp21.....	40
<b>Figure 2.2</b> -Binding of C1 domains to p23/Tmp21.....	41
<b>Figure 2.3</b> -Co-localization of GFP-fused PKC $\epsilon$ C1b and $\beta$ 2-chimaerin C1 domains with p23/Tmp21.....	42

<b>Figure 2.4</b> -Differential interaction of PKC $\epsilon$ and $\beta$ 2-chimaerin with p23/Tmp21 .....	46
<b>Figure 2.5</b> -FBS and EGF enhance the association of $\beta$ 2-chimaerin with p23/Tmp21 .....	47
<b>Figure 2.6</b> -p23/Tmp21 RNAi depletion impairs perinuclear $\beta$ 2-chimaerin translocation .....	49
<b>Figure 2.7</b> -Co-localization of $\beta$ 2-chimaerin with a Golgi marker.....	50
<b>Figure 2.8</b> -PKC $\epsilon$ (Asp257/Met278) does not co-localize with p23/Tmp21 .....	53
<b>Figure 2.9</b> -Glu227 and Leu248 in the $\beta$ 2-chimaerin C1 domain are required for perinuclear translocation.....	54
<b>Figure 2.10</b> -Glu227 and Leu248 residues in the $\beta$ 2-chimaerin C1 domain are required for the interaction with p23/Tmp21 .....	56
<b>Figure 2.11</b> -Co-localization studies of $\beta$ 2-chimaerin mutants and p23/Tmp21 .....	58
<b>Figure 2.12</b> -Identification of the $\beta$ 2-chimaerin C1 domain interacting region in p23/Tmp21 .....	61
<b>Figure 2.13</b> -Disruption of $\beta$ 2-chimaerin-p23/Tmp21 interaction leads to enhanced $\beta$ 2-chimaerin Rac-GAP activity.....	62
<b>Figure 2.14</b> -Videos for translocation experiments in Figure 2.9. ....	64

### **Chapter 3**

<b>Figure 3.1</b> -Yeast two-hybrid assay reveals that the PKC $\delta$ C1a-b domain interacts with p23/Tmp21.....	87
<b>Figure 3.2</b> -The C1b domain of PKC $\delta$ mediates perinuclear targeting and co-localizes with p23/Tmp21.....	88
<b>Figure 3.3</b> -PKC $\delta$ and p23/Tmp21 form a complex in LNCaP prostate cancer cells.....	89
<b>Figure 3.4</b> -Depletion of p23/Tmp21 potentiates PMA- and doxorubicin-induced apoptosis of LNCaP prostate cancer cells .....	91
<b>Figure 3.5</b> -Depletion of PKC $\delta$ or PKC inhibition with GF 109203X	

blocks PMA-induced apoptosis in LNCaP prostate cancer cells.....	94
<b>Figure 3.6</b> -Depletion of p23/Tmp21 accelerates PMA-induced GFP-PKC $\delta$ plasma membrane translocation.....	95
<b>Figure 3.7</b> -Depletion of p23/Tmp21 significantly enhances ROCK and JNK activation by PMA.....	96

## **Chapter 4**

<b>Figure 4.1</b> - $\gamma$ -irradiation reduces PC3 prostate cancer cell number.....	108
<b>Figure 4.2</b> -The PKC inhibitor GF 109203X radiosensitizes PC3 prostate cancer cell.....	109
<b>Figure 4.3</b> -Establishment of PC3 prostate cancer cell lines stably depleted of PKC $\alpha$ , PKC $\epsilon$ or PKC $\delta$ using shRNA.....	111
<b>Figure 4.4</b> -PKC $\alpha$ or PKC $\delta$ depletion does not affect PC3 cell radiosensitivity .....	112
<b>Figure 4.5</b> -PKC $\epsilon$ depletion enhances radiosensitivity of PC3 cells .....	114
<b>Figure 4.6</b> -Translocation of PKC $\epsilon$ after $\gamma$ -irradiation.....	115
<b>Figure 4.7</b> -NAC prevents $\gamma$ -irradiation-mediated PKC $\epsilon$ translocation.....	117
<b>Figure 4.8</b> -PKC $\epsilon$ translocation to the plasma membrane by $\gamma$ -irradiation is mediated by EGFR and PLC.....	119

## **Chapter 5**

<b>Figure 5.1</b> -Proposed model of regulation of the C1 domain-containing proteins .....	133
--	-----

# **CHAPTER 1**

## **General Introduction**

## **The lipid second messenger diacylglycerol (DAG) and phorbol esters**

1,2-diacyl-*sn*-glycerol (DAG) is a biologically active lipid second messenger that is generated in response to various extracellular stimuli, including growth factors, hormones, neurotransmitters, and a variety of other agonists. There are several sources from which DAG can derive in cells, including: 1) phosphatidylinositol (4, 5) biphosphate (PtdIns (4, 5) P<sub>2</sub>) hydrolysis through the action of a phosphoinositide-specific phospholipase C (PI-PLC); 2) phosphatidylcholine (PC) hydrolysis by phospholipase D (PLD), yielding phosphatidic acid (PA), which in turn is converted to DAG by a specific PA phosphohydrolase; 3) PC hydrolysis by PC-PLC, or phosphatidylcholine-ceramide cholinephosphotransferase, which produces DAG (**Figure 1.1**). Among these routes, hydrolysis of phosphatidylinositol-4, 5-biphosphate (PIP<sub>2</sub>) by specific PI-PLC enzymes into DAG and inositol-3,4,5-triphosphate (IP<sub>3</sub>) has been extensively studied and considered as the major pathway for the generation of DAG. Stimulation of G-protein coupled receptors (GPCRs) or receptor tyrosine kinases (RTKs) activates phospholipase C (PLC) β and PLCγ isozymes, respectively. While DAG remains in the plasma membrane and serves as a ligand for classical and novel protein kinase C (PKC) isozymes as well as “non-kinase” DAG receptors (64, 151), the soluble IP<sub>3</sub> activates Ca<sup>2+</sup> channels to release Ca<sup>2+</sup> from the endoplasmic reticulum, which also can activate classical PKC together with DAG.

Phorbol esters, natural compounds originally isolated from the plant *croton tiglium*, mimic the effects of DAG on PKC (32). Phorbol esters have generated a lot

of interest due to their tumor promoting properties in animal models of carcinogenesis (162) and have been widely used as pharmacological tools to study DAG signaling

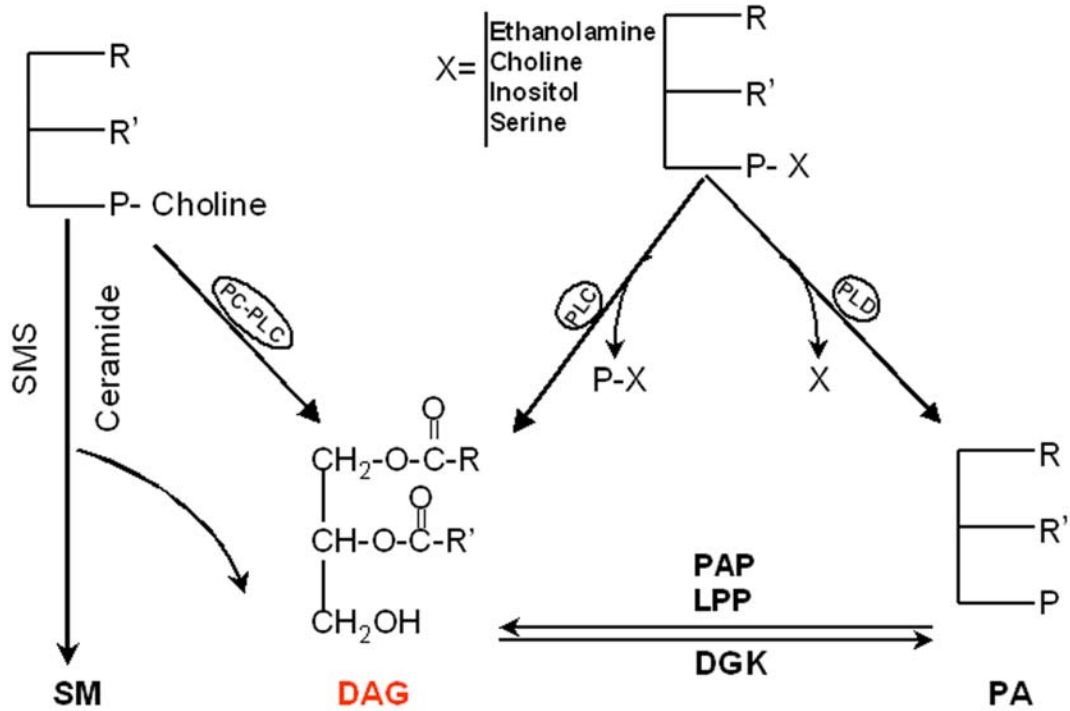


**Figure 1.1** Main pathways that lead to the production of DAG. OH is hydroxyl; R, R' are fatty acids; P is a phospho group; X is choline, ethanolamine, inositol or serine; SM, sphingomyelin; SMS, sphingomyelin synthase; LPP, lipid phosphate phosphatase; DGK, diacylglycerol kinase; PAP, phosphatidic acid phosphatase; PLC, phospholipase C; PC-PLC, phosphatidicholine specific phospholipase C; PLD, phospholipase D.

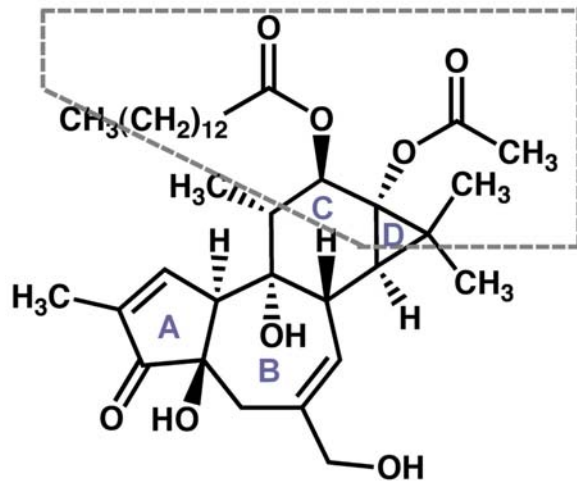
pathway due to their high potency and stability (19, 84). The basic structure of phorbols consists of four carbon rings, labeled A, B, C, and D. Substitutions in positions 12 and 13 in ring C form a DAG-like structure. The most commonly used phorbol ester is Phorbol 12-Myristate 13-Acetate (PMA), also called TPA (Tetradecanoyl Phorbol Acetate) (**Figure 1.2**).

### **PKC isozymes: the first identified DAG/phorbol ester receptors**

PKCs are a family of related serine/threonine kinases that regulate cellular proliferation, differentiation, cell cycle, apoptosis, senescence, metastasis, malignant transformation, and cancer progression (84). The enzymatic activity of PKC was first identified in rat brain by Nishizuka and co-workers as a cytoplasmic serine- and threonine-specific protein kinase (82, 171, 173). It was initially thought that this protein kinase was proteolytically activated from a proenzyme. However, later on it was found that the enzyme is reversibly activated *in vitro* by unsaturated DAG in the presence of acidic phospholipids such as phosphatidylserine (172). This finding provided the first evidence of a link between receptor-induced phosphatidylinositol hydrolysis and activation of a protein kinase (91, 136). All PKC isoforms have a highly conserved carboxyl terminal kinase domain and a more divergent amino-terminal regulatory domain linked by a hinge region. PKC in its inactive form is auto-inhibited by a pseudosubstrate sequence present in the regulatory domain that occupies the substrate-binding pocket in the otherwise functional kinase domain

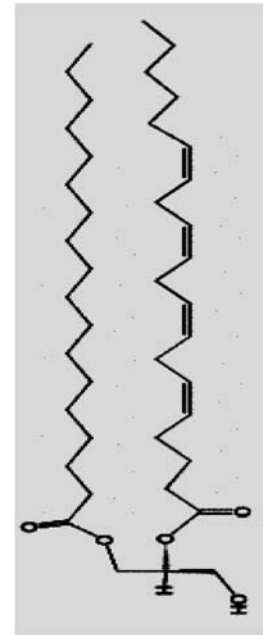


(144). PKC is activated when DAG and/or allosteric effectors bind to its regulatory domain at the plasma membrane. This binding disrupts the docking of the regulatory



**PMA (Phorbol 12-Myristate 13-Acetate)**

**TPA (Tetradecanoyl Phorbol Acetate)**



**Diacylglycerol (DAG)**

**Figure 1.2** Structures of phorbol 12-myristate 13-acetate (PMA) and diacylglycerol (DAG).

domain, which displaces the bound pseudosubstrate region from the active site, allowing for PKC kinase activation (132, 138). Based on their regulatory and biochemical properties, PKC isozymes have been classified into 3 subgroups: the “classical” or “conventional” PKCs (cPKCs) which comprise PKC $\alpha$ ,  $\beta$ I,  $\beta$ II, and  $\gamma$ ; the “novel” PKCs (nPKCs), a group that includes PKC $\delta$ , PKC $\epsilon$ , PKC $\eta$ , and PKC $\theta$ ; and the “atypical” PKCs (aPKCs) which comprise PKC $\zeta$  and PKC $\iota/\lambda$ . Both cPKCs and nPKCs are sensitive to DAG/phorbol esters, and only cPKCs are activated by calcium. Atypical PKCs do not respond to either DAG/phorbol ester or calcium (Figure 1.3).

### **PKC $\delta$ : a growth inhibitory and pro-apoptotic kinase**

Phorbol esters cause growth inhibition or cell death in many cell types. PKC $\delta$  seems to be responsible for many growth inhibitory effects, particularly through up-regulation of p21<sup>cip1</sup> (60). In many cell types, PKC $\delta$  has also been identified as a key PKC isozyme involved in apoptosis triggered by a variety of stimuli, including chemotherapy agents, H<sub>2</sub>O<sub>2</sub>, virus infection, phorbol esters, UV radiation, Fas-ligand, and ionizing radiation (3, 15, 54, 58, 59, 93, 97, 149, 152, 158, 200, 204). Studies from our laboratory and others demonstrated that in LNCaP prostate cancer cells the phorbol esters activate PKC $\delta$  to trigger an apoptotic response (58). Subsequent studies revealed that the JNK cascade acts as a mediator of phorbol ester-induced LNCaP cell apoptosis. Additional analysis found that apoptosis is triggered by the autocrine secretion of death factors, including TNF $\alpha$  and TRAIL, with subsequent

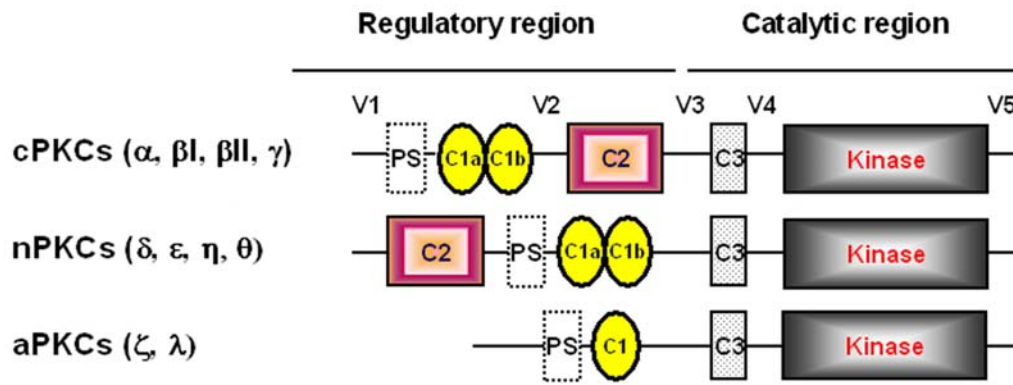


**Figure 1.3** The family of PKC isozymes.

activation of the extrinsic apoptotic cascade. A recent study by Xiao *et al.* in our laboratory revealed that the Rho-ROCK-p21<sup>cip1</sup> pathway is also implicated in phorbol ester-induced prostate cancer cell apoptosis (193).

Numerous studies have demonstrated that PKC $\delta$  is activated by caspase-3 dependent proteolytic cleavage in response to stimuli. Caspase-3 can release a 40-KDa constitutively active PKC $\delta$  catalytic fragment that subsequently phosphorylates downstream substrates involved in the apoptotic process (54, 61). Phosphorylation of tyrosine residues in PKC $\delta$  is also a critical step for its activation during apoptosis in some models. For examples, tyrosines 64 and 187 become phosphorylated upon exposure of etoposide, whereas residues of tyrosines 311, 332 and 512 become phosphorylated in response to H<sub>2</sub>O<sub>2</sub> in CHO cells (93).

Previous reports also suggested that PKC $\delta$ -triggered apoptosis depend on the cellular context and stimulation, since PKC $\delta$  redistributes to different subcellular compartments in response to apoptotic stimuli. Nuclear translocation of PKC $\delta$  can mediate DNA-damage-induced apoptosis (49), in which PKC $\delta$  can act as an inhibitor of activity of the catalytic subunit of DNA-PKs. DNA-PKs dissociate from DNA after becoming phosphorylated by PKC $\delta$ , which subsequently interrupts the DNA double strand break repair by nonhomologous end joining (14). In addition, in many cell lines, PKC $\delta$  translocates to mitochondria upon treatment with phorbol esters or by oxidative stress (20, 104, 113, 114). It is well established that translocation and activation of PKC $\delta$  decrease mitochondrial membrane potential, resulting in the release of cytochrome c, which is known to form a complex with Apaf-1 that subsequently activates caspases and induces apoptosis (137).

The involvement of PKC $\delta$  in apoptotic signaling is not universal. PKC $\delta$  activates the ERK cascade and promotes proliferation in MCF-7 cells (88), enhances cell survival and chemotherapeutic resistance in non-small lung cancer cells (40), and increases breast tumor cell anchorage-independent growth (89), arguing that PKC $\delta$  behaves differently in different cellular contexts.

### **PKC $\epsilon$ : oncogenic and pro-survival effects**

PKC $\epsilon$  is believed to function as an anti-apoptotic protein and is the only PKC isozyme shown to exhibit full oncogenic potential (8, 9, 24, 50, 62, 119, 124, 140, 161). When overexpressed in LNCaP androgen-dependent cancer cells, PKC $\epsilon$  confers androgen independence, accelerates G1/S transition, and enhances tumorigenic potential in nude mice (191, 192). PKC $\epsilon$  stimulates mitogenicity via the ERK pathway. In addition, PKC $\epsilon$  disrupts the reactivation of the tumor suppressor retinoblastoma (pRb), derepresses transcriptional elongation of the c-myc oncogene, and propagates survival signals in the absence of functional PTEN (190-192). PKC $\epsilon$  is highly expressed in many epithelial cancers (70). For example, PKC $\epsilon$  is barely detected by immunohistochemistry (IHC) in benign prostatic epithelium but is overexpressed in > 95% of prostate tumors (44). A more recent analysis found that high-grade human prostate tumors express very high PKC $\epsilon$  levels (5). PKC $\epsilon$  expression is markedly up-regulated in prostate tumors from TRAMP (transgenic adenocarcinoma mouse prostate) mice and correlates with high phospho-Akt levels (5). A positive correlation has been also found between PKC $\epsilon$  and Stat3 expression in prostate cancer cells (5). Notably, de-regulation of the PKC $\epsilon$  gene (*PRKCE*) has been

reported in other cancer types, such as in lung, breast and thyroid cancer (6, 92, 142). More recently, studies in breast cancer cells have linked PKC $\epsilon$  to Akt to protect cells against ionizing radiation induced cell death (108). Studies from our laboratory found that PKC $\epsilon$  could activate survival signaling both through Akt-dependent and Akt-independent mechanisms in prostate cancer cells (Meshki, J *et al.*, submitted for publication).

It was reported that PKC $\epsilon$  prevents both DNA damage- and receptor-mediated apoptosis. Anti-cancer drug resistance caused by overexpression of PKC $\epsilon$  has been demonstrated in many cancer types, such as ovarian, prostate, and non-small cell lung cancer as well as in embryo fibroblast cells (8, 11, 50, 56). Studies also reported that PKC $\epsilon$  plays a protective role in TNF $\alpha$ - and TRAIL-mediated cancer cell death, including in breast, glioma, and melanoma cells (9, 62, 157, 161). Several studies have established that in different cells, PKC $\epsilon$  can directly interact with Akt (108, 146, 179, 192). Akt is a downstream effector of phosphoinositol 3-kinase (PI3K) and plays an essential role in cell survival and tumorigenesis through phosphorylation of a number of downstream substrates (188). There is considerable evidence demonstrating that PKC $\epsilon$  is required for Akt phosphorylation in response to different stimuli, such as insulin, hydrogen peroxide, heat shock, and ischemia-reperfusion injury (107, 118, 146, 192, 203). PKC $\epsilon$  also enhances Akt protein stability. A number of studies also indicate that PKC $\epsilon$  pro-survival function might be linked to Bcl-2 family proteins (10). Very recently, Basu and her colleagues demonstrated that overexpression of PKC $\epsilon$  in MCF-7 cells elevates Bcl-2 mRNA levels and reciprocally decreases Bid expression (161), resulting in MCF-7 cell resistance to TRAIL. In line

with this report, a PKC $\epsilon$  inhibitory peptide could effectively inhibit Bcl-2 phosphorylation and enhance H<sub>2</sub>O<sub>2</sub>-induced apoptosis in rat cardiomyocytes (115). Overexpression of PKC $\epsilon$  renders LNCaP prostate cancer cells resistant to apoptosis, and PKC $\epsilon$ -deficiency sensitizes these cells to PMA-induced apoptosis by preventing Bax activation and translocation to mitochondria (121). However, a few reports suggested that PKC $\epsilon$  negatively regulates Akt functions (7, 71, 105, 107). Taken together, the pro-survival function of PKC $\epsilon$  appears to be dependent on the cellular context and stimuli (105, 107, 186).

### **Ionizing irradiation and PKC isozymes**

Although it has been conceived that upon ionizing radiation DNA damage/repair and cell cycle checkpoint pathways are the key mechanisms that regulate cell death/survival, accumulating evidence suggests that membrane-related signaling cascades also play critical roles in controlling cell death/survival. It has been reported that irradiation leads to PKC activation, suggesting that PKC might be a determinant factor in radiosensitivity (73, 76, 77, 90, 129, 164). An early report by Nakajima *et al.* revealed that  $\gamma$ -irradiation induces DAG production and activates PKC in cultured rat hepatocytes. Using radical scavengers and a phospholipase C inhibitor, they conclude that DAG generation and PKC activation are mediated through membrane lipid peroxidation and PLC activation (129, 130). Interestingly, irradiation induced the activation of EGFR and ERK signaling, which confers the cytoprotective effects (2). Ionizing radiation can mimic the effect of EGF and activate EGFR. Sturla *et al.* established that phosphorylation of Tyr992 in EGFR in response to ionizing

irradiation is higher than that seen with EGF, suggesting that Tyr992 is an important effector upon radiation-induced activation of EGFR (168). Phosphorylation of Tyr992 residue in EGFR promotes its coupling to PLC $\gamma$ , leading to DAG generation and [Ca<sup>2+</sup>] release which are implicated in PKC activation.

### **Novel DAG/phorbol ester receptors**

The prevalent view that PKC isozymes are the only DAG/phorbol ester receptors has been challenged after the discovery of additional DAG/phorbol ester receptors, suggesting a high degree of complexity in the signaling pathways activated by DAG/phorbol esters. At least six additional families of DAG/phorbol esters receptors have been discovered to-date (**Figure 1.4**), including chimaerins (a family of small RacGTPase activating proteins), RasGRPs (a family of guanine nucleotide exchange factor for Ras/Rap1), the serine/threonine kinase myotonic dystrophy kinase-related Cdc42-binding kinase (MRCK) family, the serine/threonine kinase protein kinase D (PKD) family, the DAG kinases (DGK)  $\beta$  and  $\gamma$ , and the mammalian unc13 (Munc13) proteins (involved in neurotransmitter secretion) (21, 86). Like classical and novel PKC isozymes, all of these DAG/phorbol ester receptors possess a cysteine-rich domain (C1 domain) that binds phorbol ester/DAG with high affinity. Moreover, the novel DAG/phorbol ester receptors are also subject to subcellular redistribution upon binding of phorbol esters or DAG, which facilitates their association with their corresponding effectors.

### **The C1 domain: a DAG/phorbol ester binding motif**



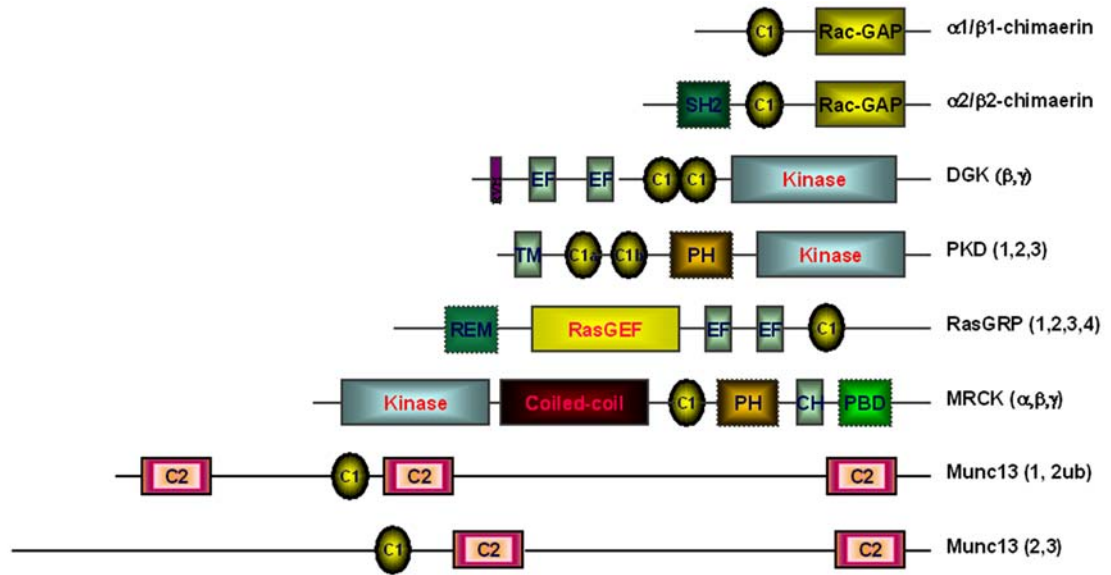


**Figure 1.4** Novel DAG/phorbol esters receptors.

C1 domains are 50-51 amino acid long cysteine-rich motifs originally identified in PKC as the binding sites for DAG and the phorbol esters. These domains contain the characteristic motif:  $HX_{12}CX_2CX_{13/14}CX_2CX_4HX_2CX_7C$ , where *H* is His, *C* is Cys, and *X* is any other amino acid. X-ray crystallography analysis revealed that C1 domains are compact globular structures coordinated through binding of two  $Zn^{2+}$  ions to conserved Cys and His residues (**Figure 1.5**). While this motif is duplicated in tandem (C1a and C1b domains) in cPKCs and nPKCs, a single copy is present in aPKCs. Structural and ligand-binding analyses demonstrated that C1 domains in cPKCs and nPKCs have the ability to bind phorbol esters and DAG. As mentioned above, recent studies revealed that DAG/phorbol ester-responsive C1 domains are also present in PKDs, MRCKs, DAG-kinases, Rac-GAPs, RasGRPs, and Munc-13s.

A distinctive aspect of most C1 domain-containing proteins is their ability to redistribute to membranes in response to phorbol esters or to stimulation of receptors that couple to DAG generation. A continuous hydrophobic surface generated by the phorbol ester or DAG facilitates the insertion of the C1 domain into lipid bilayers (**Figure 1.5**), which in the case of cPKCs and nPKCs is followed by a conformational rearrangement that leads to kinase activation.

The C1 domain of chimaerins shows a ~40% identity to those in PKCs. [ $^3H$ ]PBDu binding assays revealed that  $\beta$ 2-chimaerin binds the ligand with high affinity in the presence of PS vesicles. The dissociation constant ( $K_d$ ) value for  $\beta$ 2-chimaerin is approximately 1 nM (25), which is in the same range as those for cPKCs and nPKCs (85). However, structure-activity relationship studies demonstrated remarkable differences between PKC $\alpha$  and  $\beta$ 2-chimaerin for the ligand

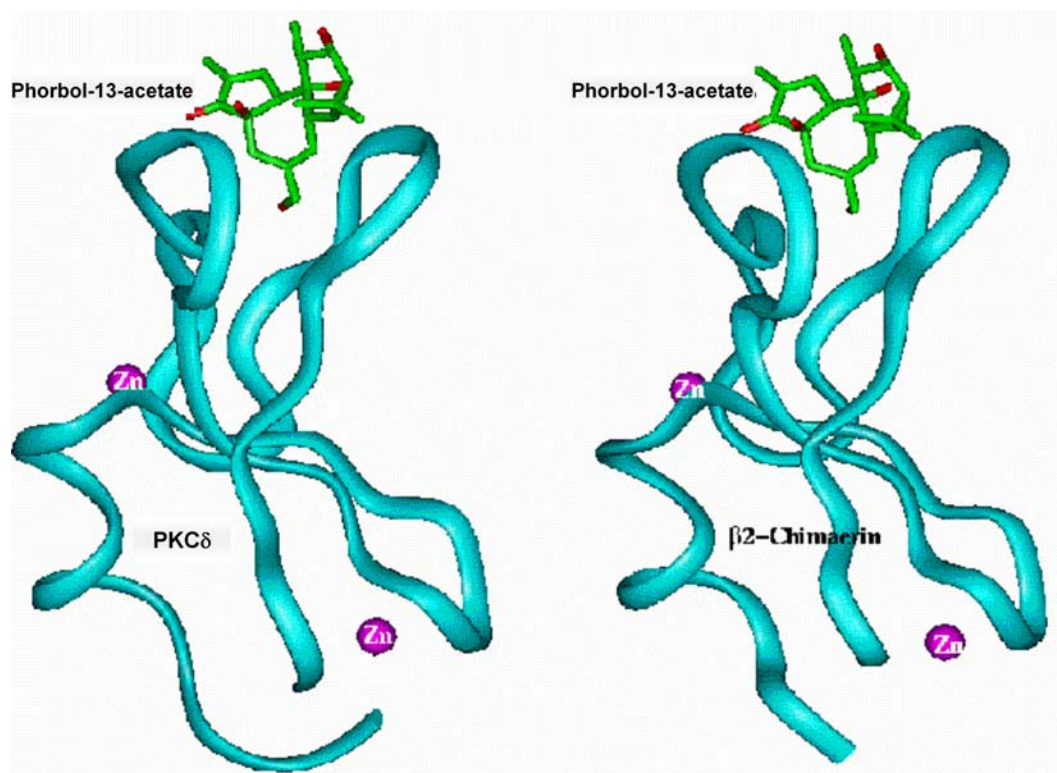


**Figure 1. 5** Structures of cysteine-rich domains (C1 domains) from PKC $\delta$  and  $\beta$ 2-chimaerin. Adapted from: Ron and Kazanietz, FASEB J. (1999) 13: 1658-1676.

thymeleatoxin. Thymeleatoxin showed significant preference for PKC $\alpha$  relative to  $\beta$ 2-chimaerin (about 60-fold). Other phorbol esters, such as 12-deoxyphorbol 13-phenylacetate, 12-deoxyphorbol 13-acetate, and mezerein also showed moderate preference for PKC $\alpha$  compared to  $\beta$ 2-chimaerin. The diacylglycerol 1-oleoyl-2-acetyl-glycerol (OAG) and the indole alkaloid (-)-indolactam V showed similar affinities for both PKC $\alpha$  and  $\beta$ 2-chimaerin (26).

### **DAG/phorbol ester receptors: protein-protein interactions**

Accumulating evidence suggests that PKC isozymes differ in their tissue distribution, substrate specificity, cofactor requirements, and subcellular localization (46). Specificity of PKC function is thought to be achieved by their association with specific interacting proteins. PKC isozymes have been reported to localize to various subcellular compartments (68, 126), including plasma membrane (69, 134), Golgi apparatus (98-100), mitochondria (113), nuclear membrane (128), and the nucleus (202). Many anchoring proteins have been identified for PKC isozymes, and they are termed receptor for activated C-kinases (RACKs) or receptor for inactivated C-kinases (53), depending if they bind to active or inactive PKCs, respectively (45, 53).

Several PKC-interacting proteins that associate with the C1 domains in PKC isozymes have been identified, which modulate either activity or cellular localization. An early study reported that the C1 and pseudosubstrate domains in PKC $\epsilon$  bind to the tyrosine kinase Btk PH domain. Upon PMA treatment, the PKC-Btk interaction was inhibited (196). Recently, Chen *et al.* demonstrated that localization of PKC $\beta$ II to centrosomes, organelles that play a central role in microtubule organization, spindle

formation and cytokinesis, is regulated by association with the scaffolding protein pericentrin via the PKC $\beta$ II C1a domain. Disruption of this interaction releases PKC $\beta$ II from the centrosomes, causing inhibition of spindle formation and cell division (34). The cell matrix protein fascin was also shown to interact with the PKC $\alpha$  C1b domain. The interaction is dependent on PKC $\alpha$  activity, and inhibition of the interaction leads to cell migration on fibronectin and fascin protrusions, arguing that the PKC $\alpha$ -fascin complex is key for regulating cell motility (4). The PKC $\gamma$  C1b domain binds 14-3-3 $\tau$  (135). This interaction is important in the regulation of Gap junction activity by PKC $\gamma$ . An interaction between the PKD1 C1 domain and 14-3-3 $\tau$  in T cells negatively regulates PKD1 functions (78). Early experiments using PKC $\epsilon$  truncated mutants revealed that C1 domains in PKC $\epsilon$  played a role in perinuclear targeting. PKC $\epsilon$  was reported to associate with Golgi membranes via its C1 domains and to modulate Golgi functions (98, 99). Mochly-Rosen's group demonstrated that  $\beta'$ -COP is a PKC $\epsilon$ -selective RACK (45).  $\beta'$ -COP is COP I (coat protein I) coatomer complex protein that is essential for Golgi budding and vesicular trafficking. Studies have linked PKC to the control of constitutive membrane trafficking and Golgi function (23, 30, 48, 87, 160, 194). Recently, Sunesson *et al.* reported that PKC $\epsilon$  C1b binds to peripherin leading to apoptosis in neuroblastoma cells (169). Moreover, PKC $\epsilon$  also was found to bind specifically to filamentous actin in a phorbol ester-dependent manner, suggesting that the interaction is dependent on the C1 domain. Taken together, all of these studies highlight the relevance of C1 domains in protein-protein interactions in addition to their well-established phorbol ester/DAG-binding properties.

### **Chimaerins: high affinity DAG/phorbol ester receptors**

In 1990 Lim and his coworkers identified a novel phorbol ester receptor highly expressed in brain. *n*-chimaerin (later renamed  $\alpha$ 1-chimaerin) resembles a “chimaera” between the regulatory region of PKC isozymes and BCR, the **breakpoint cluster region** protein involved in the translocation of Philadelphia chromosome in chronic myelogenous leukemia (1, 75). The chimaerin family of phorbol ester receptors comprises four isozymes ( $\alpha$ 1 (*n*)-,  $\alpha$ 2-,  $\beta$ 1 and  $\beta$ 2-chimaerins). In addition to a single C1 domain, chimaerins possess a C-terminal domain with Rac-GAP (GTPase-activating protein) activity that specifically accelerates GTP hydrolysis into GDP from Rac, a small GTPase that is involved in actin cytoskeleton organization, cell cycle progression, malignant transformation, adhesion, migration and metastasis (79) (**Figure 1.6**). Rac guanine nucleotide exchange factors such as Tiam 1 play a role in cell invasion and cell-cell adhesion, arguing for a key role for Rac in the metastatic cascade (123, 141, 189). Indeed, accumulating evidence revealed that Rac is involved in the progression of many tumors, such as glioma, lung, prostate and breast cancer (133).  $\alpha$ 2- and  $\beta$ 2-chimaerin have an extra N-terminal SH2 domain.  $\alpha$ 1 and  $\alpha$ 2-chimaerin are alternative splicing products of the  $\alpha$ -chimaerin gene (*CHN1*), while  $\beta$ 1 and  $\beta$ 2-chimaerin are splicing products of the  $\beta$ -chimaerin gene (*CHN2*).  $\alpha$ 2- and  $\beta$ 2-chimaerin are highly conserved, sharing 82% identity with higher degree of similarity among individual domains.  $\alpha$ 1- and  $\alpha$ 2-chimaerins are highly expressed in brain,

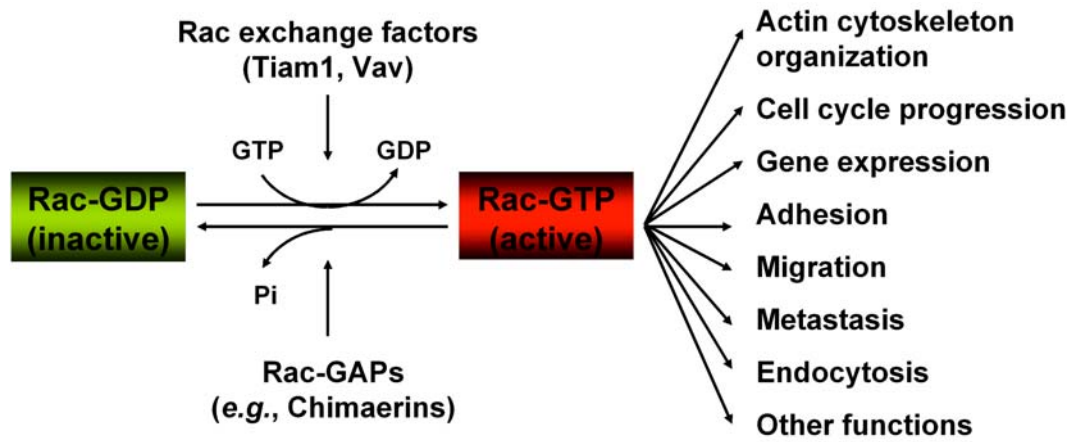


**Figure 1.6** Switches between Rac-GDP and Rac-GTP.

whereas  $\alpha$ 2-chimaerin expresses mainly in the brain cortex (74).  $\beta$ 1-chimaerin is expressed in the testis (103).  $\beta$ 2-chimaerin is ubiquitously expressed (102).

*In vitro* binding assays using [ $^3$ H]PDBu as a radioligand revealed that  $\beta$ 2-chimaerin is a high affinity phorbol ester receptor in the presence of the acidic phospholipid PS (25). DAG lactones, synthetic DAG mimetics in which the glycerol head of DAG has been constrained into a lactone ring to offer rigidity and stability, also have high affinity for  $\beta$ 2-chimaerin.

Subcellular fractionation assays in COS cells demonstrated that PMA causes  $\beta$ 2-chimaerin translocation from the cytosol to a particulate fraction in a dose-dependent and time-dependent manner (27). Deletion or mutation of critical amino acids in the C1 domain, such as Cys246, abolishes  $\beta$ 2-chimaerin translocation, arguing that the C1 domain in  $\beta$ 2-chimaerin is essential for PMA-induced translocation (27). Using GFP-fused  $\beta$ 2-chimaerin expressed in COS or HeLa cells, our laboratory showed redistribution to the plasma membrane followed by a significant perinuclear accumulation in response to phorbol esters, while no translocation of GFP- $\beta$ 2-chimaerin (C246A) was observed (**Figure 1.7**). Interestingly, unlike  $\alpha$ 2- and  $\beta$ 2-chimaerins,  $\alpha$ 1- and  $\beta$ 1-chimaerins were found predominantly in the particulate fraction even in the absence of PMA, suggesting that the SH2 domain in  $\alpha$ 2- and  $\beta$ 2-chimaerins plays a role in intracellular targeting (29). Furthermore, microscopy images demonstrated that GFP- $\alpha$ 1- and GFP- $\beta$ 1-chimaerins were found predominantly in the perinuclear region of cells (27).

To assess the regulation of  $\beta$ 2-chimaerin in a physiological context, in previous work that I carried out in the Kazanietz lab, I used epidermal growth factor receptor



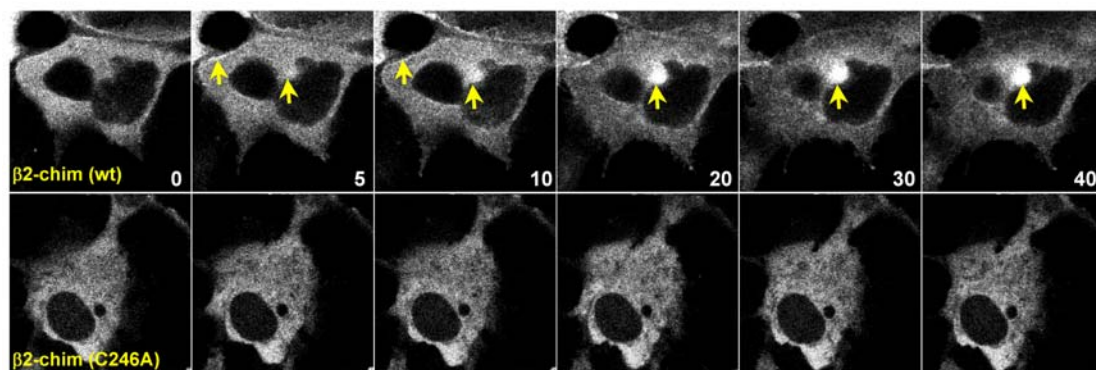


**Figure 1.7.** Time-lapse images of GFP-β2-chimaerin (wt) or GFP-β2-chimaerin (C246A) localization after PMA (3 μM) treatment.

(EGFR) activation as a paradigm for chimaerin activation since it couples to PLC $\gamma$  to generate DAG. EGFR activation also leads to Rac activation (182, 184). In that study we found that EGF promotes a transient translocation of  $\beta$ 2-chimaerin to the plasma membrane. The PLC $\gamma$  inhibitor U73122 as well as RNAi depletion of PLC $\gamma$  impair the translocation of  $\beta$ 2-chimaerin to plasma membrane, implying that  $\beta$ 2-chimaerin is a downstream effector of EGFR. Moreover, we found that the C1 domain in  $\beta$ 2-chimaerin is required for translocation since a C1 domain mutant (C246A- $\beta$ 2-chimaerin) does not translocate to plasma membrane in response to EGF.

On the other hand, we also demonstrated that  $\beta$ 2-chimaerin associates with Rac-GTP in response to EGF or PMA. First, using GST pull-down assays, we demonstrated that GST-tagged constitutively active V12Rac1 strongly associates with  $\beta$ 2-chimaerin, whereas the dominant-negative N17Rac1 does not. Second, confocal imaging studies revealed that  $\beta$ 2-chimaerin co-localizes with V12Rac1 in the plasma membrane. Lastly, I developed a fluorescence resonance energy transfer (FRET) approach that was instrumental to demonstrate a significant interaction between CFP-Rac1 and YFP- $\beta$ 2-chimaerin on the cell periphery upon EGFR stimulation. The interaction occurs as early as 1 min after EGF stimulation and is transient, returning to baseline after ~5 minutes (184).

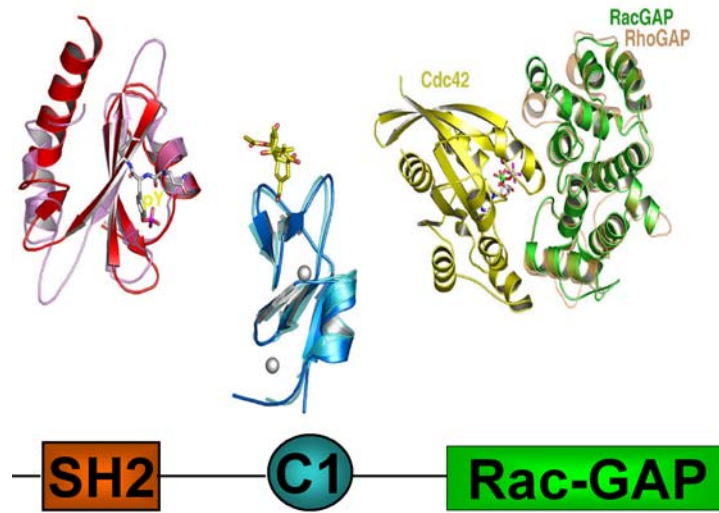
In collaboration with Dr. Jim Hurley at the NIH, our laboratory determined the 3-D structure of  $\beta$ 2-chimaerin (29). The crystal structure revealed that extensive intramolecular contacts in  $\beta$ 2-chimaerin keep the protein in a “closed” conformation. The C1 domain of  $\beta$ 2-chimaerin is buried at the heart of the structure and interacts with the N-terminus, the SH2 domain, the SH2-C1 domain linker and the Rac-GAP

domain. In addition to occluding the DAG/phorbol ester binding site, the N-terminus, the SH2 domain, the SH2-C1 domain linker and the Rac-GAP domain form hydrophobic interactions with a ring of hydrophobic side chains located around the C1 domain (29). These side chains are thought to be very important for the insertion of the C1 domain into the membrane. This may explain why  $\beta$ 2-chimaerin requires high concentration of phorbol ester to translocate to the plasma membrane as well as to interact with Rac. Mutations of residues thought to be important to keep intramolecular interactions showed enhanced PMA-induced translocation and stronger Rac-GAP activity. Based on all the experimental data and 3-D structure (**Figure 1.8**), our laboratory proposed a model for translocation and activation of  $\beta$ 2-chimaerin. Inactivated  $\beta$ 2-chimaerin exists in a “closed “ conformation in which extensive intramolecular interactions serve to occlude the DAG/phorbol ester-binding site of the C1 domain and the Rac-GAP domain. Upon PMA treatment or DAG generation by growth factor receptor stimulation,  $\beta$ 2-chimaerin undergoes a conformational rearrangement and acquires an “open” conformation. Large hydrophobic patches in “open”  $\beta$ 2-chimaerin contribute to aligning the protein at the membrane (29, 184)

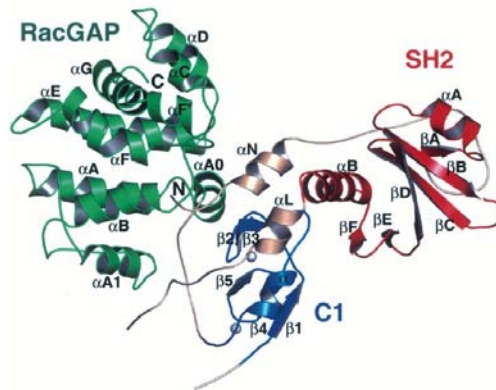
### **Chimaerins as Rac-GAPs:**

*In vitro* assays demonstrated that  $\beta$ 2-chimaerin has GAP activity towards the small G-protein Rac1, but not Cdc42 or RhoA, indicating that  $\beta$ 2-chimaerin is a Rac specific GAP (28). Ectopic expression of  $\beta$ 2-chimaerin in cells significantly reduced active Rac-GTP levels under both normal growth conditions or upon stimulation by

A.



B.



C.

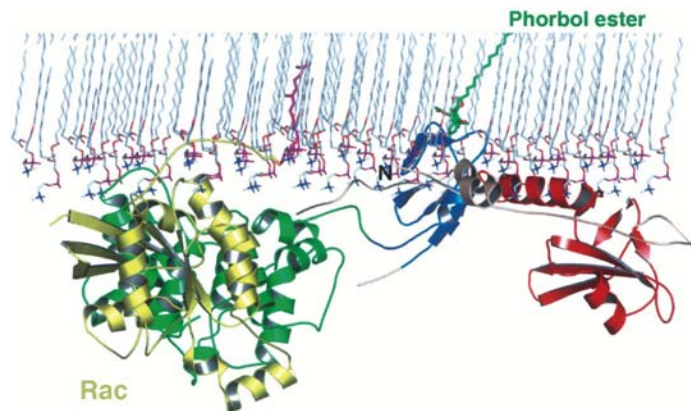


**Figure 1.8** Crystal structure of  $\beta 2$ -chimaerin. **A.** Structures of SH2 (red), C1 (blue) and Rac-GAP (green) domains. **B.** Inactive “closed” conformation of  $\beta 2$ -chimaerin. **C.** Active “open” conformation of  $\beta 2$ -chimaerin. Adapted from: Canagarajah *et al.* Cell (2004) 119: 407-418.

EGF or PMA, and the effect was dependent upon a functional C-terminal GAP domain. On the other hand, Cdc42-GTP or RhoA-GTP levels were not affected by overexpression of  $\beta$ 2-chimaerin, suggesting that it acts as a specific Rac-GAP in cells. In line with those findings, several studies demonstrated that  $\beta$ 2-chimaerin is an important regulator of Rac signaling in cells and possibly implicated in cancer progression.  $\beta$ 2-chimaerin was found to be down-regulated in high-grade astrocytomas (anaplastic astrocytomas and glioblastomas) when compared with normal brain and low-grade astrocytomas (199). A subsequent study from our laboratory demonstrated that  $\beta$ 2-chimaerin mRNA levels are significantly down-regulated in human breast cancer cell lines and breast tumors (195). Overexpression of  $\beta$ 2-chimaerin in MCF-7 breast carcinoma cells leads to inhibition of cell proliferation accompanied by decreased Rac-GTP, cyclin D1 and phosphorylated retinoblastoma protein (pRb) levels, whereas expression of V12Rac1 restored the proliferation of these cells (195).  $\beta$ 2-chimaerin also inhibits EGF-mediated effects, including actin cytoskeleton reorganization and cell migration. The inhibitory effects of  $\beta$ 2-chimaerin on cell migration could be restored by overexpression of V12Rac1 (184). In Jurkat T-cells, expression of  $\beta$ 2-chimaerin also impairs PMA-induced actin polymerization, CXCL12-induced Rac activation, cell spreading and adhesion to VCAM-1 (159). I previously demonstrated that EGF-induced activation of Rac is potentiated and prolonged when  $\beta$ 2-chimaerin is knocked-down using RNAi, suggesting that  $\beta$ 2-chimaerin acts as a mechanism for limiting the intensity and duration of Rac signaling (184). Similar results were reported later in NIH3T3 cells

upon PDGF stimulation, suggesting a role for  $\beta$ 2-chimaerin in limiting the strength of Rac-GTP activation in response to growth factors (197).

Several *in vivo* models have been used to elucidate the physiological role of chimaerins. In our laboratory we have cloned the zebrafish chimaerin gene, which encodes a protein highly homologous to  $\alpha$ 2- and  $\beta$ 2-chimaerin, with 86% and 74% amino acid identity, respectively. The zebrafish chimaerin behaves similarly to the human chimaerins, as it translocates to the plasma membrane in response to PMA and possesses Rac-GAP activity. Depletion of chimaerin by injection of antisense morpholino RNAs into zebrafish embryos at one cell stage leads to significant developmental defects. Chimaerin-deficient zebrafish embryo displayed hyperactivation of Rac and faster migration through epiboly, which results in enlarged tailbuds. Interestingly, these defects can be rescued by microinjection of chimaerin mRNA into the yolk syncytial layer. These results suggested that chimaerin is critical for regulating Rac-mediated migration during zebrafish development (101). Studies in *Drosophila* also revealed an important role for chimaerin in the modulation of Rac signaling during development. RhoGAP5a, a single ortholog for chimaerins in *Drosophila* that shares 37% identity with human  $\beta$ 2-chimaerin, is expressed in the interommatidial precursor cells of the developing fly eye. Depletion of RhoGAP5A in these cells increases numbers of cells and leads to aberrant cell-cell contacts. RhoGAP5A was also linked to EGFR signaling in the fly eye since knockdown of RhoGAP5A enhances ERK activation, implying that RhoGAP5A interacts with Rac to regulate EGFR-ERK signaling (22).

Experiments using  $\alpha 2$ -chimaerin knockout mice established an important role for  $\alpha 2$ -chimaerin in axon guidance and growth cone collapse. Mice lacking  $\alpha$ -chimaerin exhibit a hopping phenotype that is similar to that of EphA4 receptor-deficient mice. EphA4 repulsive signaling induces growth cone collapse that keeps corticospinal tract (CST) axons from crossing the midline. Axons from mice lacking  $\alpha$ -chimaerin are unresponsive to these repulsive cues, which results in aberrant midline crossing of spinal cord projections and altered motor circuit formation. These results demonstrated that  $\alpha$ -chimaerin GAP activity for inactivation of Rac is required for EphA4-induced growth cone collapse. Interestingly, Nck1-lacking mice also develop a similar phenotype to that of EphA4 and  $\alpha 2$ -chimaerin knockout mice, suggesting that Nck1 may be a critical component in the EphA4 receptor-chimaerin signaling pathway (12, 55, 83, 155, 185). One of the most remarkable recent findings has been that human CHN1 mutations that hyperactivate  $\alpha 2$ -chimaerin are the cause of Duane's retraction syndrome (DRS), which is a complex congenital eye movement disorder caused by aberrant innervation of the extraocular muscles by axons of brainstem motor neurons (125). Patients with DRS have substitution mutations in  $\alpha 2$ -chimaerin that lead to hyperactive proteins with enhanced GAP activity as well as enhanced membrane translocation (125). Remarkably, many of these mutations in  $\alpha 2$ -chimaerin are equivalent to those leading to an “open“ conformation predicted in our structural studies of  $\beta 2$ -chimaerin. Indeed, we found that mutation of Ile126 residue, which is frequently mutated in DRS, confers enhanced GAP activity and translocation in cells (43).

### **Identification of p23/Tmp21 as a chimaerin-interacting protein**

In early studies carried out in the Kazanietz lab, I identified a chimaerin-binding protein using a yeast two-hybrid approach. This screen established that p23/Tmp21, a type I transmembrane protein involved in vesicle transport and protein trafficking, interacts with both  $\alpha$ - and  $\beta$ -chimaerins. Using a series of truncation mutants, I further established that the C1 domain in chimaerins is required for the interaction. Confocal microscopy analysis demonstrated that chimaerins co-localize with p23/Tmp21 in the perinuclear region. Mutations or deletion of the C1 domain abolished the chimaerin perinuclear localization. This suggested that p23/Tmp21 might act as an anchoring protein for chimaerins. Interestingly, p23/Tmp21 inhibits  $\beta$ 2-chimaerin Rac-GAP activity in cells when co-expressed with  $\beta$ 2-chimaerin, suggesting that p23/Tmp21 may limit  $\beta$ 2-chimaerin Rac-GAP activity by sequestering it in the perinuclear region (181). More recently, our laboratory found that  $\beta$ 2-chimaerin function is regulated by another DAG/phorbol ester-regulated protein, PKC $\delta$ . Ser169 in  $\beta$ 2-chimaerin becomes phosphorylated by PKC $\delta$  upon treatment with PMA or EGF. This post-translational modification prevents  $\beta$ 2-chimaerin membrane relocation in response to stimuli and represents a means of limiting the strength of  $\beta$ 2-chimaerin Rac-GAP activity, suggesting dual roles of DAG signaling pathway in regulating  $\beta$ 2-chimaerin functions. By summarizing all the studies from our laboratory, we propose the following updated model for regulation and activation of  $\beta$ 2-chimaerin (**Figure 1.9**).



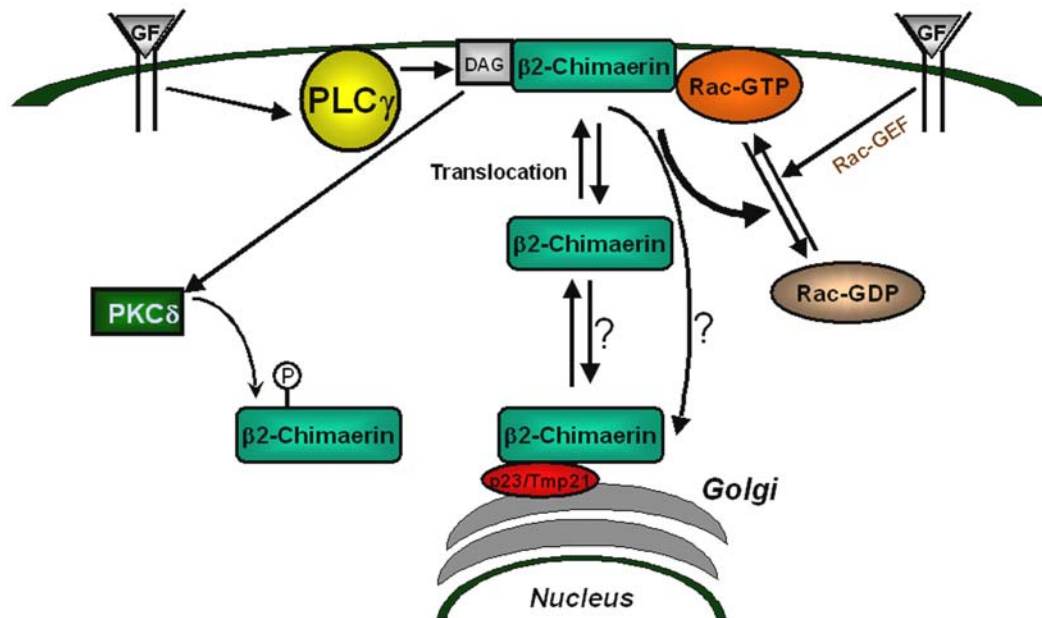


**Figure 1.9** Model of activation and regulation of  $\beta$ 2-chimaerin upon growth factor stimulation.

## **Scope and significance of my thesis research**

The overall objective of my dissertation research is to investigate the regulation and function of C1 domain-containing proteins in different paradigms. My focus will be primarily on  $\beta$ 2-chimaerin and nPKCs.

In the case of  $\beta$ 2-chimaerin, I have previously identified that it can interact with p23/Tmp21, an ER/Golgi cargo protein widely implicated in trafficking from the intermediate compartment to the Golgi (16, 18, 163). In the present studies, I elucidate how  $\beta$ 2-chimaerin interacts with p23/Tmp21. A deletional analysis in  $\alpha$ - and  $\beta$ -chimaerins revealed that the C1 domain is the p23/Tmp21-interacting motif (181). Our biochemical and imaging studies strongly support the formation of a chimaerin-p23/Tmp21 complex in cells (181), suggesting that p23/Tmp21 actually serves as a perinuclear anchoring protein for chimaerin Rac-GAPs. It is still unclear which amino acid(s) in the  $\beta$ 2-chimaerin C1 domain is (are) crucial for the interaction. It also remains to be determined if p23/Tmp21 associates with other proteins possessing C1 domains to drive their perinuclear translocation. This is relevant because proteins with C1 domains, such as PKC $\epsilon$ , have been shown to localize at the Golgi. I will focus on the ability of C1 domains to dictate intracellular localization via protein-protein interactions, which expands our view that these domains act primarily as lipid-binding motifs and also highlights the complexities of DAG signaling. These studies represent the core of Chapter 2.

It is well established that PMA and related analogs induce apoptosis in androgen-dependent prostate cancer cells, an effect primarily mediated by PKC $\delta$ . Based upon the finding that p23/Tmp21 could interact with PKC isozymes, chimaerins as well as

RasGRP, I investigated whether PKC $\delta$  could directly associate with p23/Tmp21 in LNCaP prostate cancer cells, and assessed the functional consequences of these findings. In Chapter 3, I demonstrate that p23/Tmp21 directly associates with PKC $\delta$  in LNCaP prostate cancer cells and present data showing that p23/Tmp21 acts as an anchoring protein that negatively regulates the apoptotic effects of PMA. Our findings reveal a novel function for p23/Tmp21 in DAG signaling, which is independent of its previous well-established role acting as a vesicle trafficking protein.

Many studies have reported that membrane-related signaling cascades might play important roles in controlling radiation-induced cell death. In Chapter 4 of my dissertation I present studies on the roles of PKC isozymes in the resistance to  $\gamma$ -irradiation in PC3 prostate cancer cells. Most prostate cancer cells express three DAG/phorbol ester-responsive protein kinase C (PKC) isozymes: PKC $\alpha$ , PKC $\delta$  and PKC $\epsilon$ . The role of individual PKC isozymes in prostate cancer radiosensitivity remains elusive. My results reveal that PKC $\epsilon$ , but not PKC $\alpha$  and PKC $\delta$ , confers radioresistance to androgen-independent prostate cancer cells. Moreover, C1 domain mediated translocation of PKC $\epsilon$  by  $\gamma$ -irradiation represents the key event in this paradigm.

In summary, my thesis will present novel findings on the regulation and function of C1 domain-containing proteins:  $\beta$ 2-chimaerin, PKC $\delta$ , and PKC $\epsilon$ .

## CHAPTER 2

### **p23/Tmp21 differentially targets the Rac-GAP $\beta$ 2-chimaerin and protein kinase C via their C1 domains**

This work was published in:

**Molecular Biology of the Cell**. Epub February 17, 2010 as 10.1091/mbc. E09-08-  
0735

## **ABSTRACT**

The C1 domains in PKC isozymes and other signaling molecules are responsible for binding the lipid second messenger DAG and phorbol esters, and mediate translocation to membranes. Previous studies revealed that the C1 domain in  $\alpha$ - and  $\beta$ -chimaerins, DAG-regulated Rac-GAPs, interacts with the ER/Golgi protein p23/Tmp21. Here we found that p23/Tmp21 acts as a C1 domain-docking protein that mediates perinuclear translocation of  $\beta$ 2-chimaerin. Glu227 and Leu248 in the  $\beta$ 2-chimaerin C1 domain are crucial for binding p23/Tmp21 and perinuclear targeting. Interestingly, isolated C1 domains from individual PKC isozymes differentially interact with p23/Tmp21. In the case of PKC $\epsilon$ , it interacts with p23/Tmp21 specifically via its C1b domain, however this association is lost in response to phorbol esters. These results demonstrate that p23/Tmp21 acts as an anchor that distinctively modulates compartmentalization of C1 domain-containing proteins, and it plays an essential role in  $\beta$ 2-chimaerin relocalization. Our study also highlights the relevance of C1 domains in protein-protein interactions in addition to their well-established lipid-binding properties.

## **INTRODUCTION**

C1 domains are 50-51 amino acid long cysteine-rich motifs originally identified in PKC as the binding sites for the lipid second messenger DAG and the phorbol ester tumor promoters. These domains contain the characteristic motif  $HX_{12}CX_2CX_{13/14}CX_2CX_4HX_2CX_7C$ , where  $H$  is His,  $C$  is Cys, and  $X$  is any other amino acid. X-ray crystallography analysis revealed that C1 domains are compact globular structures coordinated through binding of two  $Zn^{2+}$  ions to conserved Cys and His residues. While this motif is duplicated in tandem (C1a and C1b domains) in classical PKCs (cPKC $\alpha$ ,  $\beta$ I,  $\beta$ II and  $\gamma$ ) and novel PKCs (nPKC $\delta$ ,  $\epsilon$ ,  $\eta$  and  $\theta$ ), a single copy is present in phorbol ester/DAG unresponsive atypical PKC isozymes (aPKC $\zeta$ ,  $\iota/\lambda$ )(122, 134). C1 domains capable of binding phorbol esters and DAG are also present in other protein kinases such as protein kinase D isozymes (PKDs) and Myotonic Dystrophy Kinase-related Cdc42-binding Kinase (MRCK), lipid kinases (DAG-kinases), GTPase activating proteins ( $\alpha$ - and  $\beta$ -chimaerin Rac-GAPs), guanine nucleotide exchange factors (RasGRP GEFs), and scaffolding proteins (Munc-13s)(1, 13, 25, 39, 52, 75, 117, 156, 178).

A distinctive feature of most phorbol ester receptors with C1 domains is their ability to redistribute to membranes in response to stimulation of receptors that couple to DAG generation or phorbol esters. A continuous hydrophobic surface generated by the phorbol ester or DAG facilitates the insertion of the C1 domain into lipid bilayers, which in the case of cPKCs and nPKCs is followed by a conformational rearrangement that leads to kinase activation (46, 151, 201). It is noteworthy that upon activation PKCs relocalize not only to plasma membrane but also to other

intracellular compartments including the nuclear membrane (128), perinuclear structures (80), and mitochondria (114). A high degree of isozyme selectivity for translocation to different intracellular compartments appears to exist (126). For example, early studies established that PKC $\epsilon$  localizes to the Golgi complex in NIH 3T3 cells via the C1 domain (98, 100). Moreover, a recent study in neuroblastoma SK-N-BE(2)C cells revealed that mutation of specific residues in the PKC $\epsilon$  C1b domain impairs its perinuclear localization without affecting its translocation to the plasma membrane in response to the C1 domain ligand PMA (153).

We have previously established that  $\alpha$ 2- and  $\beta$ 2-chimaerins translocate both to the plasma membrane and the perinuclear region in response to PMA or DAG analogs via the C1 domain (27). Deletion of the C1 domain or mutations of key amino acids implicated in phorbol ester binding impairs both the peripheral and perinuclear translocation of chimaerins, thus arguing that the C1 domain is essential for chimaerin intracellular targeting (25-27, 184). Other “non-kinase” phorbol ester/DAG receptors such as RasGRP1/3 and Munc-13 also translocate to the plasma membrane and Golgi in response to PMA via their C1 domains (28, 165). The molecular basis for the translocation of proteins with C1 domains is only partially understood. Speculation has been that protein-protein interactions are key factors for determining their selective intracellular relocalization, and studies have indeed identified numerous PKC interactors that dictate compartmentalization through binding to unique motifs present in individual isoforms, such as the receptors for activated C-kinases (RACKs) (45). Interactions may require a conformational rearrangement that exposes the protein binding domain (127). Although these

mechanisms have been extensively studied for PKC isozymes, the involvement of protein partners in targeting chimaerin Rac-GAPs has not been established yet.

In a previous yeast two-hybrid screening I identified the Golgi/ER protein p23/Tmp21 (p24 $\delta$ ) as a chimaerin-interacting protein (181). p23/Tmp21, a type I transmembrane protein, belongs to the p24 protein family that has been widely implicated in trafficking from the intermediate compartment to the Golgi (16, 18, 163). A deletional analysis in  $\alpha$ - and  $\beta$ -chimaerins revealed the C1 domain as the p23/Tmp21-interacting motif (181). Biochemical and imaging studies strongly support the formation of a chimaerin-p23/Tmp21 complex in cells (181). We hypothesize that p23/Tmp21 might serve as a perinuclear anchoring protein for chimaerin Rac-GAPs. Moreover, p23/Tmp21 might also associate with other proteins containing C1 domains to drive their perinuclear translocation. This is relevant because proteins with C1 domains, such as PKC $\epsilon$ , have been shown to localize at the Golgi.

In this Chapter I present data demonstrating that p23/Tmp21 is required for the perinuclear translocation of  $\beta$ 2-chimaerin. This Rac-GAP indeed fails to redistribute to the perinuclear compartment in p23/Tmp21-deficient cells. I also identified key residues in the  $\beta$ 2-chimaerin C1 domain that specifically mediate its association with p23/Tmp21 and translocation to the perinuclear compartment. Interestingly, p23/Tmp21 also interacts with other C1 domains in isolation, including C1 domains from PKC isozymes. Our results support the notion that C1 domains act not only as lipid binding motifs but can also mediate protein-protein interactions that determine selective intracellular compartmentalization.



## RESULTS

### **The C1 domain of $\beta$ 2-chimaerin and C1b domain of PKC $\epsilon$ interact with p23/Tmp21**

In previous studies I identified p23/Tmp21, a type I transmembrane protein highly enriched in the ER and Golgi, as an  $\alpha$ - and  $\beta$ -chimaerin-interacting protein. A deletional analysis established that interaction with p23/Tmp21 occurs through a region that encompasses the chimaerin C1 domain (181). Since PKC $\epsilon$  was shown to localize at the perinuclear region via its C1 domain region (153), we speculated that C1a and/or C1b domains in PKC $\epsilon$  may interact with p23/Tmp21. To address this issue we first examined whether the C1 region of PKC $\epsilon$ , which include both C1a and C1b domains (C1 $\epsilon$ a-b), interacts with p23/Tmp21 in a yeast two-hybrid system. A pLexA construct encoding C1 $\epsilon$ a-b was generated (Figure 2.1A) and co-transformed with pB42AD-p23/Tmp21 (HA-tagged, aa 108-208, a fragment that interacts with chimaerins) into EGY48 yeast containing p8OP-LacZ vector (181). The triple vectors co-transformants were selected by plating the yeast into SD/-Ura/-His/-Trp dropout plates. pLexA-fused proteins were expressed in both galactose/raffinose (+Gal/Raf) plates and glucose plates (-Gal/Raf), while HA-tagged pB42AD-p23/Tmp21 (aa 108-208) was only expressed in galactose/raffinose induction plates (data not shown). Figure 2.1B shows that both the  $\beta$ 2-chimaerin C1 domain (C1 $\beta$ 2-ch) and C1 $\epsilon$ a-b strongly interact with p23/Tmp21, as revealed by the induction of the LacZ reporter (blue color). These interactions were also detected using a liquid  $\beta$ -galactosidase assay (Figure 2.1C).

Studies have determined that C1 $\epsilon$ b but not C1 $\epsilon$ a is essential for Golgi localization in neuroblastoma SK-N-BE(2)C cells (153), suggesting a differential involvement of each domain in perinuclear targeting. We therefore generated pLexA-fused C1 $\epsilon$ a and C1 $\epsilon$ b constructs (Figure 2.1A), co-transformed each of them with pB42AD-p23/Tmp21 into the EGY48 (p8OP-LacZ) yeast, and expressed both proteins in +Gal/Raf plates. Interestingly, a strong association was observed with C1 $\epsilon$ b, while C1 $\epsilon$ a failed to interact with p23/Tmp21 (Figure 2.1B and 2.1C). To further establish whether C1 domain specificity exists, we generated pLexA constructs encoding C1 domains of aPKC $\zeta$  (C1 $\zeta$ ), PKC $\alpha$  (C1 $\alpha$ ), PKC $\delta$  (C1 $\delta$ ), and RasGRP1. While C1 $\zeta$  failed to interact with p23/Tmp21 in the yeast two-hybrid assay (Figure 2.1B), association was detected for C1 $\alpha$  and C1 $\delta$ , and the C1 domain of the Ras/Rap1 exchange factor RasGRP1 weakly interacted with p23/Tmp21 (Figure 2.2A, 2.2B, and 2.2C).

Next, we determined the intracellular localization of C1 $\beta$ 2-ch, C1 $\epsilon$ a, and C1 $\epsilon$ b domains in mammalian cells. C1 domains were expressed as GFP-fusion proteins in HeLa cells, and localization examined by confocal microscopy (Figure 2.1D). Remarkably, individual C1 domains exhibited distinct intracellular localization. While GFP-C1 $\epsilon$ a distributed throughout the cell and had no obvious perinuclear localization, as previously reported in SK-N-BE(2)C cells (153), GFP-C1 $\epsilon$ b and GFP-C1 $\beta$ 2-ch showed a characteristic perinuclear localization. GFP-C1 $\zeta$  displayed a strong nuclear localization when expressed in HeLa cells but no obvious perinuclear staining. Thus, C1 domains, when expressed in isolation, have unique localization properties.

Next, we examined whether different C1 domains co-localize with p23/Tmp21. HeLa cells were co-transfected with pcDNA3-V5-p23/Tmp21 together with plasmids encoding different C1 domains fused to GFP, and co-localization determined by confocal microscopy. As shown in Figure 2.3, both GFP-C1 $\epsilon$ b and GFP-C1 $\beta$ 2-ch co-localized with p23/Tmp21, as judged by the yellow color observed in the overlapped images. Quantification using ImageJ and analysis using a Pearson's correlation coefficient (Rr) confirmed these results. In contrast, neither GFP-C1 $\epsilon$ a nor GFP-C1 $\zeta$  showed any obvious co-localization with p23/Tmp21. GFP alone also failed to co-localize with p23/Tmp21 in HeLa cells. We also found that full-length PKC $\alpha$ , PKC $\delta$  and RasGRP1 have some degree of co-localization with P23/Tmp21 (Figure 2.2D). These results are in agreement with those observed in the yeast two-hybrid analysis, and reveal unique patterns of intracellular localization and protein interactions for discrete C1 domains.

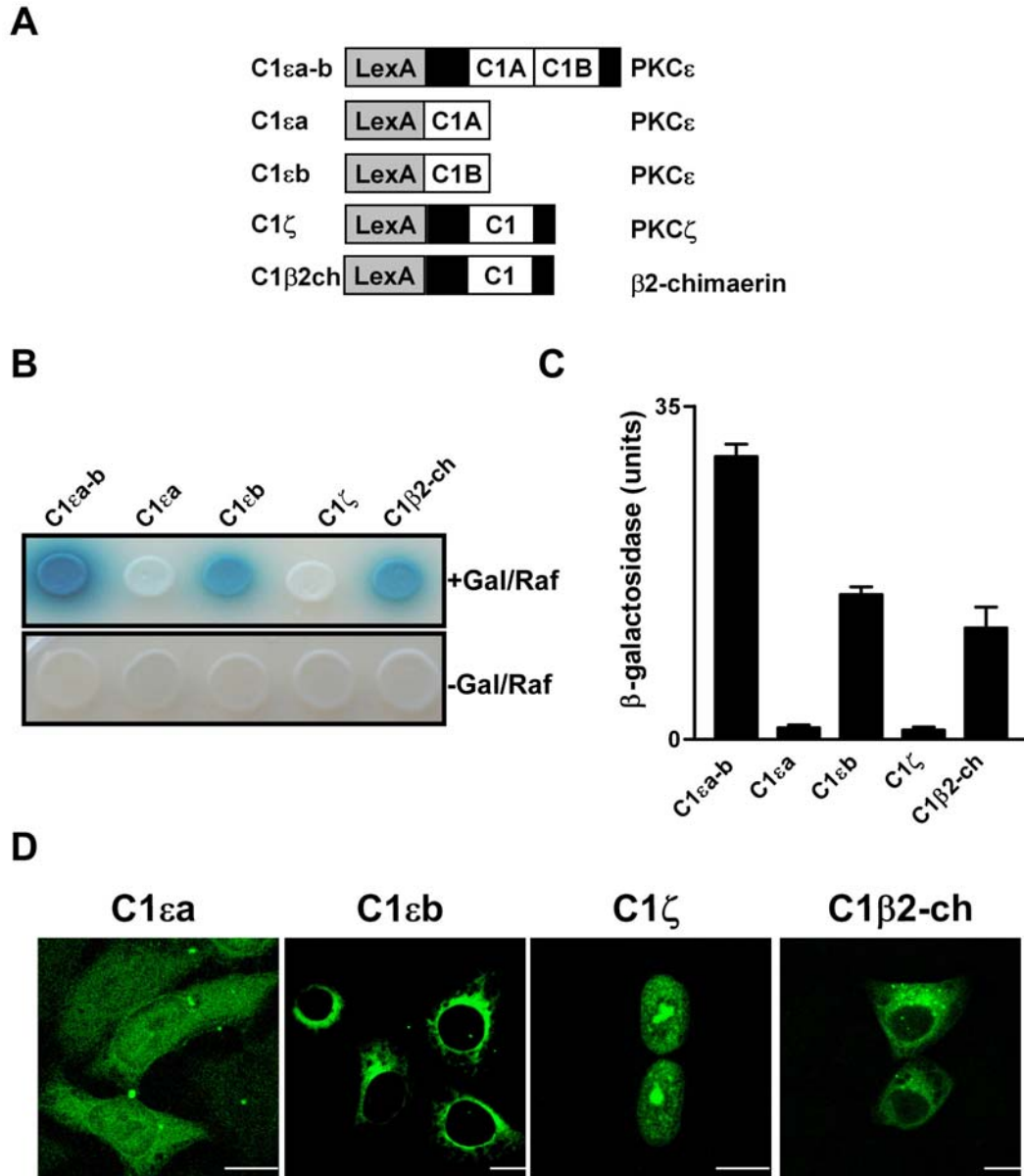


**Figure 2.1** Differential interaction of C1 domains with p23/Tmp21. **A.** Schematic representation of C1 $\epsilon$ a-b, C1 $\epsilon$ a, C1 $\epsilon$ b, C1 $\zeta$ , or C1 $\beta$ 2-ch domain fused to LexA. EGY48 yeast (containing 8op-LacZ vector) was co-transformed with pLexA encoding C1 $\epsilon$ a-b, C1 $\epsilon$ a, C1 $\epsilon$ b, C1 $\zeta$ , or C1 $\beta$ 2-ch domain, and pB42AD-HA-tagged p23/Tmp21 (aa 108-208). Assay of  $\beta$ -galactosidase activity on induction (*upper panel*) or no-induction (*lower panel*) plates was carried out 72 h after transformation. *Gal/Raf*, galactosidase/raffinose. **C.** Assay of  $\beta$ -galactosidase activity in liquid cultures using ONPG as a substrate. Results were expressed as mean  $\pm$  S.D. (n=3). **D.** GFP-CKC $\epsilon$ C1b domain localizes in the perinuclear region. HeLa cells were transfected with pEGFP-C1 $\epsilon$ a, C1 $\epsilon$ b, C1 $\zeta$ , or C1 $\beta$ 2-ch. Forty-eight h later, cells were fixed and localization examined by confocal microscopy. *Bar*, 10  $\mu$ m. All experiments have been performed at least three times with similar results.

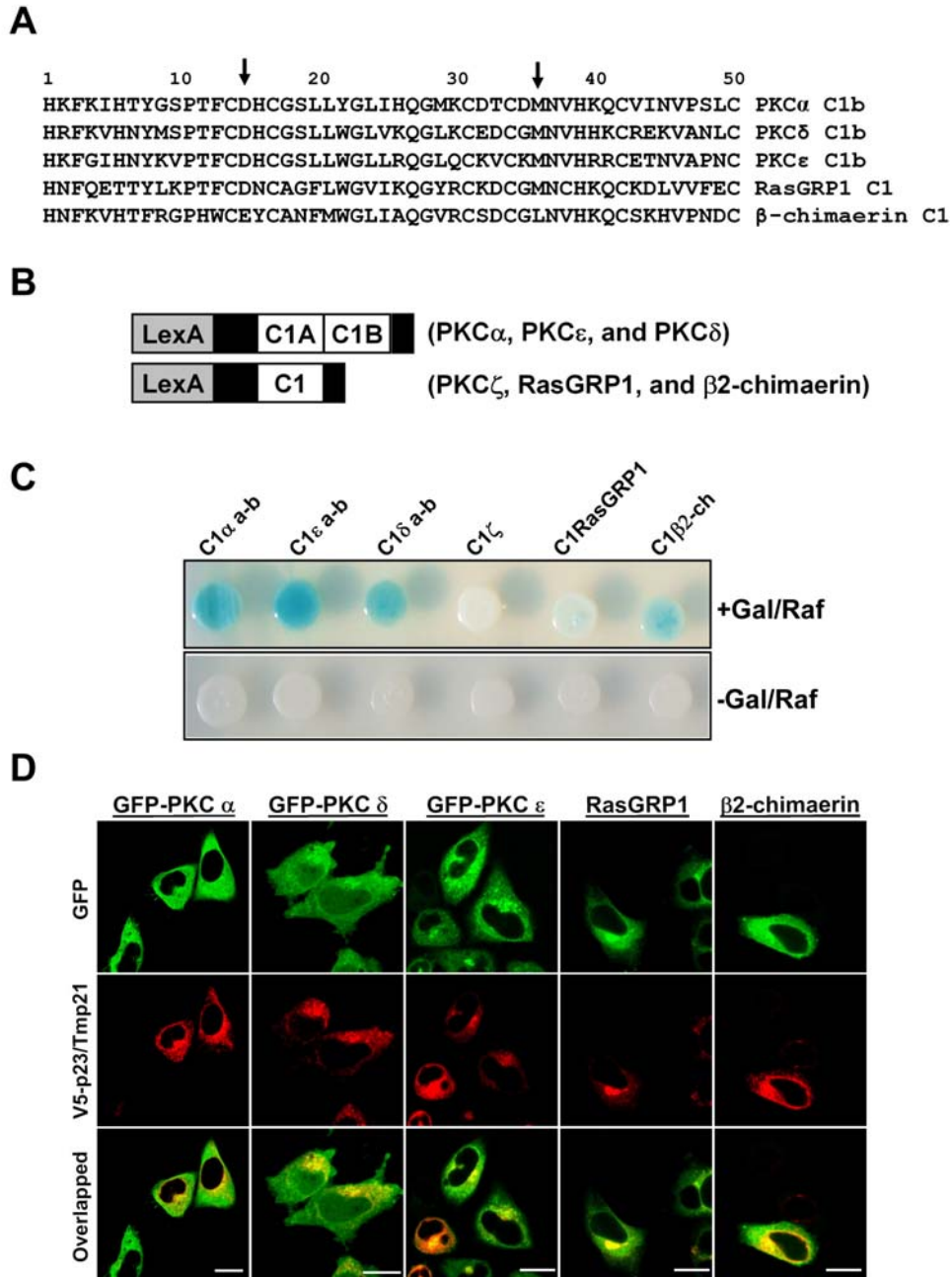


**Figure 2.2** Binding of C1 domains to p23/Tmp21. EGY48 yeast (containing 8op-LacZ vector) was co-transformed with pLexA-fused C1 domains from PKC $\alpha$  (C1 $\alpha$ -b), PKC $\epsilon$  (C1 $\epsilon$ -b), PKC $\delta$  (C1 $\delta$ -b), PKC $\zeta$  (C1 $\zeta$ ), RasGRP1 (C1RasGRP1), or  $\beta$ 2-chimaerin (C1 $\beta$ 2-ch), and pB42AD-HA-tagged p23/Tmp21 (aa 108-208). **A.** Alignment of PKC $\alpha$ , PKC $\delta$ , PKC $\epsilon$  C1b, RasGRP1, and  $\beta$ 2-chimaerin C1 domains. Positions 15 and 36 in C1 domains are indicated with arrows. **B.** Schematic representation of C1 domains fused to pLexA. **C.** Assay of  $\beta$ -galactosidase activity on induction (*upper panel*) or no-induction (*lower panel*) plates, carried out 72 h after transformation. *Gal/Raf*, galactosidase/raffinose. Two additional experiments gave similar results. **D.** HeLa cells were co-transfected with plasmids encoding GFP-PKC $\alpha$ , GFP-PKC $\delta$ , GFP-PKC $\epsilon$ , GFP-RasGRP1 or GFP- $\beta$ 2-chimaerin, and pcDNA3.1-V5-p23/Tmp21. Forty-eight h later, cells were fixed and co-localization examined by confocal microscopy. *Bar*, 10  $\mu$ m. All experiments have been performed at least three times with similar results.

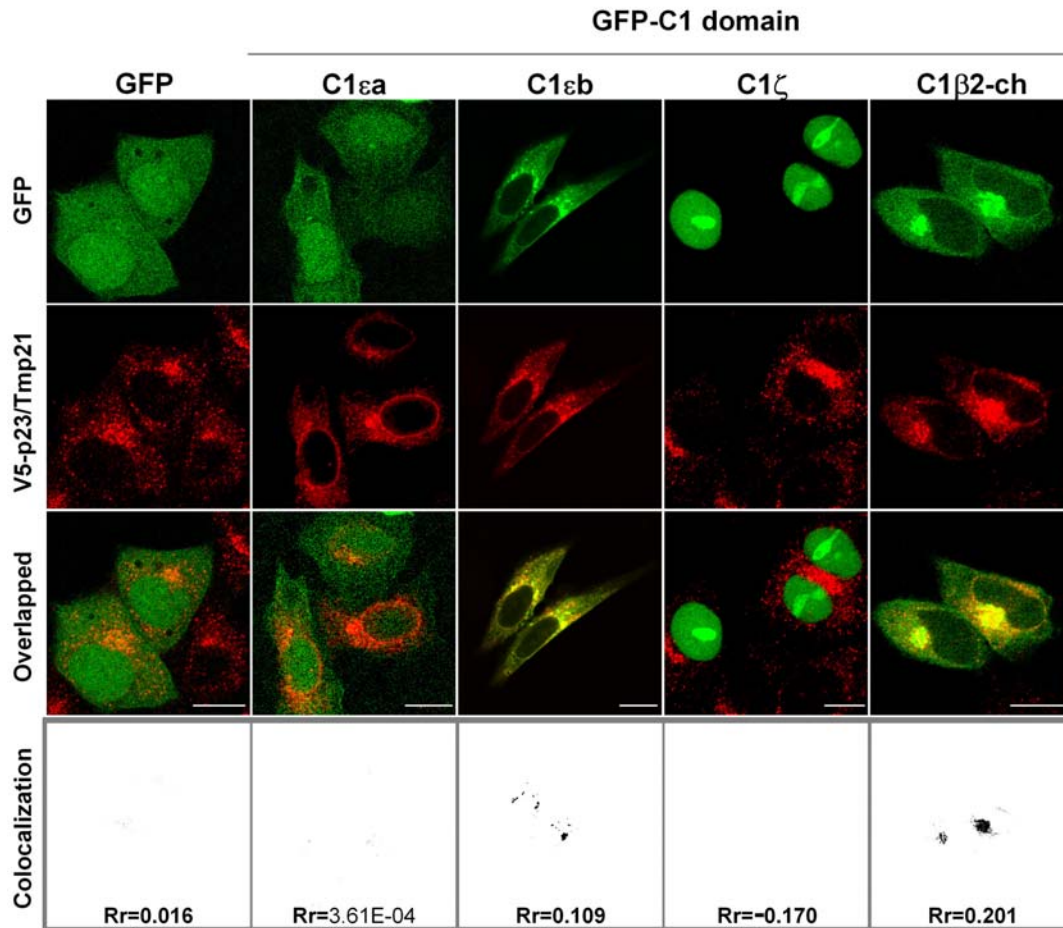


**Figure 2.3** *Co-localization of GFP-fused PKC $\epsilon$  C1b and  $\beta$ 2-chimaerin C1 domains with p23/Tmp21.* HeLa cells were co-transfected with pEGFP-fused C1 $\epsilon$ a, C1 $\epsilon$ b, C1 $\zeta$ , or C1 $\beta$ 2-ch (or empty vector) and V5-tagged full-length pcDNA3-p23/Tmp21. Forty-eight h later, cells were fixed and stained with an anti-V5 antibody, and localization examined by confocal microscopy. Co-localization images and Pearson's correlation coefficient (Rr) were generated by Image J. Similar results were observed at least in 3 independent experiments. *Bar*, 10  $\mu$ m.

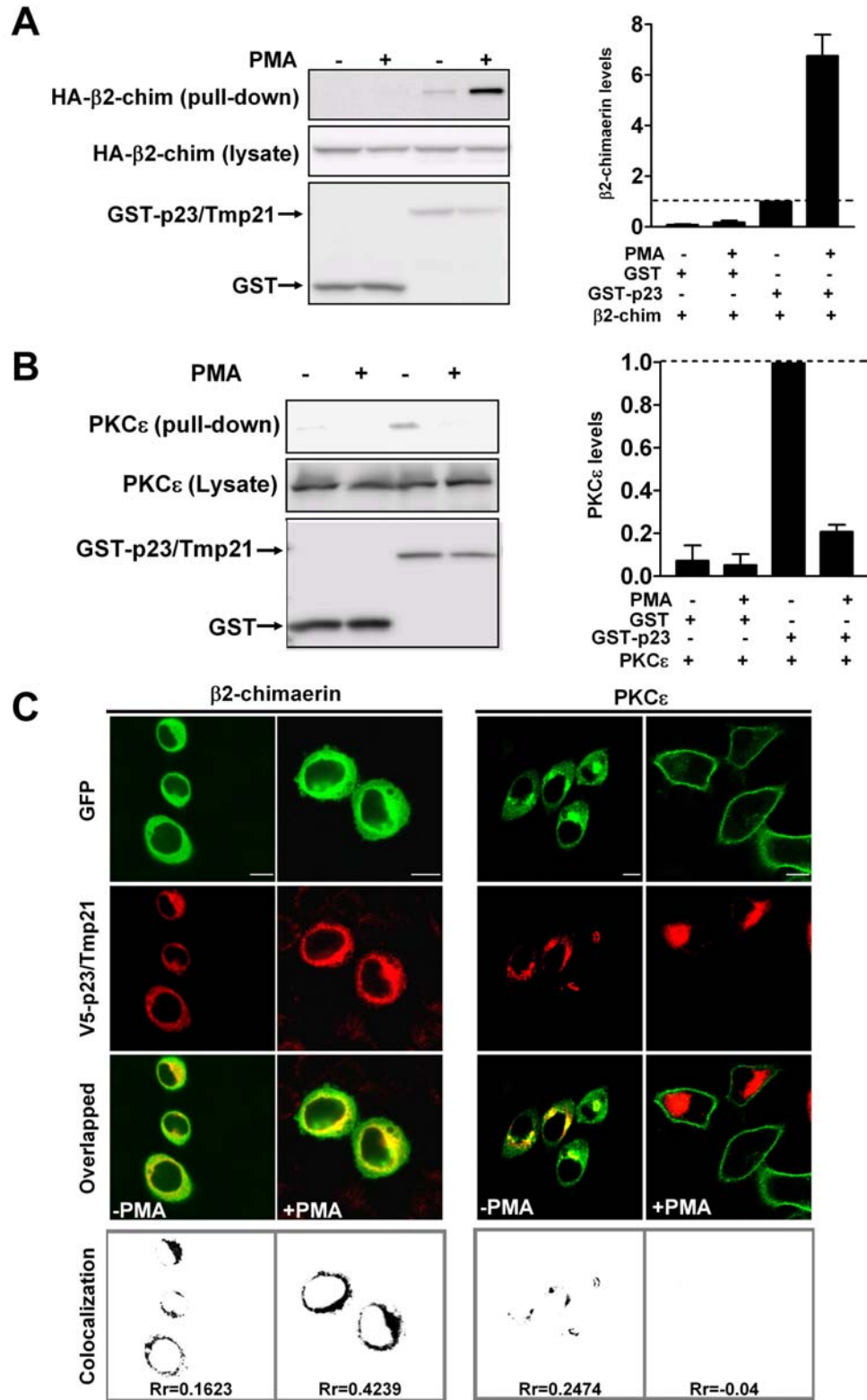
### **Co-localization of full-length PKC $\epsilon$ and p23/Tmp21**

Experiments carried out with isolated C1 domains established proof-of-principle for differential targeting, but may or may not reflect what occurs with intact proteins in cells. Therefore, we next decided to investigate the association of full-length  $\beta$ 2-chimaerin and PKC $\epsilon$  with p23/Tmp21 in mammalian cells. COS-1 cells were transfected with pEBG control vector (which encodes GST alone) (181) or pEBG-p23/Tmp21. After 24 h, cells were infected with adenoviruses for either full-length PKC $\epsilon$  or full-length  $\beta$ 2-chimaerin, and 24 h later subject to GST pull-down using glutathione Sepharose 4B beads. As shown in Figure 2.4A (*left panel*), and in agreement with our previous study (27, 181),  $\beta$ 2-chimaerin was detected in complex with GST-p23/Tmp21 but not with GST.  $\beta$ 2-chimaerin was shown to translocate to the perinuclear compartment in response to C1 domain ligands such as PMA. This effect was lost when key residues in the C1 domain are mutated but was not affected by the pan-PKC inhibitor GF 109203X, suggesting that the PMA effect was not mediated by PKCs (27, 181). Figure 2.4A (*left panel*) also shows that the association of  $\beta$ 2-chimaerin with GST-p23/Tmp21 was markedly enhanced by PMA. A densitometric analysis revealed that PMA caused a  $\sim$ 7-fold increase in the association of  $\beta$ 2-chimaerin with p23/Tmp21 (Figure 2.4A, *right panel*). The association between  $\beta$ 2-chimaerin and p23/Tmp21 can also be enhanced in cells growing in serum and in response to EGF treatment, although in this last case to a lower extent than that observed with PMA (Figure 2.5). Interestingly, PKC $\epsilon$  can be readily detected in GST-p23/Tmp21 precipitates, whereas it cannot be pulled down by GST alone, an indication that PKC $\epsilon$  and p23/Tmp21 exist as a complex. However, in contrast to  $\beta$ 2-

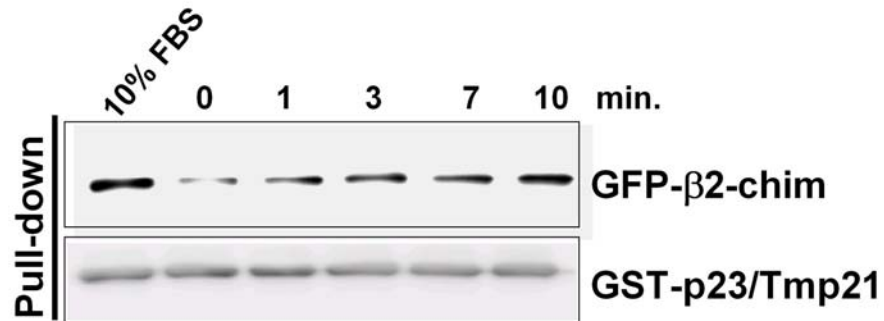
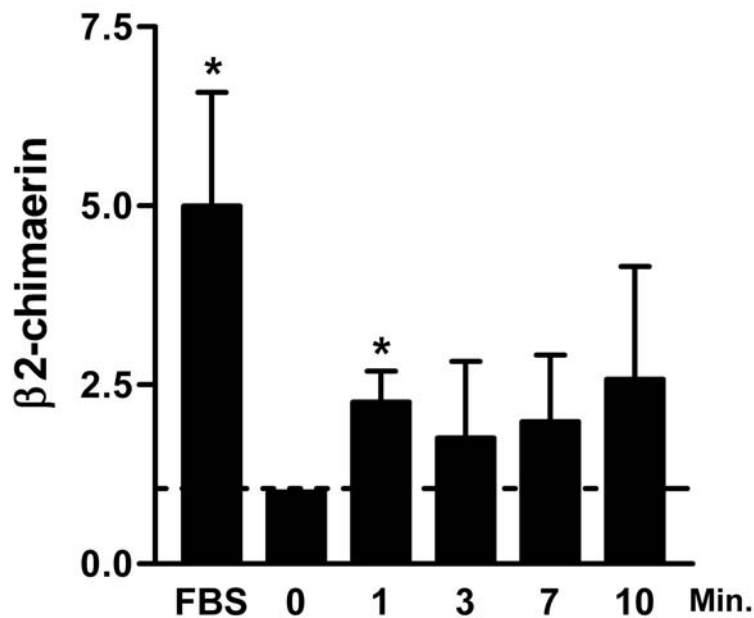
chimaerin, PKC $\epsilon$  dissociated from p23/Tmp21 when cells were treated with PMA (Figure 2.4B).

The distinct association pattern of PKC $\epsilon$  and  $\beta$ 2-chimaerin with p23/Tmp21 prompted us to examine whether they differentially re-localize in response to phorbol ester treatment. HeLa cells expressing GFP-PKC $\epsilon$  or GFP- $\beta$ 2-chimaerin (full-length) were treated with either PMA or vehicle, and localization examined by confocal microscopy. Like  $\beta$ 2-chimaerin, PKC $\epsilon$  displayed some degree of co-localization with p23/Tmp21 in the perinuclear region of vehicle-treated cells ( $R_r=0.25$ ). However, a remarkably distinct pattern of translocation for each protein was observed in response to PMA: while  $\beta$ 2-chimaerin redistributed primarily to the perinuclear compartment and co-localized with p23/Tmp21 in response to PMA ( $R_r$  increases from 0.16 to 0.42) (plasma membrane localization can be also detected)(27, 181), PKC $\epsilon$  fully translocated to the cell periphery. Coincidentally, no perinuclear PKC $\epsilon$  or co-localization with p23/Tmp21 could be observed in PMA-treated cells ( $R_r= -0.04$ ) (Figure 2.4C). These results argue for a differential interaction of PKC $\epsilon$  and  $\beta$ 2-chimaerin with p23/Tmp21 in response to stimuli. Moreover, they also suggest that domain(s) in PKC $\epsilon$  other than the C1b domain must have prominent targeting roles.





**Figure 2.4** *Differential interaction of PKC $\epsilon$  and  $\beta$ 2-chimaerin with p23/Tmp21.* **A and B.** COS-1 cells were transfected with either pEBG (empty vector) or pEBG-p23/Tmp21. Twenty-four h later, cells were infected with either HA- $\beta$ 2-chimaerin adenovirus (MOI=10 pfu/cell) (**A**) or PKC $\epsilon$  adenovirus (MOI=3 pfu/cell) (**B**). After twenty-four h, cells were treated with PMA (1  $\mu$ M) or vehicle for 30 min in the presence of the PKC inhibitor GF109203X (5  $\mu$ M) and lysed. GST or GST-p23/Tmp21 proteins were precipitated with glutathione Sepharose 4B beads and associated HA- $\beta$ 2-chimaerin detected by Western blot using an anti-HA antibody. *Left panel*, representative experiments. *Right panel*, densitometric analysis of three individual experiments, expressed as fold-change relative to GST-p23/Tmp21 in the absence (**A**) or presence (**B**) of PMA. **C.** HeLa cells were co-transfected with either pEGFP-PKC $\epsilon$  or pEGFP- $\beta$ 2-chimaerin and pcDNA3.1/V5-p23/Tmp21 (full length). Forty-eight h later, cells were treated with PMA (1  $\mu$ M) or vehicle for 30 min, fixed, and stained with an anti-V5 antibody, and localization examined by confocal microscopy. *Upper panels*, green fluorescence from GFP-PKC $\epsilon$  or GFP- $\beta$ 2-chimaerin; *middle panels*, red fluorescence from pcDNA3.1/V5-p23/Tmp21; *lower panels*, overlapped images. Co-localization images and Pearson's correlation coefficient (Rr) were generated by Image J. Similar results were obtained in 3 additional experiments. *Bar*, 10  $\mu$ m.

**A****B**

**Figure 2.5** FBS and EGF enhance the association of  $\beta 2$ -chimaerin with p23/Tmp21. COS-1 cells were co-transfected with pEBG-p23/Tmp21 and GFP- $\beta 2$ -chimaerin, and 48 h later either serum-starved for 18 h and stimulated with EGF (100 ng/ml) or left in 10% FBS. GST-p23/Tmp21 was precipitated with glutathione Sepharose 4B beads and associated GFP- $\beta 2$ -chimaerin detected by Western blot using an anti-GFP antibody. A representative example is shown together with a densitometric analysis of 3 independent experiments. \*P<0.05 between control (0 min.) vs. treatments.

### **p23/Tmp21 depletion impairs perinuclear translocation of $\beta$ 2-chimaerin**

To determine the requirement of p23/Tmp21 for  $\beta$ 2-chimaerin translocation, we established p23/Tmp21-depleted HeLa cell lines using lentiviral shRNAs. Three different lentiviruses were used, and stable cell lines were generated after selection with puromycin. Figure 2.6A shows that a significant depletion (> 80%) was observed with shRNA p23/Tmp21 lentiviruses #2 and #3, while shRNA lentivirus #1 was less effective. GFP- $\beta$ 2-chimaerin was expressed in the different stable cell lines, and its localization in response to PMA was monitored using real-time microscopy. Figure 2.6B revealed that GFP- $\beta$ 2-chimaerin efficiently translocated to the perinuclear region (marked with an arrow at 30 min time point) in control cells, as expected. Likewise, perinuclear translocation was readily detected in cells infected with p23/Tmp21 shRNA lentivirus #1, in which depletion was minimal. In contrast, perinuclear translocation of GFP- $\beta$ 2-chimaerin was essentially lost in those cell lines in which p23/Tmp21 has been markedly depleted. GFP- $\beta$ 2-chimaerin co-localized with the Cis-Golgi marker GS-28 in the resting state, and PMA treatment enhanced co-localization (Figure 2.7). Translocation of PKC $\epsilon$  to the cell periphery by PMA was not affected by shRNA p23/Tmp21 depletion (data not shown). These results suggest that p23/Tmp21 is indispensable for the translocation of  $\beta$ 2-chimaerin to the perinuclear region.

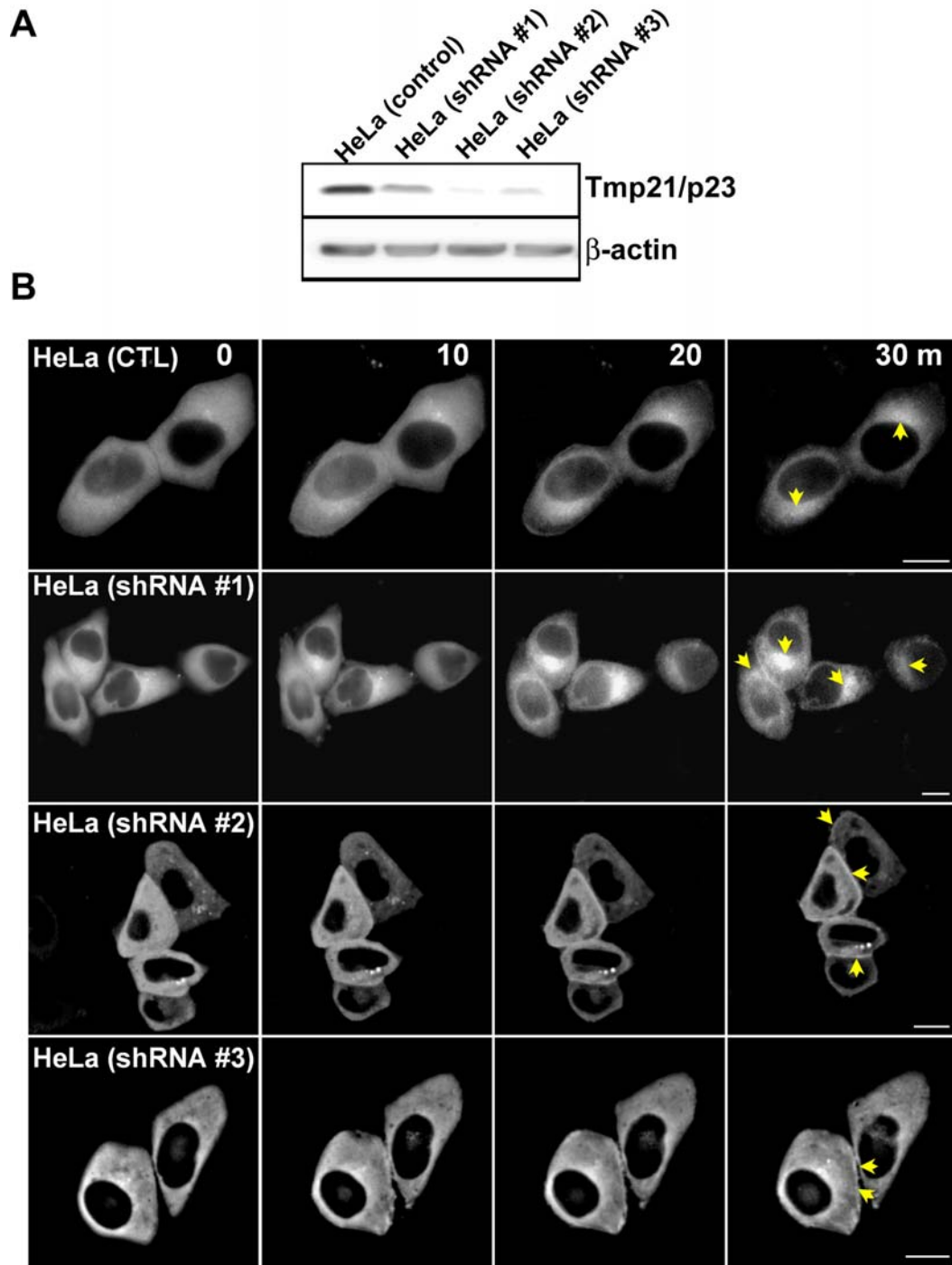


**Figure 2.6** *p23/Tmp21 RNAi depletion impairs perinuclear  $\beta$ 2-chimaerin translocation.* **A.** Expression of p23/Tmp21 in HeLa cells stably expressing different p23/Tmp21 shRNAs (shRNA#1, shRNA#2 and shRNA#3) or control cells. **B.** Cells were transfected with pEGFP- $\beta$ 2-chimaerin and 48 h later treated with PMA (3  $\mu$ M) in the presence of GF109203X (5  $\mu$ M). Time-lapse images of  $\beta$ 2-chimaerin translocation in living cells were captured at different times after PMA treatment. Perinuclear and periphery translocation were marked with arrows. Similar results were observed in 3 individual experiments. *Bar*, 10  $\mu$ m.

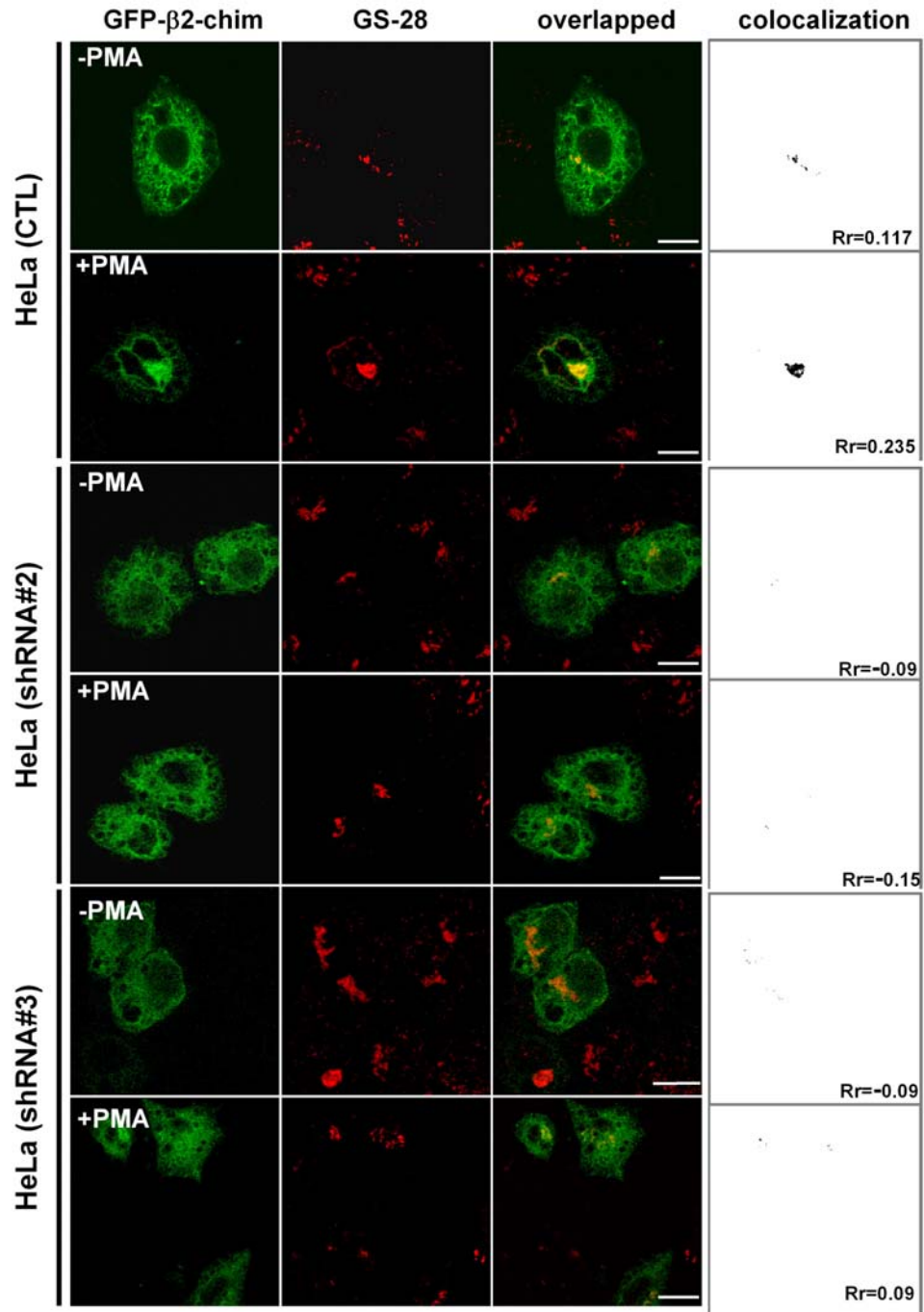


**Figure 2.7** Co-localization of β2-chimaerin with a Golgi marker. HeLa (CTL), HeLa (shRNA#2) or HeLa (shRNA#3) cells were transfected with pEGFP-β2-chimaerin and 48 h later treated with vehicle or PMA (3 μM) in the presence of GF109203X (5 μM). After 30 min., cells were fixed, stained with anti-GS28 cis-Golgi marker and examined by confocal microscopy. Co-localization images and Pearson's correlation coefficient (Rr) were generated by Image J. Similar results were observed in 3 separate experiments. *Bar*, 10 μm.

### **Glu227 and Leu248 in the $\beta$ 2-chimaerin C1 domain are critical for translocation to the perinuclear compartment**

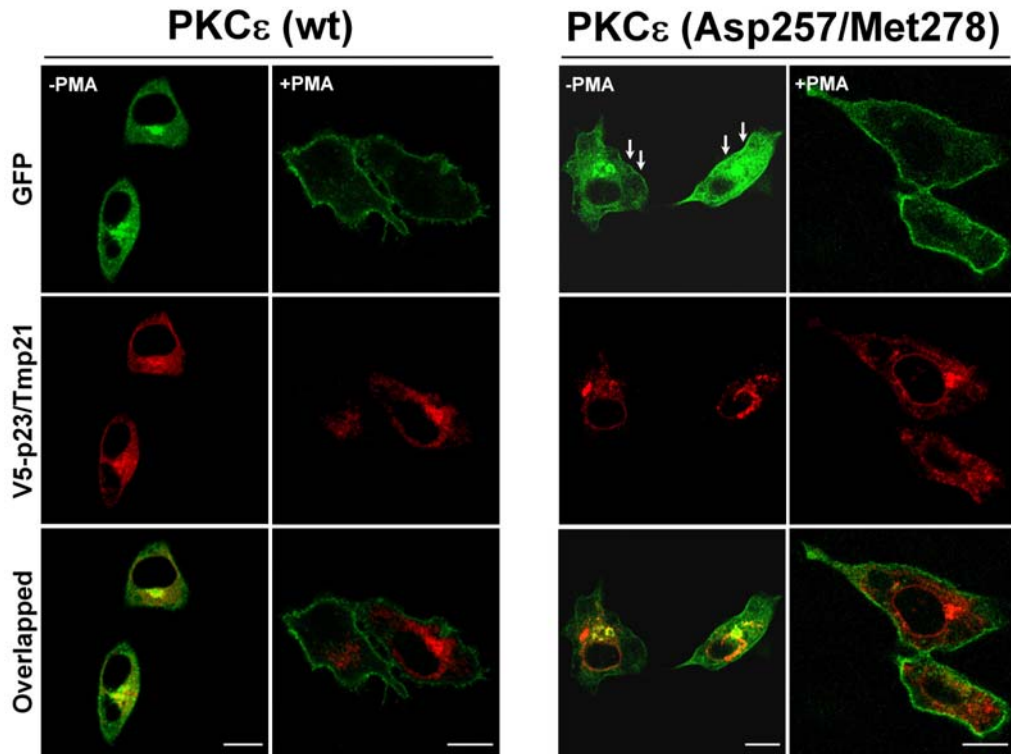
In a recent study, Schultz *et al.* showed that mutation of Asp257 and Met278 in the PKC $\epsilon$  C1b domain (amino acids 15 and 36 in the motif, respectively) abolished the perinuclear localization of PKC $\epsilon$  or its PKC $\epsilon$  C1b domain in neuroblastoma cells (153). We observed that when we mutated both Asp257 and Met278 to Gly in PKC $\epsilon$ , the resulting mutant localized to the plasma membrane even in the absence of PMA stimulation and does not co-localize with p23/Tmp21 (Figure 2.8). Alignment of C1 $\epsilon$ b with C1 domains from both  $\alpha$ - and  $\beta$ -chimaerins revealed that an acidic amino acid in position 15 and a lipophilic amino acid in position 36 of the motif were conserved (Figure 2.9A). We speculated that Glu227 and Leu248 in  $\beta$ 2-chimaerin might be implicated in perinuclear translocation. Mutants in those positions in  $\beta$ 2-chimaerin (E227G, L248A, and the double mutant E227G/L248A) were generated, expressed in HeLa cells as GFP-fused proteins, and their localization in real-time in response to PMA analyzed by microscopy. Single mutants E227G- and L248A- $\beta$ 2-chimaerin showed slightly higher translocation to the plasma membrane compared to wild-type  $\beta$ 2-chimaerin. However, perinuclear translocation after PMA treatment can still be observed. Conversely, no perinuclear translocation could be observed for the double mutant E227G/L248A- $\beta$ 2-chimaerin, while plasma membrane fluorescence was readily detected (Figure 2.9B; videos presented in Supplementary Information of MBoC paper, Figure 2.14). Therefore, residues in the  $\beta$ 2-chimaerin C1 domain homologous to those in C1 $\epsilon$ b play a significant role in targeting  $\beta$ 2-chimaerin to the perinuclear compartment.

## **The double mutant E227G/L248A-β2-chimaerin fails to interact with p23/Tmp21**

We speculated that the lack of perinuclear translocation of the double mutant E227G/L248A-β2-chimaerin by PMA was due to its inability to bind p23/Tmp21. We tested this hypothesis using a yeast two-hybrid assay. pLexA-fused constructs for E227G-, L248A-, and E227G/L248A-β2-chimaerin C1 domain mutants were generated (E227G-C1β2-ch, L248A-C1β2-ch, and E227G/L248A-C1β2-ch respectively). The pLexA plasmids were co-transformed with pB42AD-p23/Tmp21 into EGY48 (p8OP-LacZ) yeast. As shown in Figure 2.10A, single mutants E227G-C1β2-ch and L248A-C1β2-ch retained their ability to bind p23/Tmp21, as revealed by the induction of the LacZ reporter gene (blue). In contrast, the double mutant E227G/L248A-C1β2-ch was unable to interact with p23/Tmp21. A mutant with a Cys essential for C1 domain folding mutated to Ala (C246A-C1β2-ch) also failed to interact with p23/Tmp21, consistent with the lack of translocation of C246A-β2-chimaerin in PMA-treated cells (27, 181).

In the next experiments, we determined the association of GFP-β2-chimaerin mutants with p23/Tmp21 in COS-1 cells using a co-precipitation approach. Cells were co-transfected with pEBG (empty vector) or pEBG-p23/Tmp21, together with GFP-β2-chimaerin (wt), GFP-β2-chimaerin (E227G/L248A) or GFP-β2-

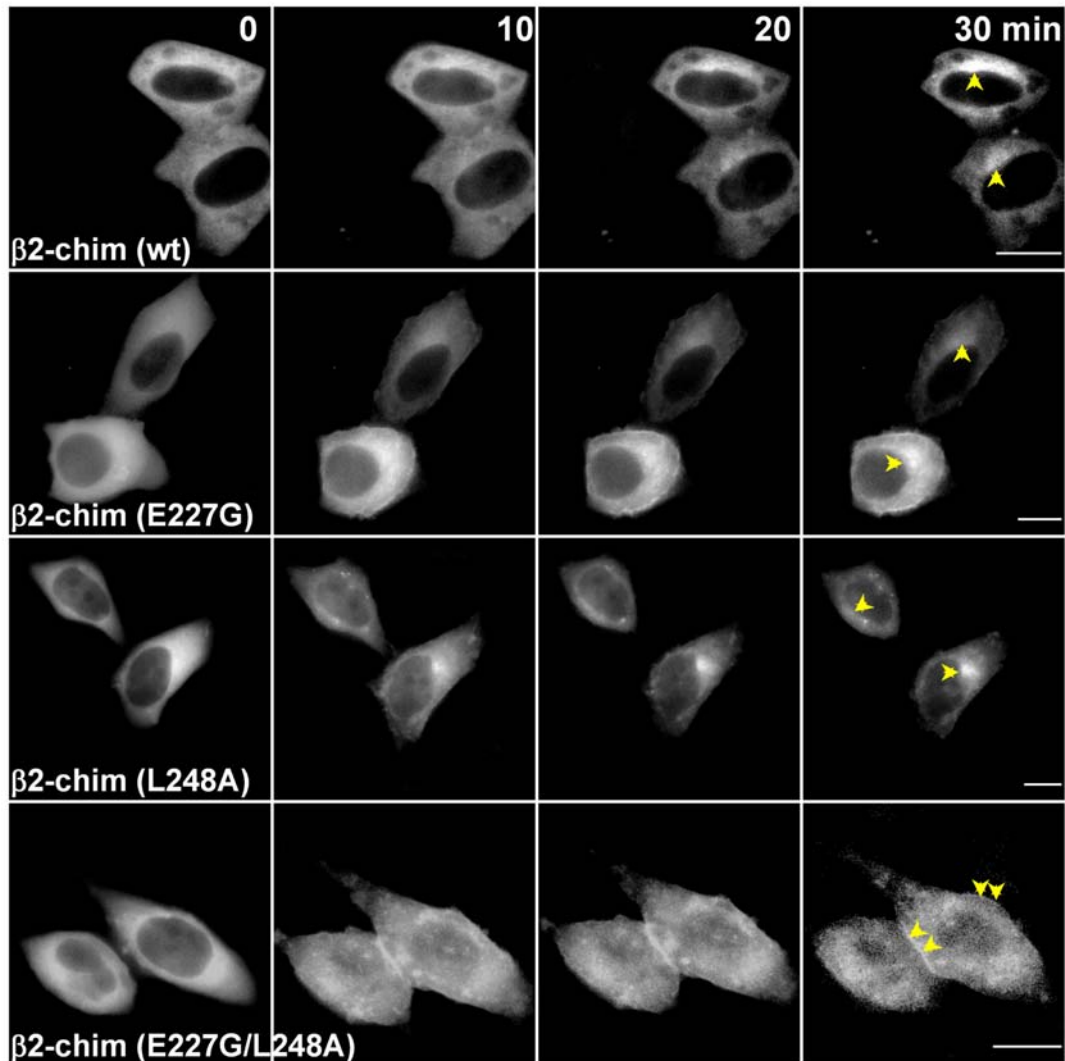




**Figure 2.8** *PKC $\epsilon$  (Asp257/Met278)* does not co-localize with *p23/Tmp21*. HeLa cells were co-transfected with either pEGFP-PKC $\epsilon$  (wt) or pEGFP-PKC $\epsilon$  (Asp257/Met278) and pcDNA3.1/V5-p23/Tmp21 (full-length). Forty-eight h later, cells were treated with PMA (1  $\mu$ M) or vehicle for 30 min, fixed, and visualized by confocal microscopy. *Upper panels*, green fluorescence from GFP-PKC $\epsilon$  or GFP-PKC $\epsilon$  (Asp257/Met278); *middle panels*, red fluorescence from pcDNA3.1/V5-p23/Tmp21; *lower panels*, overlapped images. *Bar*, 10  $\mu$ m. Similar results were obtained in 3 independent experiments. Peripheral localization is marked with arrows.

**A**

1	10	↓	20	30	↓	40	50	
HKFGIHNHYKVPTFCDHCGSLLWGLLRQGLQCKVKMNVHRRCEITNVAPNC								PKCε C1b
HNFKVHTFRGPHWCEYCANFMWGLIAQGVKCADCGLNVHKQCSKMPNDC								α-chimaerin C1
HNFKVHTFRGPHWCEYCANFMWGLIAQGVRCSDCGLNVHKQCSKHVPNDC								β-chimaerin C1

**B**

**Figure 2.9** *Glu227 and Leu248 in the β2-chimaerin C1 domain are required for perinuclear translocation.* **A.** Alignment of PKCε C1b and α- and β-chimaerin C1 domains. Positions 15 and 36 are indicated with an arrow. **B.** HeLa cells were transfected with pEGFP-β2-chimaerin (wt), pEGFP-β2-chimaerin (E227G), pEGFP-β2-chimaerin (L248A), or pEGFP-β2-chimaerin (E227G/L248A). Forty-eight h later, cells were treated with PMA (3 μM) in the presence of GF109203X (5 μM). Time-lapse images of translocation of GFP-β2-chimaerin or its mutants in living cells were captured by fluorescence microscopy at different times after PMA treatment. Perinuclear and periphery translocation were marked with arrows. Similar results were observed in 5 independent experiments. *Bar*, 10 μm.

chimaerin (C246A). After 36 h, cells were subject to a pull-down assay using glutathione Sepharose 4B beads. As shown in Figure 2.10B (*left panel*), while  $\beta$ 2-chimaerin (wt) was readily detected in complex with GST-p23/Tmp21, no co-precipitation was observed for  $\beta$ 2-chimaerin (E227G/L248A) or  $\beta$ 2-chimaerin (C246A). A quantitative analysis of multiple experiments is presented in Figure 2.10B (*right panel*).

Furthermore, imaging studies using confocal microscopy showed that while perinuclear translocation and co-localization with p23/Tmp21 in response to PMA could still be observed for full-length GFP- $\beta$ 2-chimaerin in which Glu227 and Leu248 have been mutated individually, the double mutant GFP-E227G/L248A- $\beta$ 2-chimaerin was unable to redistribute to the perinuclear compartment or to co-localize with p23/Tmp21 in cells (Figure 2.11). As also shown in Figure 2.9B, significant plasma membrane translocation could be detected with the double mutant. In agreement with previous studies (27, 181), the PMA-unresponsive mutant C246A- $\beta$ 2-chimaerin was unable to translocate in response to the phorbol ester.

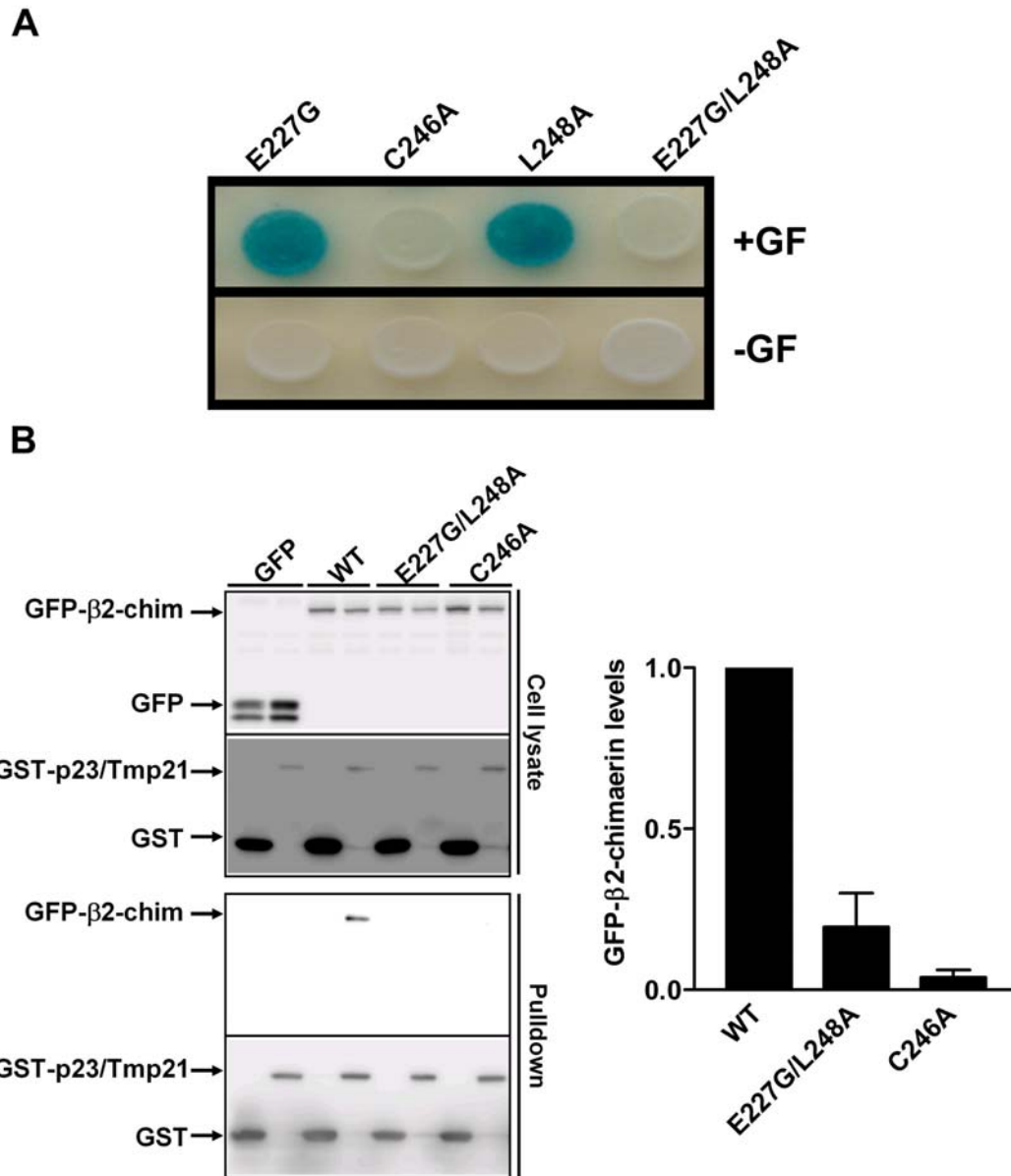


**Figure 2.10** *Glu227 and Leu248 residues in the  $\beta$ 2-chimaerin C1 domain are required for the interaction with p23/Tmp21.* **A.** EGY48 yeast (containing 8op-LacZ vector) was co-transformed with pLexA- $\beta$ 2-chim-C1 (E227G), pLexA- $\beta$ 2-chim-C1 (L248A), pLexA- $\beta$ 2-chim-C1 (E227G/L248A), or pLexA- $\beta$ 2-chim-C1 (C246A), and pB42AD-HA-tagged p23/Tmp21 (aa 108-208). Assay of  $\beta$ -galactosidase activity on induction (*upper panel*) or no-induction (*lower panel*) plates was carried out 72 h after transformation. *Gal/Raf*, galactosidase/raffinose. **B.** COS-1 cells were co-transfected with either pEBG (empty vector) or pEBG-p23/Tmp21 and GFP vector, GFP- $\beta$ 2-chimaerin (wt), GFP- $\beta$ 2-chimaerin (E227G/L248A) or GFP- $\beta$ 2-chimaerin (C246A). After twenty-four h, cells were lysed. GST or GST-p23/Tmp21 proteins were precipitated with glutathione Sepharose 4B beads and associated GFP-fused proteins detected by Western blot using an anti-GFP antibody. *Left panel*, representative experiments. *Right panel*, densitometric analysis of three individual experiments, expressed as fold-change relative to GST-p23/Tmp21 bound  $\beta$ 2-chimaerin (wt).

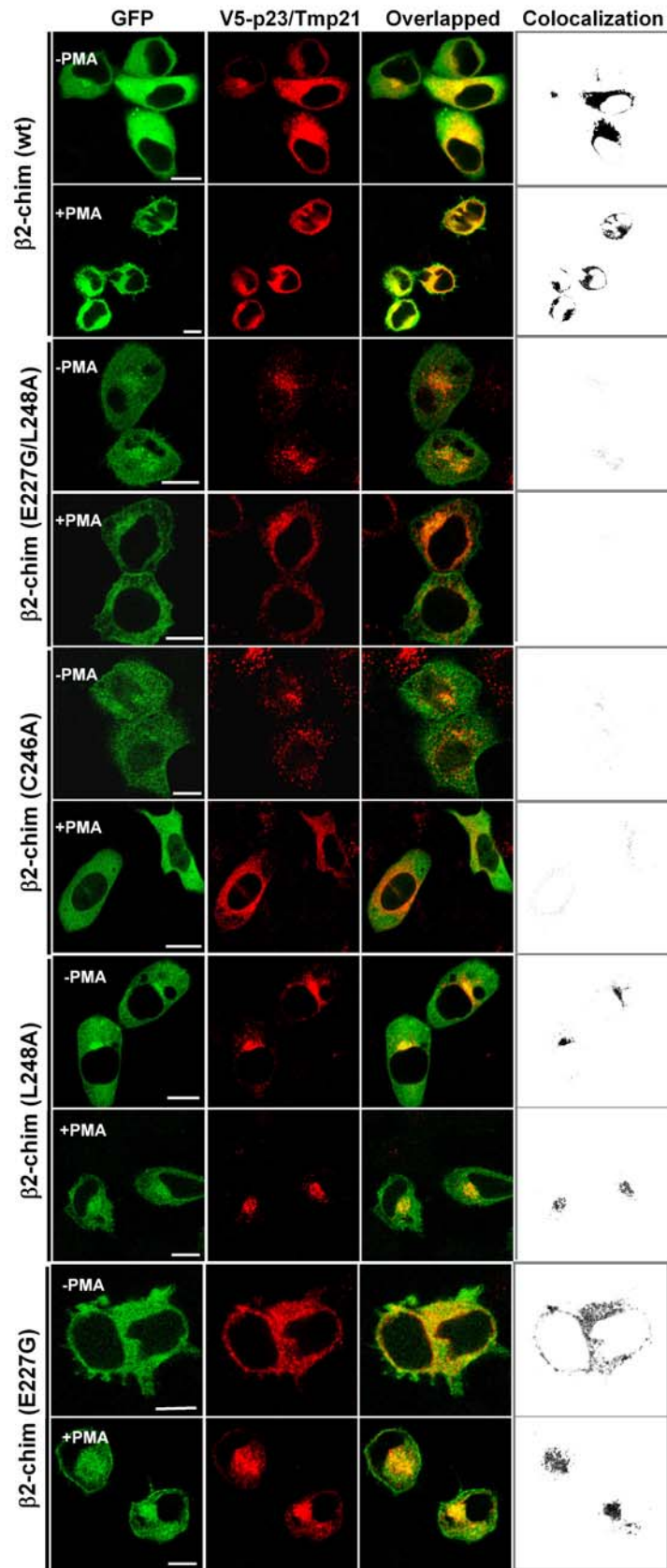


**Figure 2.11** *Co-localization studies of  $\beta$ 2-chimaerin mutants and p23/Tmp21.* HeLa cells were co-transfected with pEGFP- $\beta$ 2-chim (wt), pEGFP- $\beta$ 2-chim (C246A), pEGFP- $\beta$ 2-chim (E227G), pEGFP- $\beta$ 2-chim (L248A), or pEGFP- $\beta$ 2-chim (E227G/L248A) and V5-tagged pcDNA-p23/Tmp21. Forty-eight h later, cells were treated with PMA (3  $\mu$ M) or vehicle for 30 min in the presence of GF 109203X (5  $\mu$ M). Cells were then washed and visualized by confocal microscopy. *Left panel*, green fluorescence from GFP- $\beta$ 2-chimaerin (wild-type or mutants); *middle panels*, red fluorescence from pcDNA3.1/V5-p23/Tmp21; *right panels*, overlapped images. *Far right panels*, co-localization images generated by Image J. Similar results were obtained in 3 different experiments. *Bar*, 10  $\mu$ m.

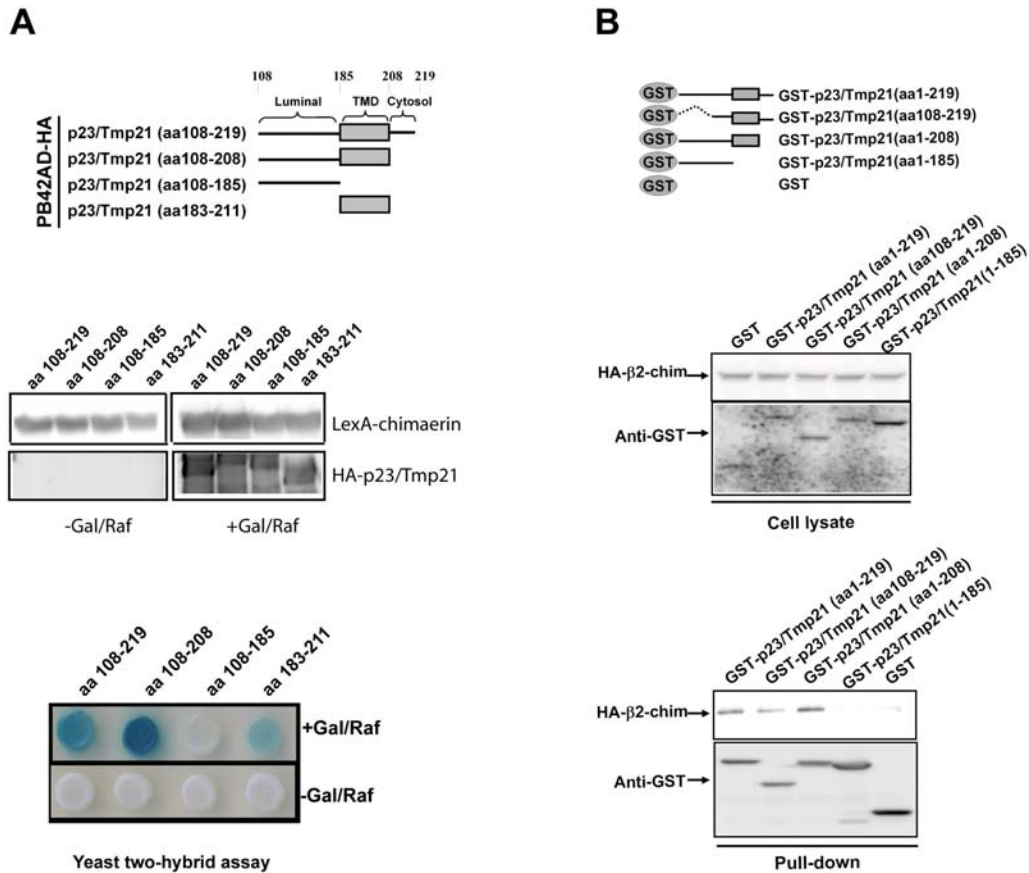
### Identification of the chimaerin binding domain in p23/Tmp21

In the next set of experiments we mapped the domain in p23/Tmp21 that interacts with the C1 domain in chimaerins using a yeast two-hybrid approach. p23/Tmp21 comprises a luminal domain and a short cytoplasmatic tail linked by a transmembrane domain. Deletions for each domain were generated, and the corresponding deleted mutants subcloned into pB42AD-HA as shown in Figure 2.12A (*upper panel*). EGY48 (p8OP-LacZ) yeast was co-transformed with either mutant together with pLexA- $\alpha$ -chimaerin (aa 1-147) (it has similar interacting properties as the  $\beta$ -isoforms) and proteins expressed in Gal/Raf plates (Figure 2.12A, *middle panel*). A strong interaction could be detected even when the cytosolic tail ( $\Delta$ 208-219) was deleted. On the other hand, deletion of amino acids 185-208, which correspond to the transmembrane domain, impaired the association. Expression of the transmembrane domain alone was sufficient to observe interaction (Figure 2.12A, *lower panel*). A  $\beta$ -galactosidase liquid assay also revealed that the transmembrane domain alone interacts with chimaerin (data not shown). These results were confirmed using a co-precipitation approach. Deletion mutants were generated and subcloned into pEBG vector (Figure 2.12B, *upper panel*). GST or GST-fused p23/Tmp21 mutants were mixed with COS-1 cell lysates expressing HA- $\beta$ 2-chimaerin (Figure 2.12B, *middle panel*). While association of GST-p23/Tmp21 (aa 1-219; aa108-219; aa 1-208) with HA- $\beta$ 2-chimaerin was readily detected, GST-p23/Tmp21 (aa 1-185), which has the transmembrane domain deleted, failed to associate with  $\beta$ 2-chimaerin (Figure 2.12B, *lower panel*). These results suggest that p23/Tmp21 transmembrane domain is implicated in the interaction.

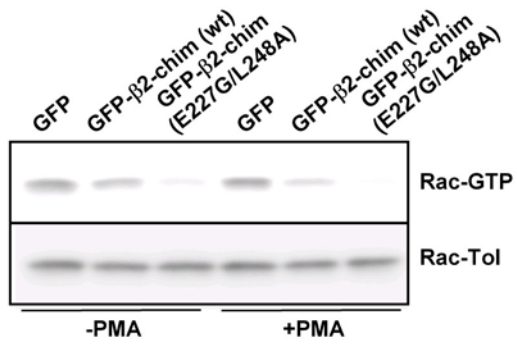
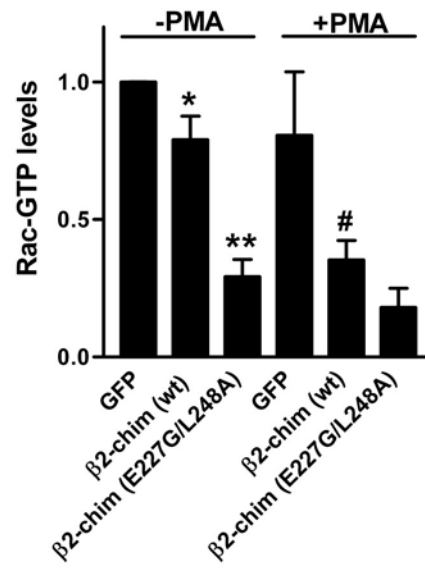
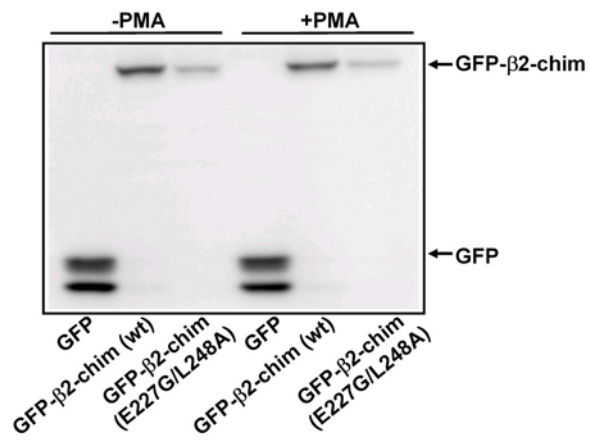
### **Disruption of the $\beta$ 2-chimaerin-p23/Tmp21 complex leads to enhanced $\beta$ 2-chimaerin Rac-GAP activity**

We have previously shown that the expression levels of p23/Tmp21 may influence the ability of  $\beta$ 2-chimaerin to regulate Rac-GTP (active) levels (181). Conceivably, when complexed with p23/Tmp21,  $\beta$ 2-chimaerin cannot access the plasma membrane to inactivate Rac. It is still elusive whether disruption of the  $\beta$ 2-chimaerin-p23/Tmp21 complex affects  $\beta$ 2-chimaerin Rac-GAP activity. We predicted that dissociation of this complex should result in enhanced availability of  $\beta$ 2-chimaerin for Rac inactivation. To address this issue, we compared the Rac-GAP activity of  $\beta$ 2-chimaerin (wild-type) and E227G/L248A- $\beta$ 2-chimaerin in COS-1 cells using a PBD pull-down assay. As shown in Figure 2.13, the double mutant is more active as a Rac-GAP than wild-type- $\beta$ 2-chimaerin is when expressed at comparable levels. PMA significantly enhanced Rac-GAP activity of wild-type  $\beta$ 2-chimaerin. These results suggest that binding of  $\beta$ 2-chimaerin to p23/Tmp21 limits the availability of this Rac-GAP for inhibiting Rac activity.





**Figure 2.12** Identification of the  $\beta$ 2-chimaerin C1 domain interacting region in p23/Tmp21. EGY48 yeast (containing 8op-LacZ vector) was co-transformed with pLexA-fused  $\alpha$ 1-chimaerin (aa 1-147) (181) and pB42AD-HA-tagged p23/Tmp21 truncated mutants. **A**. *Upper panel*, schematic representation of p23/Tmp21 constructs used in the yeast two-hybrid assay. *Middle panel*, chimaerin expression in yeast lysates, as determined by Western blot using an anti-pLexA antibody; and expression of p23/Tmp21 truncated proteins in yeast lysates using an anti-HA antibody. *Lower panel*, assay of  $\beta$ -galactosidase activity on induction or no-induction plates, carried out 72 h after transformation. *Gal/Raf*, galactosidase/raffinose. **B**. COS-1 cells were transfected with either pEBG (empty vector) or pEBG-p23/Tmp21, and infected with a HA- $\beta$ 2-chimaerin adenovirus (MOI=10 pfu/cell). Thirty-six h later, GST or GST-p23/Tmp21 proteins were precipitated with glutathione Sepharose 4B beads and associated HA- $\beta$ 2-chimaerin detected by Western blot using an anti-HA antibody. *Upper panel*, schematic representation of GST-p23/Tmp21 constructs used in the co-precipitation assays. *Middle panel*, expression of GST-p23/Tmp21 or its mutants and HA- $\beta$ 2-chimaerin in cell lysates. *Lower panel*, associated HA- $\beta$ 2-chimaerin and GST-p23/Tmp21 or its mutants in pull-down assay were detected by Western blot using anti-HA and anti-GST antibody respectively. Similar results were observed in two additional experiments.

**A****B****C**

**Figure 2.13** *Disruption of  $\beta$ 2-chimaerin-p23/Tmp21 interaction leads to enhanced  $\beta$ 2-chimaerin Rac-GAP activity.* **A.** COS-1 cells were transfected with pEGFP, pEGFP- $\beta$ 2-chimaerin (wt), or pEGFP- $\beta$ 2-chimaerin (E227G/L248A). Forty-eight h later, Rac-GTP levels were assayed using a GST-PBD pull-down assay. **B.** Densitometric analysis of Rac-GTP levels relative to control (GFP alone). Data are expressed as mean  $\pm$  S.E. of 5 independent experiments. \* $p < 0.05$  between GFP vs. GFP- $\beta$ 2-chim (wt); \*\* $p < 0.01$  between GFP- $\beta$ 2-chim (wt) vs. GFP- $\beta$ 2-chim (E227D/L248A). # $p < 0.01$  between GFP- $\beta$ 2-chim (wt) (-PMA) vs. GFP- $\beta$ 2-chim(wt) (+PMA). **C.** Western blot show GFP, GFP- $\beta$ 2-chim (wt) and GFP- $\beta$ 2-chim (E227D/L248A) protein expression.

Videos can be viewed at: <http://www.molbiolcell.org/cgi/content/full/E09-08-0735/DC1>

**Figure 2.14** *Videos for translocation experiments in Figure 2.9.* Time-lapse images of translocation of GFP- $\beta$ 2-chimaerin or its mutants in living cells were captured by fluorescence microscopy at different time points after PMA treatment. AVI files (movies) were made using Northern Eclipse software (version 6.0).

## **DISCUSSION**

In this Chapter we showed that p23/Tmp21 is an anchoring protein for the Rac-GAP  $\beta$ 2-chimaerin and is required for its translocation to the perinuclear compartment. The interaction is mediated through the  $\beta$ 2-chimaerin C1 domain. Interestingly, we found that C1 domains from other proteins, such as the second C1 domain of PKC $\epsilon$  (C1 $\epsilon$ b), have the ability to interact with p23/Tmp21. However, a comparative analysis between  $\beta$ 2-chimaerin and PKC $\epsilon$  suggests that p23/Tmp21 plays differential roles in targeting C1 domain-containing proteins, as only the former interacts with p23/Tmp21 in response to phorbol ester activation. We also identified key amino acids in the  $\beta$ 2-chimaerin C1 domain required for the interaction that when mutated prevent the formation of the complex.

### **C1 domains as targeting modules**

It is well established that C1 domains play a fundamental role in targeting PKC isozymes and other molecules from the cytosol to membranes both in response to phorbol esters or DAG generated upon receptor activation (42). For classical and novel PKCs, this membrane targeting is essential for allosteric activation. C1 domains in other phorbol ester/DAG receptors also play key roles in translocation, as it has been extensively demonstrated for PKDs, RasGRPs, and chimaerin Rac-GAPs. X-Ray crystallography studies of the C1b domain of PKC $\delta$  established that it is constituted of two  $\beta$  sheets and a small  $\alpha$  helix at the end of the C-terminus. The  $\beta$  sheets form a pocket where phorbol esters and DAG bind (201). Modeling analysis revealed that all C1 domains including those in chimaerins, have remarkable

structural resemblance (26). The C1 domain in  $\alpha$ - and  $\beta$ -chimaerins binds phorbol esters and DAG analogs with affinities similar to PKC C1 domains and utilizes similar mechanisms for insertion into lipid bilayers (26). It is remarkable, however, that individual C1 domains from phorbol ester/DAG receptors have quite distinct properties for ligand recognition and localize to entirely different compartments when expressed in cells. Various examples of differential ligand affinities have been reported for C1a and C1b domains in PKC isozymes. For example, a study showed that while in PKC $\delta$  the C1a domain preferentially binds DAG, the C1b domain has higher affinity for phorbol esters (166). Site-directed mutagenesis of individual C1 domains in PKCs has also established distinct roles in translocation, and it was suggested that this disparity relates to a differential exposure of C1a and C1b domains (148). The non-equivalency of C1 domains in PKCs is also exemplified by their differential ability to localize to the Golgi complex: while isolated C1a domains generally localize throughout the cell rather than specifically in the perinuclear region, C1b domains of cPKCs and nPKCs show co-localization with a Golgi marker (153), as we have also demonstrated for full-length  $\beta$ 2-chimaerin and its isolated C1 domain (27), and brefeldin can disrupt their localization (111). In PKDs, a family of PKC-related kinases, C1a and C1b domains also have differential biochemical and targeting properties (36, 109). Altogether, this suggests that mechanisms alternative or in addition to ligand binding may account for the selective intracellular compartmentalization.

Growing evidence suggests that C1 domains in PKCs and PKDs act as protein-interaction modules that regulate their cellular localization and/or activation. For

example, the C1b domain of PKC $\alpha$  interacts with the cell matrix protein fascin, and disruption of this interaction affects cell motility (4). 14-3-3 $\tau$  binding sites have been identified within the C1b domain of PKC $\gamma$  (135). The association between the PKD1 C1 domain and 14-3-3 $\tau$  in T cells negatively regulates PKD1 (78). The recent identification of a 20 amino acid module in PKC $\epsilon$  that directs localization to cell-cell contacts via protein-protein interaction is another remarkable example (51). The PKC $\epsilon$  C1b binds to peripherin to induce its aggregation, leading to apoptosis in neuroblastoma cells (169). Localization of PKC $\beta$ II to centrosomes is mediated by the scaffolding protein pericentrin and involves the PKC $\beta$ II C1a domain, and dissociation of this complex impairs spindle formation and cell division (34). Newton and co-workers identified a novel E3 ubiquitin ligase that interacts with the C1a domain of PKC $\beta$ II (33).

The identification of p23/Tmp21 as a  $\beta$ 2-chimaerin interactor allowed us to postulate an anchoring role for this Golgi protein. In this study we showed that RNAi depletion of p23/Tmp21 prevents the translocation of  $\beta$ 2-chimaerin to the perinuclear region, an indication that binding to p23/Tmp21 is a requisite for relocalization. Deletion of the C1 domain in  $\beta$ 2-chimaerin prevents  $\beta$ 2-chimaerin interaction with p23/Tmp21 (181), and this is also supported by the failure of the C1 domain mutant C246A- $\beta$ 2-chimaerin to associate with p23/Tmp21 observed in the present study. We also investigated the role of two highly conserved amino acids in the C1b domains of PKCs. Previous studies by Schultz *et al.* showed that Asp257 and Met278 in PKC $\epsilon$  (positions 15 and 36 in the C1 domain consensus) or the equivalent residues in PKC $\theta$  (Glu246 and Met267) are required for Golgi targeting (153). Like PKC C1b domains,

the C1 domain in  $\beta$ 2-chimaerin possesses an acidic residue in position 15 (Glu227) and a hydrophobic residue in position 36 (Leu248). We found that mutation of both residues abolishes perinuclear translocation of  $\beta$ 2-chimaerin. It is unclear why single mutants were not as effective, but Shultz *et al.* also described similar results for single mutants in PKC $\theta$  (153). It is interesting that, unlike  $\beta$ 2-chimaerin, PKC $\epsilon$  loses its perinuclear localization in response to PMA and mobilize to a peripheral compartment. Most likely the forces that drive membrane translocation are sufficiently strong to overcome the PKC $\epsilon$ -p23/Tmp21 interaction. The C1a domain in PKC $\epsilon$  may suffice to drive plasma membrane localization, as the tandem C1a-C1b domain mobilizes to the plasma membrane in response to PMA (data not shown). In addition to its perinuclear relocalization,  $\beta$ 2-chimaerin translocates to the plasma membrane in response to stimuli (184). It remains to be determined whether signals could lead to the dissociation of the complex and release  $\beta$ 2-chimaerin to make it available for membrane translocation or whether different intracellular pools that respond differentially to stimuli exist. The ability of chimaerins to interact with other proteins independently of the C1 domain (Colon-Gonzalez, H.W., and M.G.K., manuscript in preparation) clearly suggests complex regulatory mechanisms controlling relocalization and activation of this family of Rac-GAPs.

A key finding was the identification of amino acids 15 and 36 in the C1 domain consensus as essential for the interaction with p23/Tmp21. Mutation of both residues in  $\beta$ 2-chimaerin impairs the interaction with p23/Tmp21 in a yeast two-hybrid assay. Likewise, mutation of amino acids Asp257 and Met258 in PKC $\epsilon$  leads to dissociation of this kinase from the perinuclear compartment (see Figure 2.8). The differential



interaction of PKCε C1a and C1b domains with p23/Tmp21 may also reflect the differences in amino acids present in those positions (Ser and Cys in C1a). While at the present time there is no structural information on the C1 domain-p23/Tmp21 interaction, 3D studies clearly showed that amino acids in position 15 and 36 are in close proximity and possibly not inserted into the membrane bilayer (153, 201), thus making them available for interactions with other partners.

### **p23/Tmp21 as an anchoring protein for β2-chimaerin**

p23/Tmp21 is a type I protein belonging to the p24 family that has a receptor-like luminal domain and a short cytoplasmatic tail. Members of the p24 family have been widely implicated as coat protein (COP) vesicle cargo receptors, and they participate in COP vesicle budding and the organization of the Golgi apparatus. The cytoplasmic tail of p23/Tmp21 carries motifs that bind to COPI, and this association is crucial for the retention and retrieval of cargo proteins in the early secretory pathway (65). Our deletional analysis revealed that this C-terminal tail is not involved in binding to chimaerins. Despite multiple studies implicating p24 proteins in vesicle trafficking, insights into the actual function of p23/Tmp21 remain elusive. Recent studies have established that p23/Tmp21 is a component of the presenilin complex that modulates γ-secretase activity (35). p23/Tmp21 can also localize in post-Golgi compartments and even traffic to the plasma membrane (17). In addition, emerging evidence suggests that p23/Tmp21 is implicated in the regulation of small GTPase function. Studies identified a mechanism of recruitment of the small GTPase ARF1 (ADP-ribosylation factor 1) to the Golgi via p23/Tmp21 (65, 112). More recently, studies

found that ARF1-dependent assembly of actin in the Golgi apparatus may involve Cdc42/Rac and is dependent on p23/Tmp21 (57). While early studies showed that Rac1 is present in the perinuclear region, primarily in an inactive GDP-bound state (95), functional studies on perinuclear Rac are scarce. Moreover, it is unclear what the relative contribution of this perinuclear-associated Rac is to the pool of active plasma membrane Rac generated in response to stimuli. It may be possible that recruitment of chimaerin Rac-GAPs via p23/Tmp21 contributes to the maintenance of the perinuclear Rac inactive pool. There is a precedent for the interaction of endogenous Rac and a Rac-GAP protein, OCRL1, at the trans-Golgi network, however the mechanisms involved in targeting these proteins to the perinuclear region are yet to be established.

### **Conclusion of Chapter 2**

We identified p23/Tmp21 as an anchoring protein for  $\beta$ 2-chimaerin via its C1 domain. Depletion of p23/Tmp21 from cells leads to reduced perinuclear translocation of  $\beta$ 2-chimaerin, suggesting that when complexed with p23/Tmp21 its availability to mobilize to the plasma membrane and inactivate Rac is limited. Our studies also provide evidence for a marked selectivity of C1 domains for binding to p23/Tmp21, as some C1 domains from PKC isozymes and potentially other phorbol ester/DAG receptors have the ability to bind p23/Tmp21. In the case of PKC $\epsilon$  it seems that p23/Tmp21 anchors this kinase via the C1b domain and that the PKC $\epsilon$ -Tmp21 complex dissociates in response to stimuli. Whether this is also true for other PKC isozymes or phorbol ester/DAG receptors such as PKD and RasGRP isozymes

remains to be determined. In summary, the ability of C1 domains to dictate intracellular localization via protein-protein interactions expands our view that these domains act solely as lipid-binding motifs and highlight the complexity of DAG signaling.

## **MATERIALS AND METHODS**

*Materials-* PMA and GF109203X were purchased from LC Laboratories (Woburn, MA). Cell culture reagents were obtained from Invitrogen (Carlsbad, CA). Reagents for the expression and purification of recombinant glutathione S-transferase (GST)-fusion proteins and glutathione Sepharose 4B beads were purchased from GE Healthcare (Piscataway, NJ). COS-1 and HeLa cells were obtained from the American Type Culture Collection (ATCC, Manassas, VA). Yeast strain EGY48, and yeast culture reagents and media were obtained from Clontech Laboratories, Inc. (Mountain View, CA). ONPG (*O*-nitrophenyl- $\beta$ -D-galactopyranoside) and MISSION<sup>®</sup> Lentiviral Transduction shRNAs particles were obtained from Sigma (St. Louis, MO). The following primary antibodies were used: anti-pLexA (Santa Cruz, CA), anti- $\beta$ -actin (Sigma), anti-V5 (Invitrogen), anti-p23/Tmp21 (ProSci Incorporated, Poway, CA), anti-GST, anti-HA and anti-GFP (Covance, Emeryville, CA), anti-Rac1 (Millipore, Billerica, MA), anti-PKC $\epsilon$  (Cell Signaling, Danvers, MA), and anti-GS28 (BD Biosciences, San Jose, CA).

*Plasmid construction-* Generation of pB42AD-p23/Tmp21 (amino acid (aa) 108-219), pEBG-p23/Tmp21 (aa 1-219) and pEBG-p23/Tmp21 (aa 108-219) are described elsewhere (181). Truncated p23/Tmp21 mutants were generated by PCR and subcloned into *EcoRI-XhoI* sites in pB42AD-HA vector or *BamHI /SpeI* sites in pEBG vector. C1 regions from PKC $\epsilon$ , PKC $\zeta$  and  $\beta$ 2-chimaerin were isolated by PCR and fragments subcloned into *EcoRI-BamHI* sites in pLexA to generate pLexA-C1 $\epsilon$ a-

b (aa 134-309), pLexA-C1 $\zeta$  (aa 95-197), and pLexA-C1 $\beta$ 2-ch (aa 179-281), respectively. C1 domain fragments were also subcloned into *EcoRI-BamHI* sites in pEGFP-C1 to generate pEGFP-C1 $\epsilon$ a-b, pEGFP-C1 $\zeta$ , and pEGFP-C1 $\beta$ 2-ch. Individual C1a and C1b domains from PKC $\epsilon$  (comprising aa 168-222 and aa 241-294, respectively) were subcloned into *EcoRI-BamHI* sites in pEGFP-C1 and pLexA to generate pEGFP-C1 $\epsilon$ a, pEGFP-C1 $\epsilon$ b, pLexA-C1 $\epsilon$ a, and pLexA-C1 $\epsilon$ b. The primers used for PCR cloning are listed in [Table 2-1](#). All constructs were confirmed by sequencing.

*Site-directed mutagenesis-* For PCR-based mutagenesis we employed the QuikChange® XL Site-Directed Mutagenesis Kit (Stratagene, La Jolla, CA), using GFP- $\beta$ 2-chimaerin, GFP-C1 $\beta$ 2-ch, or pLexA-C1 $\beta$ 2-ch as templates. For the mutant E227G- $\beta$ 2-chimaerin we used the following primers (mutated nucleotides are underlined):

forward, 5'-  
CGAGGCCACACTGGTGTGGATATTGTGCCAATTCATG; reverse, 5'-  
CATGAAATTGGCACAATATCCACACCAGTGTGGGCCTCG. For the mutant L248A- $\beta$ 2-chimaerin we used:

forward, 5'-  
GTCCGGTGCTCAGACTGTGGAGCTAACGTACACAAACAG; reverse, 5'-  
CTGTTTGTGTACGTTAGCTCCACAGTCTGAGCACCGGAC. For PKC $\epsilon$  (E257G) we used:

forward, 5'-  
GGTCCCACGTTCTGTGGCCACTGTGGGTCCCTGC; reverse, 5'-  
GCAGGGACCCACAGTGGCCACAGAACGTGGGGACC. For PKC $\epsilon$  (M278G) we used:

forward, 5'-

GCAGTGTAAGTCTGCAAAGGGAATGTTACACCGTCGATGTG; reverse, 5'-CACATCGACGGTGAACATTCCCTTTGCAGACTTTACACTGC.

*Cell culture, transfections, and adenoviral infections-* HeLa and COS-1 cells were cultured in Dulbecco's modified Eagle's medium (Invitrogen) supplemented with 10% fetal bovine serum (Cyclone), 100 units/ml penicillin, and 100 µg/ml streptomycin in a humidified 5% CO<sub>2</sub> atmosphere at 37 °C. Cells in 6-well plates at ~50% confluence were transfected with different mammalian expression vectors (1 µg) using Lipofectamine 2000 (Invitrogen) following the manufacturer's protocol. Adenoviral infections were carried out essentially as previously described (101).

*Generation of p23/Tmp21-depleted cell lines using shRNA lentiviruses-* HeLa cells were infected with 3 different MISSION<sup>®</sup> Lentiviral Transduction particles encoding p23/Tmp21 shRNAs. p23/Tmp21 shRNA target sequences were as follows: #1, CCGGGAGATTCACAAGGACCTGCTACTCGAGTAGCAGGTCCTTGTGAATC TCTTTTT; #2, CCGGCCAACTCGTGATCCTAGACATCTCGAGATGTCTAGGATCACGAGTT GGTTTTT. #3, CCGGCGCTTCTTCAAGGCCAAGAACTCGAGTTTCTTGGCCTTGAAGAAG CGTTTTT; Stable cell lines (pools) were generated by selection with puromycin (1 µg/ml).

*Yeast two-hybrid assay-* pLexA expression vectors, which contain a *His* marker, were co-transformed into the yeast strain EGY48 together with pB42AD-HA-tagged expression vectors, which have a *Trp* marker, and the p8OP-LacZ reporter vector (*Ura* marker). Transformants were plated on yeast dropout medium lacking *Trp*, *Ura*, and *His*, thereby selecting for the plasmids encoding proteins capable of two-hybrid interaction as evidenced by transactivation of the LacZ reporter gene (181).

For  $\beta$ -galactosidase liquid assays, yeast was cultured in galactose/raffinose/-His/-Ura/-Trp liquid SD selection medium until the cells were in mid-log phase (OD600 = 0.5-0.8). Cells were pelleted at 14,000 x g for 30 sec, and resuspended in 300  $\mu$ l of a buffer (pH 7.0) containing 60 mM Na<sub>2</sub>HPO<sub>4</sub>, 40 mM NaH<sub>2</sub>PO<sub>4</sub>.H<sub>2</sub>O, 10 mM KCl, 1 mM MgSO<sub>4</sub>, and 0.27% (v/v)  $\beta$ -mercaptoethanol. One hundred  $\mu$ l of the cell suspension were then frozen and thawed 3 times in liquid nitrogen and a 37°C water bath, respectively, and additional 700  $\mu$ l of resuspension buffer were added. ONPG was then added (final concentration: 670  $\mu$ g/ml), and the reaction initiated by addition of Na<sub>2</sub>CO<sub>3</sub> (final concentration: 300  $\mu$ g/ml).  $\beta$ -galactosidase activity was determined as previously determined (181). One unit of  $\beta$ -galactosidase activity is defined as the amount that hydrolyzes 1  $\mu$ mol of ONPG to o-nitrophenol and D-galactose per min and per cell.

*Immunostaining and confocal microscopy-* Plasmids encoding for full-length PKC $\epsilon$  or  $\beta$ 2-chimaerin together with p23/Tmp21 in V5 epitope-tagged pcDNA3.1 were co-transfected into HeLa cells using Lipofectamine 2000. After 24 h, cells were treated with PMA for 30 min, washed twice with PBS, and fixed with 4% paraformaldehyde

for 20 min at room temperature. After washing once with PBS containing 0.5% SDS and 5%  $\beta$ -mercaptoethanol (37°C, 30 min), and twice with PBS alone, cells were incubated with an anti-V5 monoclonal antibody (1:500). A donkey anti-mouse antibody conjugated with Cy3 was used as secondary antibody (1:1,000). Slides were mounted using Fluoromount-G (SouthernBiotech, Birmingham, AL) and viewed with a Carl Zeiss LSM 710 laser scanning microscope. The confocal images were processed with LSM Image Browser. All the images shown are individual middle sections of projected Z-series mounting. For quantification, images (RGB) from Red and Green channels were converted into 8-bits images in ImageJ and the Pearson's correlation coefficient ( $R_r$ ) calculated using this software.

*Time-lapse microscopy*- HeLa cells were seeded into glass-bottomed culture dishes (MatTek, Ashland, MA) for 20 h. pEGFP-PKC $\epsilon$  or pEGFP- $\beta$ 2-chimaerin plasmids (wild-type or mutants) were transfected using Lipofectamine 2000 according to the manufacturer's protocols. Cells were cultured for 20 h in Phenol red-free RPMI-1640 medium containing 10% FBS and 5 mM HEPES. Cells were monitored under a fluorescence microscope (Nikon Eclipse TE2000U) at a 488 nm excitation wavelength with a 515 nm-long pass barrier filter at 25°C.

*Co-precipitation using glutathione Sepharose 4B beads*- COS-1 cells at ~50% confluency were co-transfected with pEBG-p23/Tmp21 (full-length) or empty vector (pEBG). After 24 h, cells were washed twice with cold PBS, and then lysed for 10 min at 4°C in 400  $\mu$ l of a lysis buffer containing 50 mM Tris-HCl, pH



7.5, 150 mM NaCl, 1% Nonidet P-40, 0.5% deoxycholate, 0.1% SDS, and protease inhibitor cocktail (Sigma). Ten  $\mu$ l of glutathione Sepharose 4B beads were added to the lysate and incubated for 1 h at 4°C. The beads were extensively washed in lysis buffer and boiled. Samples were resolved in a 12% SDS-polyacrylamide gel and transferred to a polyvinylidene difluoride membrane (Millipore Co., Bedford, MA) for Western blot analysis.

*In vitro protein-protein binding assay-* Cell lysates were prepared from COS-1 cells expressing pEBG, pEBG-p23/Tmp21 (aa 1-219), pEBG-p23/Tmp21 (aa 1-208), pEBG-p23/Tmp21 (aa 108-219) or pEBG-p23/Tmp21 (aa 1-185). A fixed amount of GST or GST-fused p23/Tmp21 (wild-type or truncated mutants) were incubated with lysates of COS-1 cells expressing HA- $\beta$ 2-chimaerin at 4°C for 2h, and then incubated with glutathione Sepharose 4B beads for 1 h. After extensive washing, the beads were boiled in loading buffer and subjected to Western blot with an anti-HA antibody.

*Determination of Rac-GTP levels-* Experiments were carried out as previously described (181). Briefly, cells were lysed in a buffer containing 8  $\mu$ g of GST-PBD (p21-binding domain), 20 mM Tris-HCl, pH 7.5, 1 mM dithiothreitol, 5 mM MgCl<sub>2</sub>, 150 mM NaCl, 0.5% Nonidet P-40, 5 mM  $\beta$ -glycerophosphate, and protease inhibitors cocktail (Sigma). Lysates were centrifuged at 14,000  $\times$  g (4°C, 10 min) and then incubated with glutathione Sepharose 4B beads (4°C, 1 h). After extensive washing, the beads were boiled in loading buffer and subject to Western blot analysis using an anti-Rac1 antibody.

*Western blot-* Non-specific binding in membranes was blocked by incubation with 5% nonfat milk or 5% bovine serum albumin for 2 h. Membranes were then incubated with primary antibodies for 2 h at room temperature, followed by incubation with peroxidase-conjugated goat anti-mouse or anti-rabbit IgG (1:3,000 or 1:10,000) for 1 h at room temperature. Immunoreactivity was visualized with a FUJIFILM LAS3000 image reader using an enhanced chemoluminescence detection kit (Amersham).

**Table 2.1 Primers used to generate constructs**

<b>Constructs</b>	<b>Primers</b>
pB42AD-Tmp21 (aa 108-208):	
Forward:	ccggaattctgttttgagagcaaggggaacaggg
Reverse:	ccgctcgagcaggtagaagacctgccag
pB42ADTmp21 (aa108-185):	
Forward:	ccggaattctgttttgagagcaaggggaacaggg
Reverse:	ccgctcgagccgagtgtttgttgactcgttgg
pB42ADTmp21 (aa183-211):	
Forward:	ggaattcgtcctatacttcagcatcttttcaatggtctgtctcattggactagctacctg
Reverse:	ccttaagcaggatagaagt cgtagaaaagt tacaagacagagtaacctgatcgatggac
pEBG-p23/Tmp21 (aa 1-219)	
Forward:	ccgctcgaggatccatgtctggtttgtctggccc
Reverse:	gactagtctactcaatcaatttcttgccc
pEBG-p23/Tmp21 (aa 108-219)	
Forward:	gaagatctctcgaggatccatgtgttttgagagcaaggg
Reverse:	gactagtctactcaatcaatttcttgccc
pEBG-p23/Tmp21 (aa 1-208)	
Forward:	ccgctcgaggatccatgtctggtttgtctggccc
Reverse:	gactagtctagcgtcgaggtagaagacc
pEBG-p23/Tmp21 (aa 1-185)	
Forward:	ccgctcgaggatccatgtctggtttgtctggccc
Reverse:	gactagtctaccgagtgtttgttgactcg
PKC $\alpha$ C1a-b	
Forward	ccggaattcatggetgacgttttcccgggcaacga
Reverse	cgcggtatccctaaacctcagcctttaggtaaatcc
PKC $\epsilon$ C1a-b	
Forward	ccggaattctcgtcgggtgaagcccctaaagacaatg
Reverse	cgcggtatccctaggtaacgcccaggtcggccagtactttg
PKC $\delta$ C1a-b	
Forward	ccggaattcgaggacgtggattgcaaacagtctatg
Reverse	cgcggtatccctatctctgggtgacttggttcaaggcct
PKC $\zeta$ C1	
Forward	ccggaattcgttttcccagcaccctgagcagcctg
Reverse	cgcggtatccctaaagactctgccccagggctaagcaaatc
RasGRP1 C1	
Forward	ccggaattcttctgtgtgatggacaaagatagg
Reverse	cgcggtatcccacagagctgatgttttctgtgg
$\beta$ 2-chimaerin C1	
Forward	ccggaattcaaaacaaacgtcacacatgaagaacacacagc
Reverse	cgcggtatccctatgttgtgaggtcacaacagtacact
PKC $\epsilon$ C1a	
Forward	gaattcaacggccacaagttcatg
Reverse	ggatccccagcacactttgtgatta
PKC $\epsilon$ C1b	
Forward	gaattcatgccccacaagttcggtat
Reverse	ggatcccactccacagttgggag

## **CHAPTER 3**

**p23/Tmp21, an ER/Golgi cargo protein, regulates phorbol ester-induced apoptosis in LNCaP prostate cancer cells via direct association with PKC $\delta$**

## **ABSTRACT**

It has been established that androgen-dependent prostate cancer cells undergo apoptosis in response to phorbol esters treatment, and that this effect was primarily mediated by nPKC $\delta$ . In the present chapter we demonstrate that depletion of p23/Tmp21 significantly potentiates PMA-induced apoptosis in LNCaP cells. The effect was rescued by PKC $\delta$  RNAi depletion or the pan-PKC inhibitor GF 109203X, suggesting that the enhancing apoptotic effect of p23/Tmp21 depletion was mediated by PKC $\delta$ . Yeast two-hybrid assay revealed that the PKC $\delta$  C1a-b domain interacts with p23/Tmp21. In addition, co-localization analysis by confocal microscopy demonstrated that GFP-PKC $\delta$  C1b domain co-localizes with p23/Tmp21 in the perinuclear region. More importantly, the authenticity of the interaction between PKC $\delta$  and p23/Tmp21 was confirmed by showing that endogenous PKC $\delta$  co-immunoprecipitated and co-localized with endogenous p23/Tmp21 in LNCaP cells. Interestingly, disruption of PKC $\delta$ -p23/Tmp21 association by depletion of p23/Tmp21 significantly accelerated PMA-induced PKC $\delta$  translocation to the plasma membrane and activated PKC $\delta$  downstream effectors. Furthermore, our experiments also demonstrated that depletion of p23/Tmp21 potentiates apoptosis induced by the DNA damage agent doxorubicin. In summary, our data provide evidence that PKC $\delta$  associates with p23/Tmp21, and suggest that p23/Tmp21 acts as an anchoring protein that retains PKC $\delta$  at the perinuclear region, thus limiting its availability for signaling.

## **INTRODUCTION**

As described in Chapter 2, we identified p23/Tmp21 as a binding protein for chimaerin Rac-GAPs and showed that p23/Tmp21 negatively regulates the Rac-GAP activity of  $\beta$ 2-chimaerin. Mutation or deletional analysis demonstrated that the interaction is mediated by the C1 domain in chimaerins (181). We also showed in Chapter 2 that p23/Tmp21 associates with the PKC $\epsilon$  C1b domain. Interestingly, a yeast two-hybrid assay also revealed that p23/Tmp21 could interact with C1 domains from other phorbol ester/DAG receptors, including RasGRP1, PKC $\alpha$ , and PKC $\delta$  (183). The functional relevance of the C1 domain-p23/Tmp21 association has not been thoroughly elucidated in the context of PKC-mediated responses.

PKC $\delta$  is an important pro-apoptotic kinase in androgen-dependent prostate cancer cells (58, 66, 147, 174, 193, 198). Activation of PKC $\delta$  by PMA induces apoptosis in LNCaP cells (58). The signaling events downstream of PKC $\delta$  include the activation of the small GTPase RhoA and its target ROCK (193), activation of JNK and p38 MAPK (174), and dephosphorylation of Akt (174). It has been reported that PKC $\delta$  activity is also required for the apoptotic effect of DNA damage agents such as etoposide and doxorubicin in cancer cells (49, 143). A yeast two-hybrid assay demonstrated that p23/Tmp21 can interact with the PKC $\delta$  C1a-b domain. We propose that p23/Tmp21 may regulate PKC $\delta$ -mediated apoptosis through their interaction.

In the present chapter we investigate the functional relevance of the PKC $\delta$ -p23/Tmp21 association in LNCaP prostate cancer cells. A remarkable finding is that the association between p23/Tmp21 and PKC $\delta$  modulates apoptosis in LNCaP prostate cancer cells induced by PMA and doxorubicin. p23/Tmp21 possibly anchors

PKC $\delta$  in the ER/Golgi compartment and in this manner limits the ability of PKC $\delta$  to translocate to the plasma membrane. Our study also revealed a novel function for p23/Tmp21 in regulating apoptotic cell death in addition to its well-established role in vesicle formation and cargo trafficking.

## RESULTS

### **p23/Tmp21 directly interacts with PKC $\delta$ in LNCaP prostate cancer cells**

Our studies have demonstrated that p23/Tmp21 interacts with  $\alpha$ -,  $\beta$ - chimaerin, and PKC $\epsilon$  through their C1 domains (181, 183). We speculated that there is a direct interaction between p23/Tmp21 and PKC $\delta$  through the same region. We first addressed this issue by using a yeast two-hybrid approach. pLexA constructs encoding C1 $\delta$ a-b, C1 $\zeta$  or C1 $\beta$ 2-chim were generated (Figure 3.1A, *upper panel*) and co-transformed with pB42AD-p23/Tmp21 (HA-tagged, aa 108-208, a fragment that interacts with C1 domain of chimaerins) into EGY48 yeast containing p8OP-LacZ vector (181, 183). The triple vector co-transformants were selected by plating the yeast into SD/-Ura/-His/-Trp dropout plates. pLexA-fused proteins were expressed in both galactose/raffinose (+Gal/Raf) plates and glucose plates (-Gal/Raf), while HA-tagged pB42AD-p23/Tmp21 (aa 108-208) was only expressed in galactose/raffinose induction plates (Figure 3.1A, *lower panel*). Figure 3.1A (*middle panel*) shows that the C1 $\delta$ a-b and C1 $\beta$ 2-chim (positive control) interacted with p23/Tmp21, as revealed by the induction of the LacZ reporter (blue color). In agreement with our previous results, C1 $\zeta$  (negative control) did not interact with p23/Tmp21. These interactions were also detected using a liquid  $\beta$ -galactosidase assay (data not shown).

To confirm the interaction between p23/Tmp21 and PKC $\delta$  at the cellular level, we first used a co-precipitation approach. COS-1 cells were transfected with pEBG vector (encoding GST protein) or pEBG-p23/Tmp21 (encoding GST-p23/Tmp21). Twenty-four h later, cells were infected with PKC $\delta$  adenovirus (3 MOI) and cultured



for 24 h. As shown in Figure 3.1B, no association was detected with GST alone, whereas significant PKC $\delta$  was detected in association with GST-p23/Tmp21.

In the next experiment we assessed the localization of various PKC $\delta$ -deleted mutants. HeLa cells were transfected with pEGFP-fused PKC $\delta$  (full-length), PKC $\delta$  C1a-b, PKC $\delta$  C1a, or PKC $\delta$  C1b. As shown in Figure 3.2B, PKC $\delta$  C1a and C1b domains differentially localize in cells. While PKC $\delta$  C1b domain mainly localized in the perinuclear region, the PKC $\delta$  C1a domain evenly distributes in the cells without any significant perinuclear localization. In that regard, these results resembled those observed for PKC $\epsilon$  (see Chapter 2). To demonstrate co-localization of PKC $\delta$  and p23/Tmp21, HeLa cells were co-transfected with the different pEGFP-PKC $\delta$  plasmids together with pcDNA3-V5-p23/Tmp21, a plasmid encoding V5-tagged p23/Tmp21, and co-localization was determined by confocal microscopy. We observed that PKC $\delta$  full-length and the PKC $\delta$  C1b domain co-localized with p23/Tmp21 in the perinuclear region, as judged by the yellow color observed in the overlapped images (Figure 3.2C).

As PKC $\delta$  plays a critical role in PMA-induced apoptosis in LNCaP cells, we next decided to use this paradigm to examine any potential modulation by p23/Tmp21. We speculated that the association between PKC $\delta$  and p23/Tmp21 regulates PKC $\delta$ -mediated apoptosis in LNCaP cells. First, we performed co-immunoprecipitation experiments to examine the association of *endogenous* PKC $\delta$  and p23/Tmp21 in LNCaP cells. In this experiment we used an anti-PKC $\delta$  antibody to pull-down *endogenous* PKC $\delta$ , and examined if p23/Tmp21 co-precipitates with PKC $\delta$ . As shown in Figure 3.3A, the interaction between PKC $\delta$  and p23/Tmp21 could be

readily detected in LNCaP cells. We then examined co-localization of PKC $\delta$  and p23/Tmp21 in LNCaP cells by confocal microscopy. LNCaP cells expressing GFP-PKC $\delta$  were immunostained for *endogenous* p23/Tmp21. As shown in Figure 3.3 B, GFP-PKC $\delta$  co-localized with p23/Tmp21 in the perinuclear region as judged by the yellow color in the overlapped images. Furthermore, by using immunostaining analysis we found that *endogenous* PKC $\delta$  and p23/Tmp21 co-localized in LNCaP cells (Figure 3.3C). Collectively, these results confirmed that PKC $\delta$  interacts with p23/Tmp21 in LNCaP prostate cancer cells.

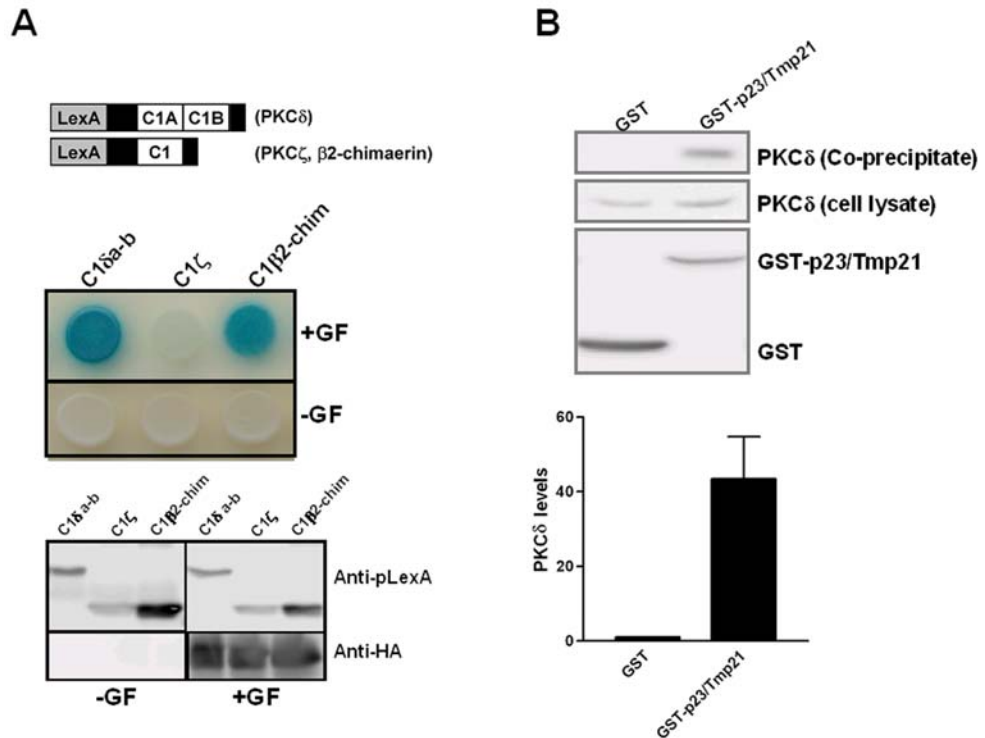


**Figure 3. 1** **A.** Yeast two-hybrid assay reveals that the PKC $\delta$  C1a-b domain interacts with p23/Tmp21. Schematic representation of C1 $\delta$ a-b, C1 $\zeta$ , or C1 $\beta$ 2-ch domain fused to pLexA (upper panel). EGY48 yeast (containing 8op-LacZ vector) was co-transformed with pLexA encoding C1 $\delta$  a-b, C1 $\zeta$ , or C1 $\beta$ 2-ch domain, and pB42AD-HA-tagged p23/Tmp21 (aa 108-208). Assay of  $\beta$ -galactosidase activity on induction (+GF) or no-induction (-GF) plates was carried out 72 h after transformation. GF, galactosidase/raffinose (middle panel). Expression of pLexA fused C1 $\delta$ a-b, C1 $\zeta$  and C1 $\beta$ 2-chim using an anti-pLexA antibody and expression of pB42AD-HA-p23/Tmp21 (aa 108-208) using an anti-HA antibody (lower panel). **B.** PKC $\delta$  forms a complex with p23/Tmp21 in COS-1 cells. COS-1 cells were transfected with either pEBG (empty vector) or pEBG-p23/Tmp21. Twenty-four h later, cells were infected with PKC $\delta$  adenovirus (MOI=3 pfu/cell). After twenty-four h, GST or GST-p23/Tmp21 proteins were precipitated with glutathione Sepharose 4B beads and associated PKC $\delta$  detected by western blot using an anti-PKC $\delta$  antibody. Upper panel, representative experiment. Lower panel, densitometric analysis of three individual experiments, expressed as fold-change relative to GST.

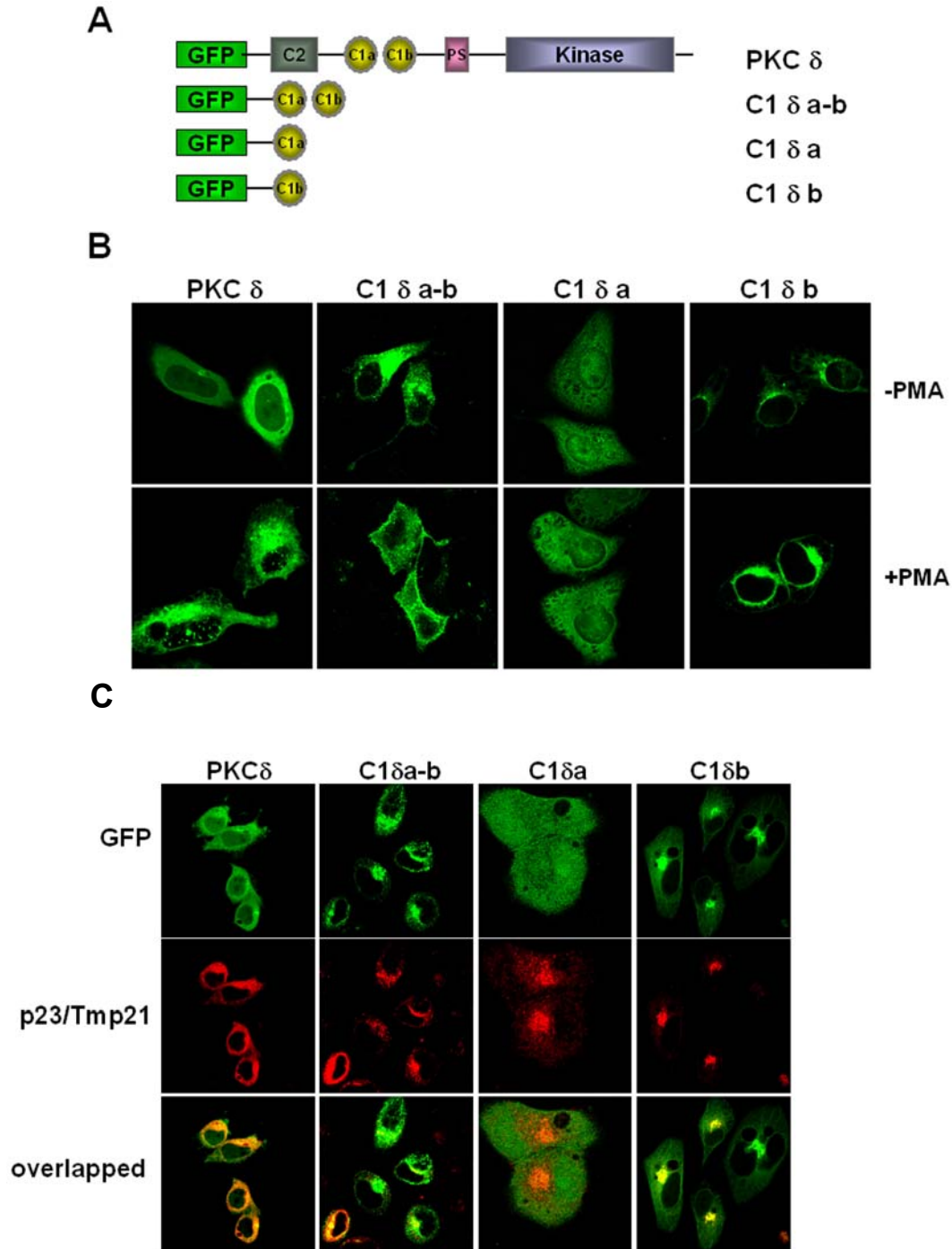


**Figure 3.2** The C1b domain of PKC $\delta$  mediates perinuclear targeting and co-localizes with p23/Tmp21. **A.** Schematic representation of C1 $\delta$ a-b, C1 $\delta$ a, C1 $\delta$ b, or full-length PKC $\delta$  fused to GFP. **B.** C1 $\delta$ b localizes in the perinuclear region. HeLa cells were transfected with pEGFP-fused PKC $\delta$ , C1 $\delta$ a-b, C1 $\delta$ a, or C1 $\delta$ b. Forty-eight h later, cells were treated with PMA (1  $\mu$ M, 30 min) or vehicle, fixed, and localization examined by confocal microscopy. **C.** HeLa cells were co-transfected with pEGFP-PKC $\delta$  plasmids together with pcDNA3.1-V5-p23/Tmp21. Forty-eight h later, cells were fixed and co-localization examined by confocal microscopy. Similar results were observed in three independent experiments.

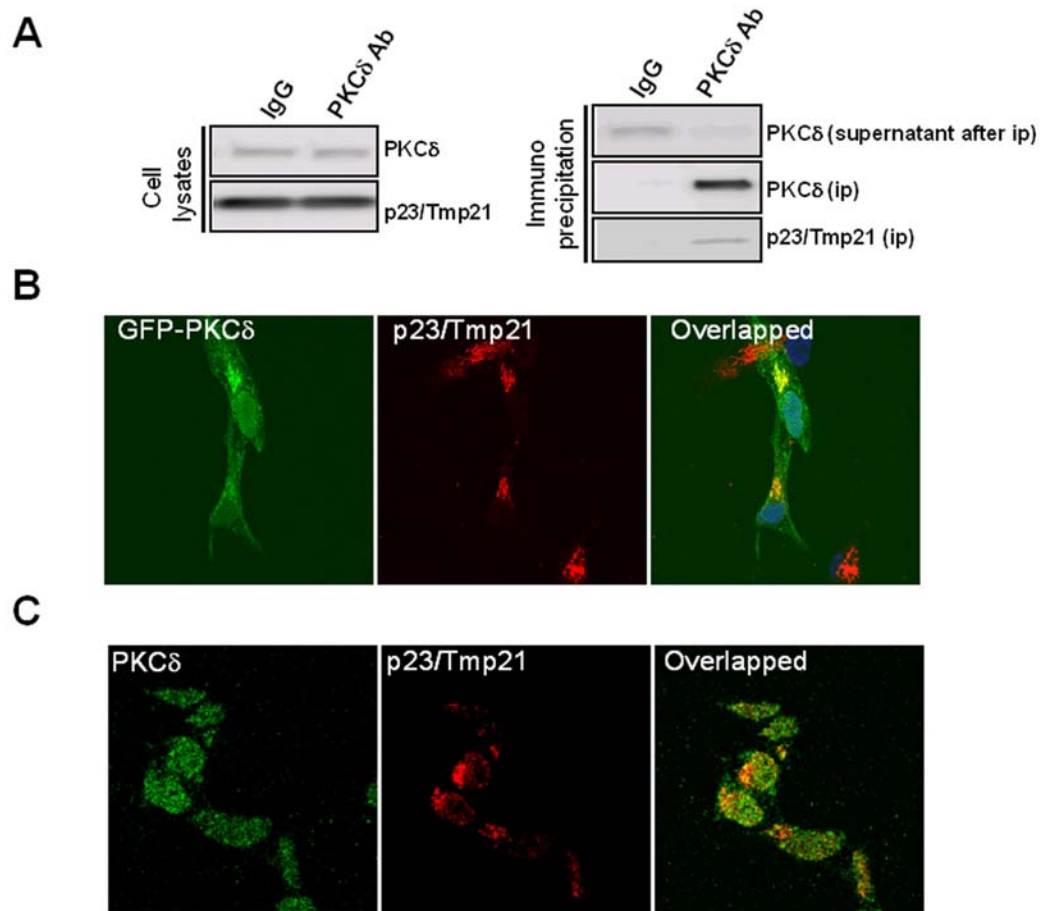


**Figure 3.3** *PKC $\delta$*  and *p23/Tmp21* form a complex in LNCaP prostate cancer cells. **A.** LNCaP cells were lysed. Cell lysates were centrifuged at 14, 000 $\times$  g for 10 min and the supernatant precleared with 15  $\mu$ l of protein A agarose beads (*invitrogen*) for 1 h at 4 $^{\circ}$ C. After a short centrifugation, the supernatant was used for immunoprecipitation with an anti-PKC $\delta$  antibody or control IgG (4 $^{\circ}$ C, 2 h). Representative western blots of the supernatant and the immunoprecipitation are shown. **B.** pEGFP-PKC $\delta$  co-localizes with p23/Tmp21 in LNCaP prostate cancer cells. GFP-PKC $\delta$  was transfected into LNCaP cells using the Amaxa Nucleofector following the instructions provided by the manufacturer. Forty-eight h later, cells were fixed and p23/Tmp21 was stained with and anti-p23/Tmp21 primary antibody followed by a Cy3-conjugated secondary antibody. Co-localization was examined by confocal microscopy. **C.** Co-localization of *endogenous* PKC $\delta$  and p23/Tmp21. All experiments have been performed three times with similar results.

### **p23/Tmp21 modulates apoptotic responses in LNCaP cells**

To determine the role of p23/Tmp21 in PMA-induced apoptosis in LNCaP cells, we depleted p23/Tmp21 from LNCaP cells using a p23/Tmp21 specific RNAi duplex, and then treated cells with PMA to assess the apoptotic response. Remarkably, depletion of p23/Tmp21 significantly potentiated PMA-induced apoptosis of LNCaP cells (Figure 3.4A). To further confirm this effect, we used p23/Tmp21 knockdown stable cell lines (see Chapter 2). In agreement with results in transiently depleted cells, stable depletion of p23/Tmp21 also resulted in a higher PMA-induced apoptotic response relative to control cells (Figure 3.4B). Our results suggest that p23/Tmp21 plays a negative role in regulating PMA-induced apoptosis. In addition, we found that depletion of p23/Tmp21 by RNAi also enhanced the apoptotic effect of the DNA damage doxorubicin in LNCaP cells (Figure 3.4C). Interestingly, several reports showed PKC $\delta$  mediates the death effect of DNA damaging agents in prostate cancer cells (15).

### **p23/Tmp21 regulates PMA-induced apoptosis through PKC $\delta$**

Previous studies have demonstrated that PKC $\delta$  played a central role in PMA-induced apoptosis of LNCaP cells. Inhibition or RNAi depletion of PKC $\delta$  abolishes PMA-induced apoptosis in LNCaP cells (66). To determine if the potentiating effect of p23/Tmp21 depletion on PMA-induced apoptosis is mediated through PKC $\delta$ , we examined if PKC $\delta$  depletion could prevent this effect. As shown in Figure 3.5B, PKC $\delta$ /p23/Tmp21 double knockdown cells had significantly decreased apoptosis, suggesting that the potentiating effect of p23/Tmp21 depletion on PMA-mediated.

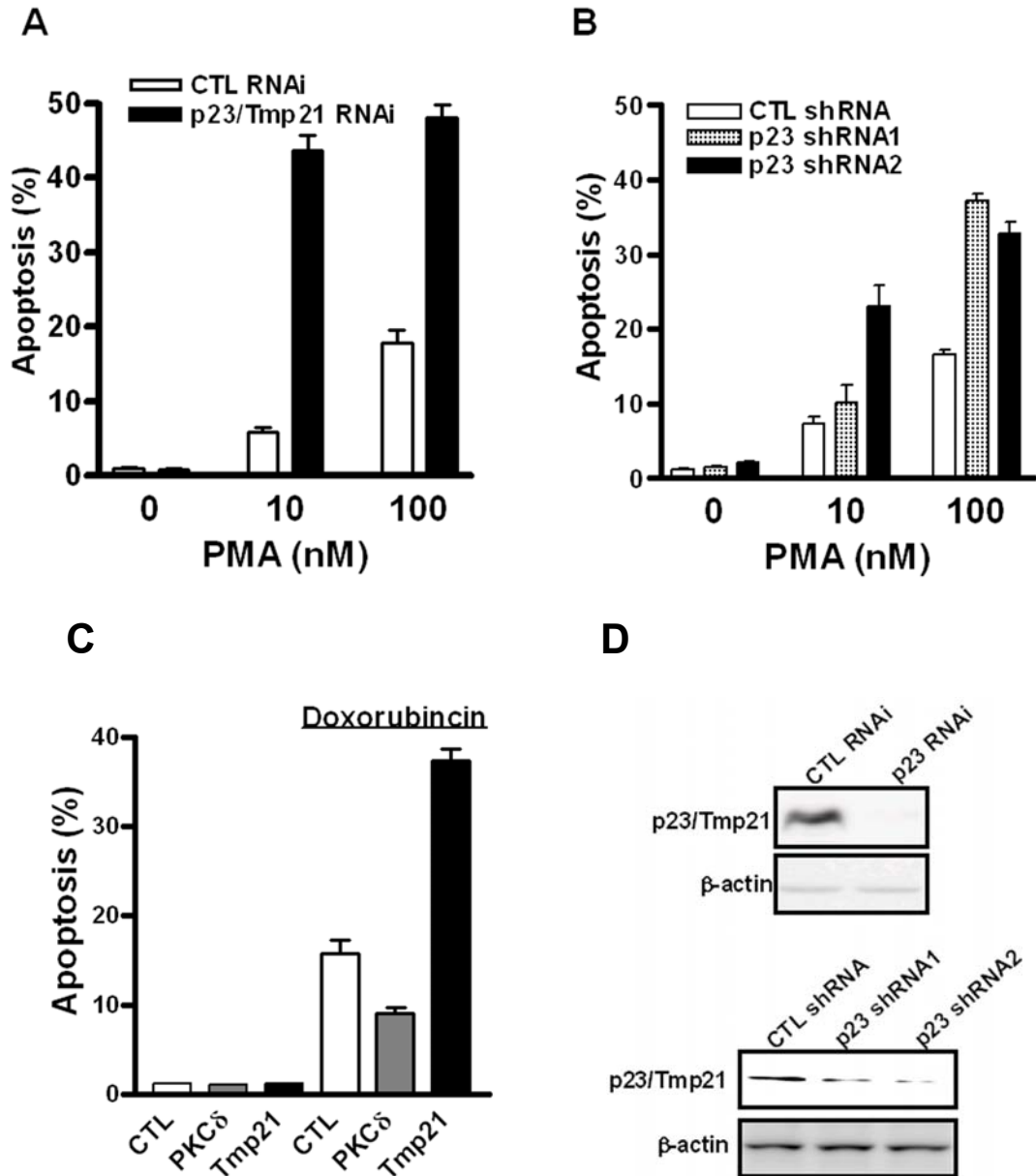


**Figure 3.4** Depletion of p23/Tmp21 potentiates PMA- and doxorubicin-induced apoptosis in LNCaP prostate cancer cells. **A.** LNCaP cells were transiently transfected with p23/Tmp21 or control (CTL) RNAi duplexes. After 48 h, cells were treated with vehicle or PMA and the incidence of apoptosis determined 24 h later. **B.** LNCaP cells stably expressing different p23/Tmp21 shRNAs (shRNA#1, or shRNA#2) or control shRNA were treated with vehicle or PMA, and the incidence of apoptosis determined 24 h later. **C.** LNCaP cells were transiently transfected with p23/Tmp21, PKC $\delta$  or control (CTL) RNAi duplexes. After 48 h, cells were treated with vehicle or doxorubicin (1  $\mu$ g/ml for 2 h) and the incidence of apoptosis determined 24 h later. **D.** Western blot for the expression of p23/Tmp21 in LNCaP cells transiently depleted of p23/Tmp21 (*upper panel*) and LNCaP stable cell lines expressing p23/Tmp21 shRNA (*lower panel*).

apoptosis in LNCaP cells is mediated through PKC $\delta$ . As a second approach, we analyzed the effect of GF 109203X, a pan-PKC inhibitor. As shown in Figure 3.5C, GF 109203X essentially abolished apoptosis in response to PMA treatment both in control and p23/Tmp21 knockdown cells. These results suggest that p23/Tmp21 depletion potentiates PMA-induced apoptosis through enhanced PKC $\delta$  activation.

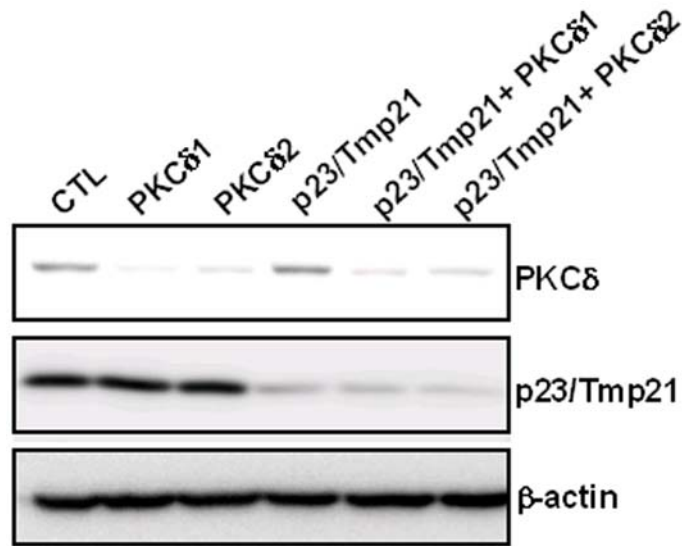
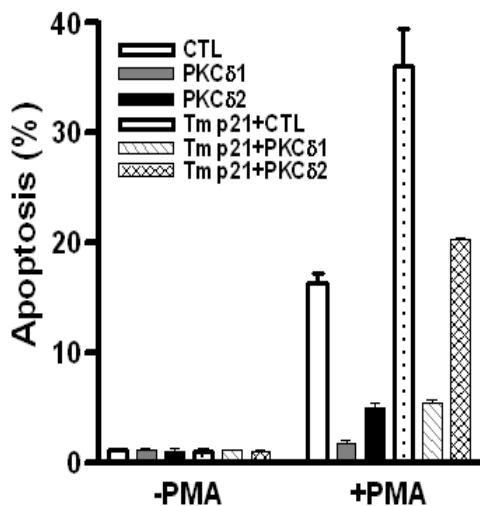
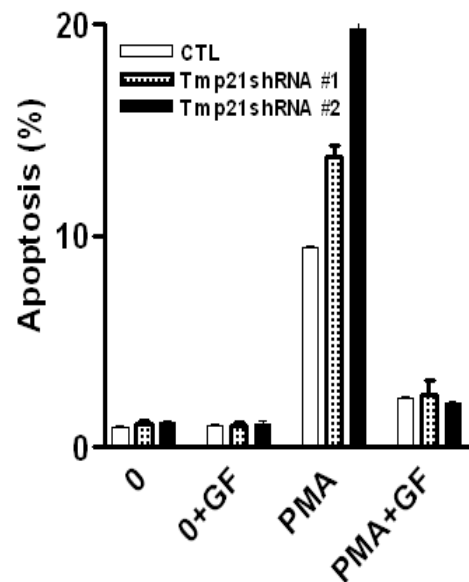
### **Depletion of p23/Tmp21 facilitates PKC $\delta$ translocation to the plasma membrane**

To establish if depletion of p23/Tmp21 affects PKC $\delta$  activation in LNCaP cells, we first examined PMA-induced translocation of GFP-PKC $\delta$ . LNCaP cells were treated with 30 nM PMA, a concentration at which translocation of PKC $\delta$  is not readily detected by microscopy in LNCaP cells. Interestingly, significant plasma membrane translocation of GFP-PKC $\delta$  could be observed at about 5-10 min in p23/Tmp21-depleted LNCaP cells under this experimental condition (Figure 3.6B). These results demonstrated that depletion of p23/Tmp21 facilitates PMA-induced PKC $\delta$  plasma membrane translocation and therefore its activation.

Our laboratory recently reported that ROCK and JNK are downstream effectors of PKC $\delta$  that mediate the apoptotic effect of PMA in LNCaP prostate cancer cells (193). PMA at 100 nM caused significant activation of JNK, as assessed with an anti-phospho-JNK antibody. PMA treatment also activates Rho and ROCK, and it induces the phosphorylation of the ROCK effector MYPT-1 in Thr850. Notably, we found a significant potentiation of JNK and MYPT-1 phosphorylation in response to PMA in p23/Tmp21 knockdown LNCaP cells compared to control cells. Figure 3.7 shows a representative experiment using 30 nM PMA, a concentration that causes only a

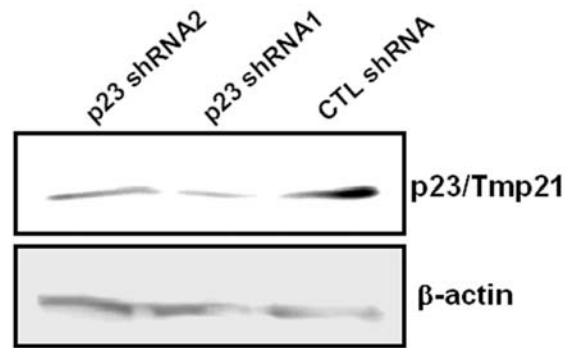


partial response and allows better detection of a potentiation effect. Taken together, these results suggest that p23/Tmp21 depletion in LNCaP cells enhances PKC $\delta$  activation upon PMA stimulation.

**A****B****C**

**Figure 3.5** Depletion of PKC $\delta$  or PKC inhibition with GF 109203X blocks PMA-induced apoptosis in LNCaP prostate cancer cells. **A.** Western blots for the expression of PKC $\delta$  and p23/Tmp21 in LNCaP cells. **B.** LNCaP cells were transiently transfected with either control, PKC $\delta$ , or PKC $\delta$  RNAi duplexes combined with a p23/Tmp21 RNAi duplex. Forty-eight h later, cells were treated with 30 nM PMA for 1 h and apoptosis was assessed 24 h following PMA treatment. **C.** Effect of the PKC inhibitor GF 109203 X (5  $\mu$ M). GF 109203 X (5  $\mu$ M) was added 1 h before PMA treatment. LNCaP cells expressing p23/Tmp21 shRNA were treated with 30 nM PMA for 1 h and apoptosis was assessed 24 h later.

**A.**



**B.**

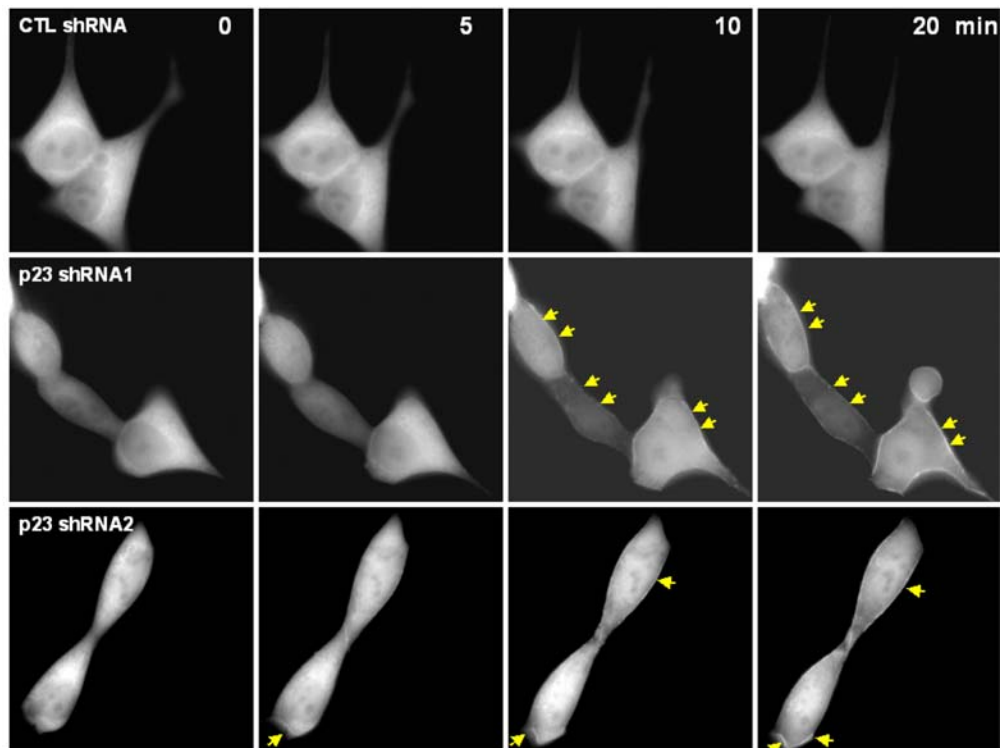


**Figure 3.6** Depletion of p23/Tmp21 accelerates PMA-induced GFP-PKC $\delta$  plasma membrane translocation. **A.** Expression of p23/Tmp21 in LNCaP cells stably expressing different p23/Tmp21 shRNAs (shRNA#1 and shRNA#2) or control shRNA cells. **B.** pEGFP-PKC $\delta$  was transfected into different LNCaP cell lines using the Amaxa Nucleofector. Forty-eight h later, cells were treated with PMA (30 nM). Time-lapse images of GFP-PKC $\delta$  translocation in living cells were captured at different times after PMA treatment. Peripheral translocation is marked with arrows. Similar results were observed in two additional experiments.

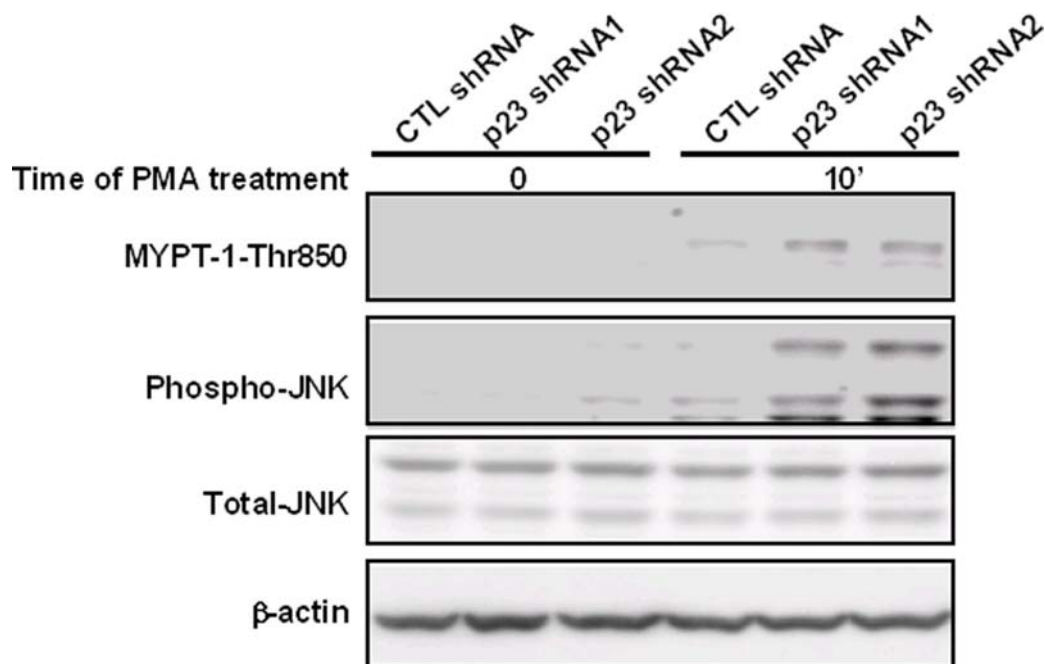


**Figure 3.7** Depletion of *p23/Tmp21* significantly enhances *ROCK* and *JNK* activation by *PMA*. LNCaP cells with stable *p23/Tmp21* depletion or control cells were treated with *PMA* (30 nM) or vehicle for 10 min. MYPT1-Thr850 and phospho-JNK were determined by Western blot. Two additional experiments gave the same results.

## **DISCUSSION**

In this chapter we report that p23/Tmp21, an ER/Golgi protein, negatively regulates apoptosis of LNCaP prostate cancer cells in response to stimuli. p23/Tmp21 associates with PKC $\delta$ , and RNAi depletion of p23/Tmp21 results in enhanced apoptotic death of LNCaP cells upon PMA or doxorubicin treatment. The interaction is mediated by the PKC $\delta$  C1a-b domain. Moreover, we demonstrated that upon PMA treatment, depletion of p23/Tmp21 enhances activation of PKC $\delta$ , as suggested by the enhanced PKC $\delta$  plasma membrane translocation and the activation of PKC $\delta$  downstream effectors ROCK and JNK. We conclude that p23/Tmp21 serves as a perinuclear anchoring protein for PKC $\delta$  that limits PKC $\delta$  activation.

Recently, the involvement of p24 family proteins in apoptotic cell death was reported. Brefeldin A, which causes ER stress by inhibiting protein transport into the Golgi, significantly induces ERS25 gene expression. ERS25 is a novel identified oxidative stress-responsive protein. Remarkably, shRNA-directed inhibition of ERS25 attenuates oxidative stress-induced ROS and abrogates apoptotic cell death in yeast upon H<sub>2</sub>O<sub>2</sub> treatment (81). Thus, the p24 family proteins may contribute to apoptotic death induced by ER stress. However, it is still elusive what is the exact role of individual members of the p24 family in apoptotic cell death in response to different stimuli.

Our previous studies in COS and HeLa cells, together with our yeast two-hybrid analysis, demonstrated that p23/Tmp21 interacts with C1 domains in  $\alpha$ -,  $\beta$ -chimaerin, and PKC $\epsilon$  (182). Our results support a model in which p23/Tmp21 serves as an

anchoring protein receptor for C1 domain-containing proteins, that sequesters them in the ER/Golgi region and prevents their translocation and activation. Likewise, our present results demonstrate that depletion of p23/Tmp21 enhances PKC $\delta$  plasma membrane translocation upon PMA treatment, suggesting a role for p23/Tmp21 as a negative regulator of PKC $\delta$  translocation to the cell membrane or possibly other compartments.

In many cell types, it has been demonstrated that PKC $\delta$  mediates apoptotic responses initiated by a variety of stimuli, including chemotherapy agents, H<sub>2</sub>O<sub>2</sub>, viral infection, phorbol esters, UV radiation, Fas-ligand, and ionizing radiation. In our laboratory, we have established that PKC $\delta$  plays a critical role in mediating apoptosis in androgen-sensitive prostate cancer cells. Using adenoviral overexpression of PKC $\delta$ , it was revealed that PKC $\delta$  significantly enhances PMA-induced apoptosis of LNCaP cells, whereas kinase-deficient PKC $\delta$  can substantially block PMA-induced apoptosis of LNCaP cells, arguing that PKC $\delta$  is critical in regulation of apoptosis of LNCaP cells (58). Recently, we identified a novel autocrine pro-apoptotic loop triggered by PKC $\delta$  activation in prostate cancer cells. Blocking antibodies against TNF $\alpha$  and TRAIL significantly inhibited apoptotic effects mediated by conditioned medium collected from PMA-treated cells, suggesting that the release of death receptor ligands by activation of PKC $\delta$  plays an important role in PMA-induced apoptosis of androgen-dependent prostate cancer cells (66). Blocking TNF receptor 1 signaling significantly inhibited ER stress-induced cell death (105). ER stress signals induced by docetaxel are mediated by JNK activation downstream of PKC $\delta$  activation, as revealed by the fact that PKC $\delta$  RNAi significantly inhibit ER stress

signaling. Interestingly, our previous experiments demonstrated that PKC $\delta$ -mediated apoptosis in LNCaP prostate cancer cells is dependent on the JNK pathway (66, 193). One speculation is that the ER stress signaling pathway possibly mediates PMA-induced apoptosis of LNCaP cells, and that p23/Tmp21 might be involved in ER stress. Indeed, as mentioned above, one of p24 family member proteins, ERS25, contributes to apoptotic cell death in yeast upon ER stress stimulus (81).

In summary, here we provide the first evidence that PKC $\delta$ -mediated apoptosis in LNCaP cells can be negatively regulated by the ER/Golgi protein p23/Tmp21 through their direct association. In addition, enhanced translocation of PKC $\delta$  to the plasma membrane and activation of downstream effectors such as ROCK and JNK, were observed in p23/Tmp21-depleted cells. This suggests a role for p23/Tmp21 in anchoring PKC $\delta$  in the perinuclear compartment, which possibly impedes PKC $\delta$  activation and translocation to the plasma membrane.

## **MATERIAL AND METHODS**

*Cell Culture*- LNCaP human prostate cancer cells were cultured in RPMI 1640 medium (ATCC) supplemented with 10% fetal bovine serum and penicillin (100 units/ml)-streptomycin (100 µg/ml). HeLa and COS-1 cells were cultured in Dulbecco's modified Eagles's medium (Invitrogen) supplemented with 10% fetal bovine serum and penicillin (100 units/ml)-streptomycin (100 µg/ml). All cells were cultured at 37 °C in a humidified 5% CO<sub>2</sub> atmosphere.

*Generation of p23/Tmp21- depleted cell lines using shRNA lentivirus* - LNCaP cells were infected with 2 different MISSION® Lentiviral Transduction particles encoding p23/Tmp21 shRNAs following the manufacture's instructions. p23/Tmp21 shRNA target sequences were as follows:

#1,CCGGCCAACCTCGTGATCCTAGACATCTCGAGATGTCTAGGATCACGAG  
TTGGTTTTT.

#2,CCGGCGCTTCTTCAAGGCCAAGAACTCGAGTTTCTTGGCCTTGAAGA  
AGCGTTTTT. Stable cell lines (pools) were generated by selection with puromycin (1 µg/ml).

*Yeast two-hybrid assays*- Yeast two-hybrid assays were carried out essentially as described in Chapter 2.

*Western Blot analysis*- Western blot was carried out essentially as described in Chapter 2. The following primary antibodies were used: anti-PKCδ (Transduction



Laboratories, Lexington, KY); anti-actin (Sigma); anti-phospho-JNK and anti-JNK (Cell Signaling Technology, Beverly, MA); anti-p23/Tmp21 (Santa Cruz Biotechnology, Inc., Santa Cruz, CA); and anti-phospho-MYPT1 (myosin phosphatase target subunit 1)-Thr<sup>850</sup> (Millipore, Billerica, MA). All antibodies were used at a 1:1000 dilution except for the anti-actin antibody, which was used at a 1:20,000 dilution.

*Apoptosis assays*- The incidence of apoptosis was determined as we previously described (58). Briefly, Cells were trypsinized, mounted on glass slides, fixed in 70% ethanol, and then stained for 20 min with 1 mg/ml 4',6-diamidino-2-phenylindole (Sigma). Apoptosis was characterized by chromatin condensation and fragmentation when examined by fluorescence microscopy. The incidence of apoptosis in each preparation was analyzed by counting ~500 cells.

*RNA interference*- 21-bp double-stranded RNAs were purchased from Dharmacon Research, Inc. (Dallas, TX) or Ambion (Austin, TX), and transfected into LNCaP cells using the Amaxa Nucleofector (Amaxa Biosystems, Gaithersburg, MD) following the instructions provided by the manufacturer. Experiments were performed 48 h after transfection. The following targeting sequences were used: CCATGAGTTTATCGCCACCTT (PKC $\delta$ 1), CCATGTATCCTGAGTGGAA (PKC $\delta$ 2), GCCAUAUUCUCUACUCCAAUU (p23/Tmp21) (35). As a control we used the Silencer<sup>®</sup> negative control 7 siRNAi (Ambion).

*Immunostaining and confocal microscopy*- Immunostaining and confocal microscopy were carried out essentially as described in Chapter 2.

*Time-lapse microscopy*- LNCaP cells were transfected with pEGFP-PKC $\delta$  using the Amaxa Nucleofector and seeded into glass-bottomed culture dishes (MatTek, Ashland, MA) for 48 h. Cells were cultured for 20 h in Phenol red-free RPMI-1640 medium containing 10% FBS and 5 mM HEPES. Cells were monitored under a fluorescence microscope (Nikon Eclipse TE2000U) at a 488 nm excitation wavelength with a 515 nm-long pass barrier filter at 25°C.

*Co-immunoprecipitation*- LNCaP cells were washed once with PBS, and then lysed for 10 min at 4°C in 800  $\mu$ l of a lysis buffer containing 20 mM Tris-HCl, pH 7.5, 100 mM NaCl, 0.5 mM EDTA, 0.5 mM EGTA, 0.5% TritonX 100, 1 mM beta-glycerophosphate and a protease inhibitor cocktail (Sigma). Cell lysates were centrifuged at 14,000  $\times$  g and the supernatant was precleared with 15  $\mu$ l of protein A agarose beads (*Invitrogen*) for 1 h at 4°C. After a short centrifugation, the supernatant was used for immunoprecipitation with an anti-PKC $\delta$  antibody or control IgG (4 °C, 2 h). Protein A beads (20  $\mu$ l) were then added and the mixture was incubated at 4°C for 2 h. The beads were extensively washed in lysis buffer and boiled. Samples were resolved in a 12% SDS-polyacrylamide gel and transferred to a polyvinylidene difluoride membrane (Millipore Co., Bedford, MA) for Western blot analysis.

## **CHAPTER 4**

### **C1 domain-mediated translocation of PKC $\epsilon$ : implications for prostate cancer radioresistance**

## **ABSTRACT**

The molecular mechanisms for radioresistance of cancer cells are not completely understood. Epidermal growth factor receptor (EGFR) activation by ionizing radiation has been documented as one of the major mechanisms of cytoprotection. As EGFR couples to PLC $\gamma$  and DAG generation, we decided to investigate whether C1 domain-containing proteins modulate radiosensitivity. The role of individual PKC isozymes in prostate cancer radiosensitivity still remains elusive. Here, we provide evidence that PKC isozymes play distinct roles in PC3 prostate cancer cell radiosensitivity. The PKC inhibitor GF 109203X radiosensitizes PC3 cells in a dose-dependent manner. Using a lentiviral approach to silence PKC $\alpha$ , PKC $\delta$  or PKC $\epsilon$ , we demonstrated that only PKC $\epsilon$  confers radioresistance to PC3 cells. Interestingly, a clinically relevant dose of  $\gamma$ -irradiation (2 Gy) significantly enhanced PKC $\epsilon$  translocation from the cytosol to a particulate fraction. Confocal microscopy studies demonstrated that upon  $\gamma$ -irradiation, the EGFR inhibitor AG1478 as well as PLC inhibitor U73122 significantly impair PKC $\epsilon$  translocation to the plasma membrane. Furthermore, the reactive oxygen species (ROS) scavenger N-acetylcysteine (NAC) also blocked PKC $\epsilon$  translocation to the plasma membrane. Our study revealed a potential role for DAG and C1 domain-containing proteins in the control of ionizing irradiation-induced cell death/survival.

## **INTRODUCTION**

Ionizing radiation is widely used to treat different types of solid tumors. However, radioresistance occurs in many cases and is likely to be the underlying mechanism of selection and repopulation in tumors. DNA damage/repair and cell cycle checkpoint pathways are key regulatory mechanisms that determine the fate of cancer cells after irradiation (72, 96, 110). In addition, many studies revealed that cell membrane-related signaling events are also involved in survival/death responses. Studies by many laboratories demonstrated that ionizing radiation activates receptor tyrosine kinases (RTK), mitogen-activated protein kinases (MAPKs), and PKCs (41, 76, 77, 90, 154, 167, 176, 177, 187). EGFR, a member of ErbB family of RTKs, could be activated by clinically relevant doses of ionizing radiation (1-5 Gy), confirming that ionizing radiation can mimic EGF effects and lead to the activation of cytoprotective signaling pathways, primarily the MAPK cascades (2, 168). Ionizing radiation also stimulates sphingomyelin-to-ceramide conversion via sphingomyelinases. Ceramide is a sphingolipid-derived second messenger capable of initiating apoptotic cascades in response to various stressful stimuli (38, 73, 116). Interestingly, DAG is also generated from cell membranes by ionizing radiation (129). Moreover, DAG analogs such as the phorbol esters can block ceramide-dependent apoptosis by various stimuli, including H<sub>2</sub>O<sub>2</sub> (63), TNF $\alpha$  (47, 139), chemotherapy agents (67), and ionizing radiation (73, 120, 131, 175), arguing that DAG-dependent signaling pathways may play an anti-apoptotic role in some contexts.

Extensive studies have established the relative contribution of individual PKC isozymes to cancer initiation, cell cycle progression, transformation, apoptosis, and

senescence (70). However, the role of individual PKCs in radiation-induced cancer cell death remains unknown. As radiotherapy is widely used to treat prostate cancer, we chose PC3 androgen-independent prostate cancer cells as a model to explore the relevance of individual PKCs in radiation-induced cancer cell death. Most prostate cancer cells express three DAG/phorbol ester responsive PKCs: PKC $\alpha$ , PKC $\delta$  and PKC $\epsilon$  (58). Based on the established roles of PKC isozymes in controlling cell fate in response to stimuli and their ability to regulate apoptotic and survival pathways, we hypothesize that PKC isozymes can modulate the sensitivity of cells to radiation. One attractive scenario is that PKC $\epsilon$ , which is widely implicated in the control of survival signals to promote resistance to radiation-induced death. The results of our analysis revealed that PKC isozymes played differential roles in irradiation-mediated PC3 cell death. Depletion of PKC $\epsilon$  significantly radiosensitizes PC3 cells, suggesting that PKC $\epsilon$  confers cytoprotection to PC3 prostate cancer cells in response to  $\gamma$ -irradiation. Moreover, we established a key role for DAG, the C1 domain ligand, in plasma membrane translocation of PKC $\epsilon$  by  $\gamma$ -irradiation.

## **RESULTS**

### **$\gamma$ -irradiation inhibits the growth of PC3 androgen-independent prostate cancer cells**

In clinic, radiotherapy has been widely used to treat prostate cancer. PC3 androgen-independent prostate cancer cells ( $5 \times 10^4$ /well) were seeded (DMEM with 10% FBS) in six-well plates. As shown in Figure 4.1A, the cell number was counted at 24, 48, 72, and 96 h after the culture. The number of PC3 cells increased about 60-fold after 96 h. As shown in Figure 4.1C and Figure 4.1D, PC3 cell number was significantly reduced upon  $\gamma$  irradiation in a dose-dependent manner. Apoptosis analysis by DAPI staining revealed that  $\gamma$ -irradiation (8 Gy) causes only about 10% apoptosis (Figure 4.1B), suggesting that  $\gamma$ -irradiation-mediated inhibition of PC3 cell growth involves primarily other mechanisms.

### **The PKC inhibitor GF 109203X (GF) radiosensitizes PC3 prostate cancer cells**

To examine a potential involvement of PKC isozymes on  $\gamma$ -irradiation-mediated prostate cancer cell death *in vitro*, PC3 cells were pre-treated with the pan-PKC isozyme inhibitor GF for 30 min and then subject to a clonogenic survival assay. As shown in Figure 4.2A, the PKC inhibitor significantly radiosensitizes PC3 prostate cancer cells.  $\gamma$ -irradiation (8 Gy) alone causes about 8% apoptosis. GF enhanced  $\gamma$ -irradiation-induced apoptosis to 13% and 20% at the concentration of 1  $\mu$ M and 5  $\mu$ M, respectively. Our results suggest that inhibition of PKC isozymes by GF radiosensitizes PC3 androgen-independent prostate cancer cells.

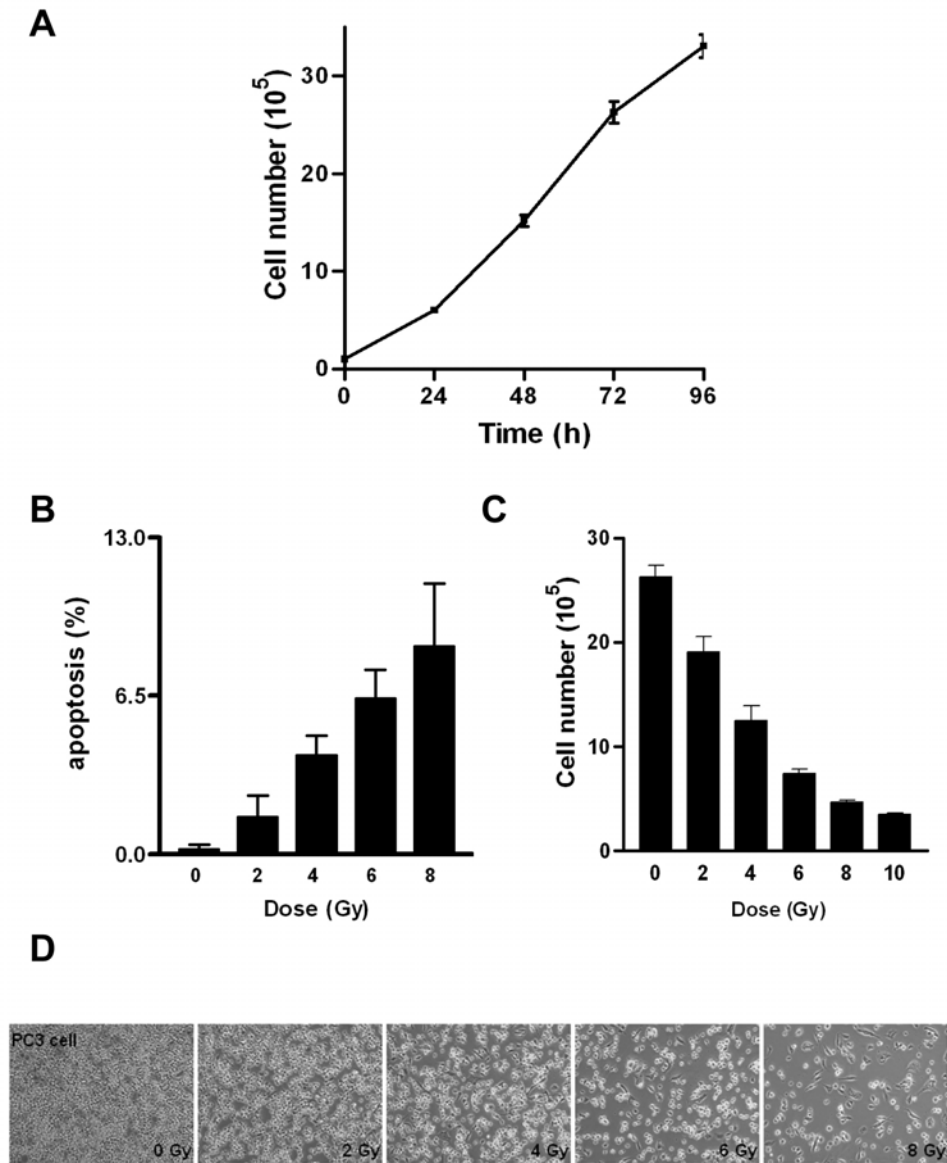


**Figure 4.1**  $\gamma$ -irradiation reduces PC3 prostate cancer cell number. PC3 prostate cancer cells ( $5 \times 10^4$ /well) were seeded into six-well plates and irradiated by different dose of  $\gamma$ -irradiation. Cell number was determined at 24, 48, 72 and 96 h after irradiation. **A.** PC3 prostate cancer cell growth curve. Cell number was determined at 24, 48, 72, and 96 h. **B.** Apoptosis was analyzed by DAPI staining 72 h after  $\gamma$ -irradiation (2, 4, 6, and 8 Gy). The results are from 3 separate experiments (mean  $\pm$  SE). **C.** PC3 cells were trypsinized and cell number was determined 72 h after different  $\gamma$ -irradiation doses. **D.** Representative images of PC3 cell density 72 h after  $\gamma$ -irradiation.



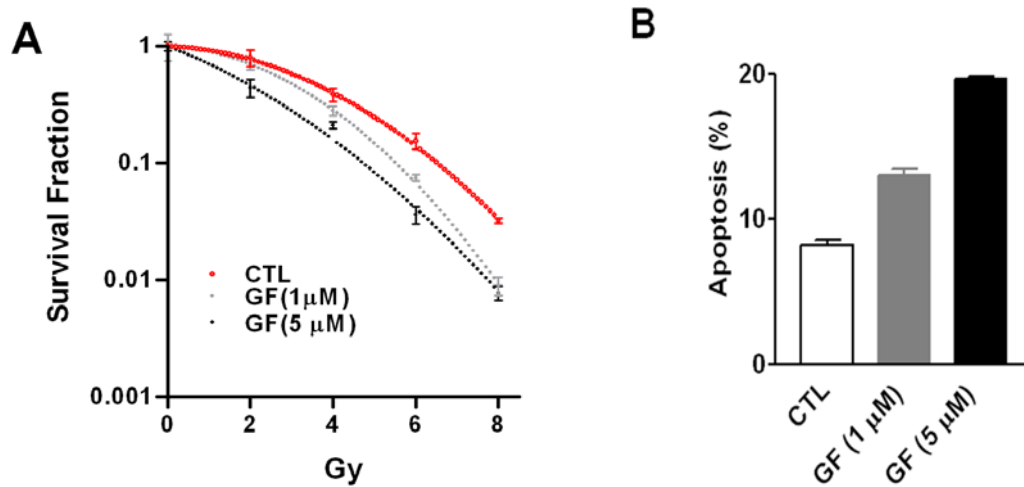


**Figure 4.2** *The PKC inhibitor 109203X (GF) radiosensitizes PC3 prostate cancer cell.* **A.** PC3 cells were serum-starved for 72 h, treated with different concentrations of the PKC inhibitor GF for 30 min and subject to  $\gamma$ -irradiation. After irradiation, cells were seeded into 60 mm Petri dishes and colonies in each plate counted after 15 days. The survival fraction was calculated as: colonies / [cells seeded x (plating efficiency)/100]. Each sample was done in triplicate. Two additional experiments showed similar results. **B.** Apoptosis was measured by DAPI staining 72 h after  $\gamma$ -irradiation (8 Gy). The results are from 3 separate experiments (mean  $\pm$  SE).

## **Establishment of PC3 prostate cancer cell lines stably depleted of PKC $\alpha$ , PKC $\epsilon$ and PKC $\delta$**

In order to determine the role of individual DAG-responsive PKC isoforms in PC3 cell radiosensitivity, we used shRNA lentiviruses to specifically knockdown PKC $\alpha$ , PKC $\delta$ , or PKC $\epsilon$ , the main PKC isozymes expressed in prostate cancer cells. As a control, we used a non-target sequence shRNA lentivirus. Stable cell lines (pools) were selected using puromycin. As shown in Figure 4.3, PC3 prostate cancer cell lines with >50% depletion of PKC $\alpha$ , PKC $\delta$ , or PKC $\epsilon$  could be successfully established using this approach. We picked two cell lines for each PKC that show isozyme-specific depletion (#2 and #3 for PKC $\alpha$ ; #2 and #4 for PKC $\delta$ ; #1 and #4 for PKC $\epsilon$ ).

### **PKC $\epsilon$ depletion significantly radiosensitizes PC3 prostate cancer cells**

In the next series of experiments, we assessed the effect of specific PKC isozyme depletion on PC3 cell radiosensitivity. Clonogenic survival assays revealed that depletion of PKC $\delta$  has no sensitizing effect on  $\gamma$ -irradiation (Figure 4.4A). Likewise, PKC $\alpha$  depletion has no significant effects on clonogenic survival (Figure 4.4B). It has been reported that PKC $\epsilon$  confers androgen independence, accelerates G1/S transition, and enhances tumorigenic potential in nude mice when overexpressed in LNCaP cells. PKC $\epsilon$  also activates the mitogenic ERK pathway, and propagates survival signals in the absence of functional PTEN (190-192). Notably, human prostate tumors display very high levels of PKC $\epsilon$  (5, 44, 94, 121).

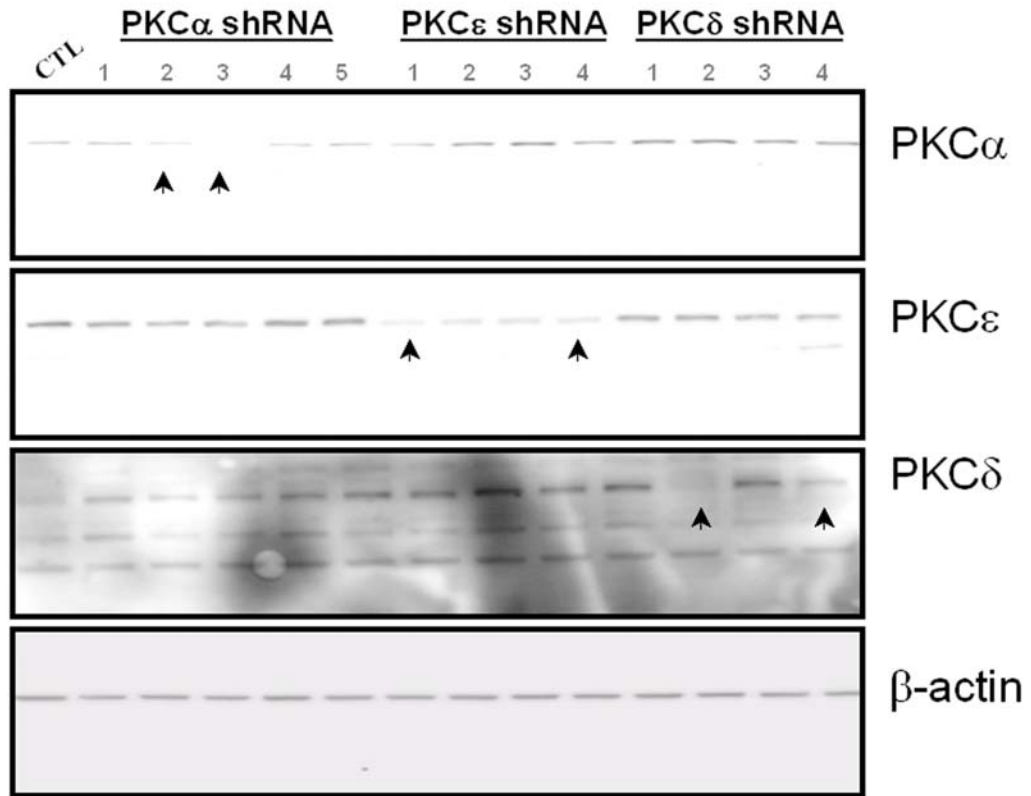


**Figure 4.3** Establishment of PC3 prostate cancer cell lines stably depleted of PKC $\alpha$ , PKC $\epsilon$  or PKC $\delta$  by using shRNA lentiviral expression system (MISSION® lentiviral particles, Sigma). PKC $\alpha$  (#2, #3), PKC $\epsilon$  (#1, #4) and PKC $\delta$  (#2, #4) PC3 cell lines were chosen for subsequent experiments.

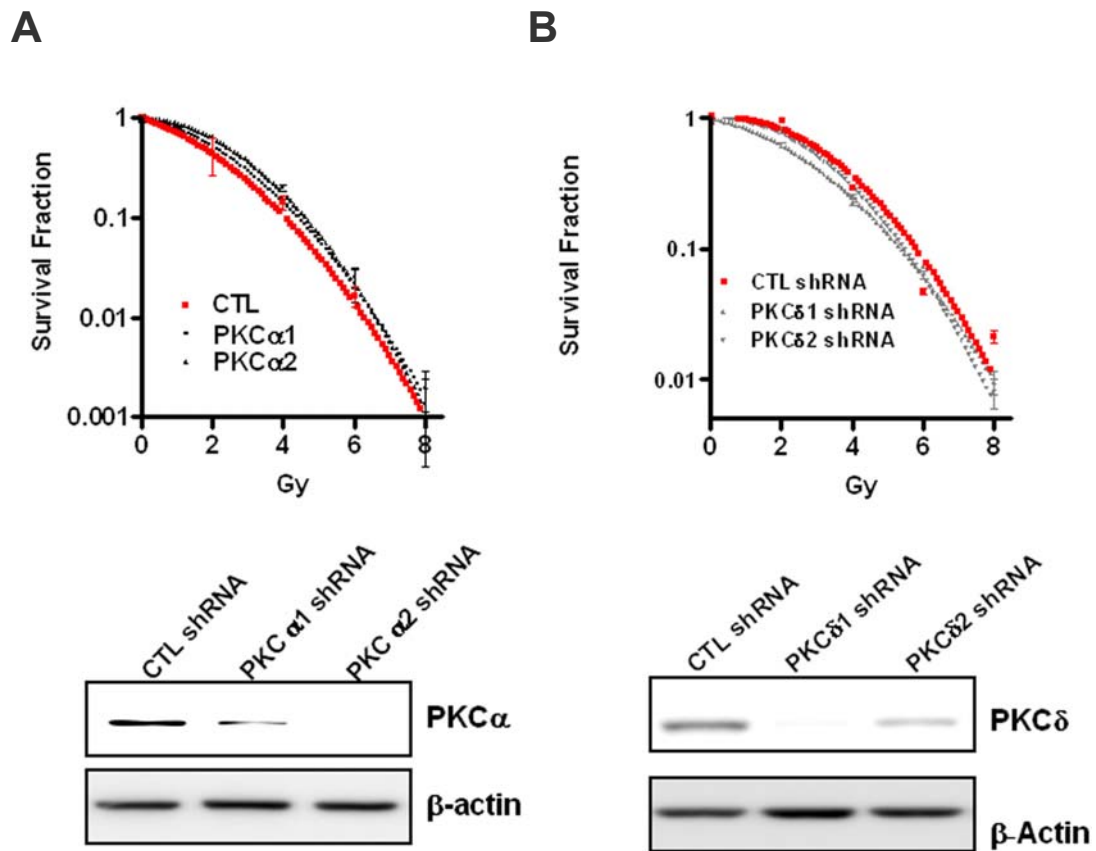
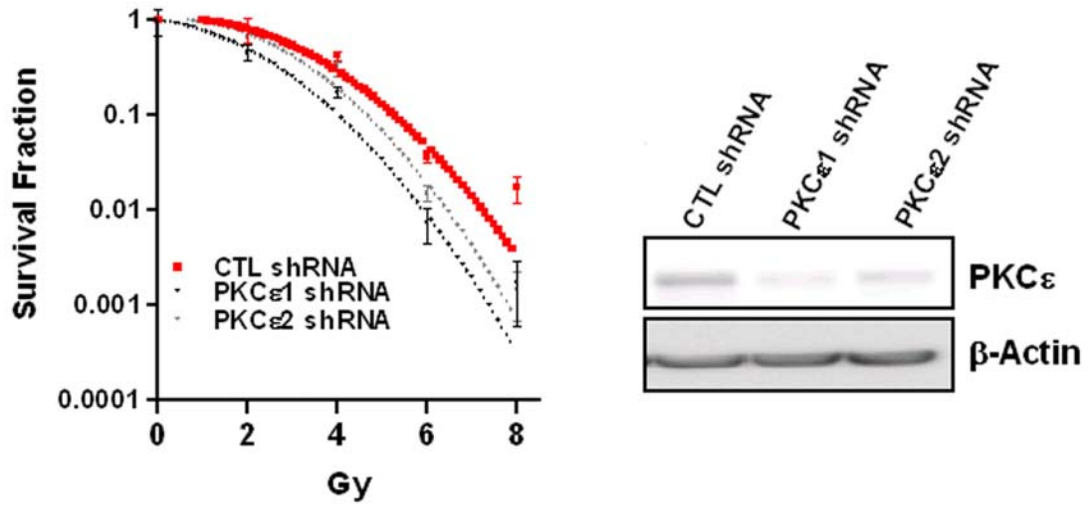


**Figure 4.4** *PKC $\alpha$  or PKC $\delta$  depletion does not affect PC3 cell radiosensitivity. A.* Survival curve for PKC $\alpha$ -depleted PC3 cell lines. **B.** Survival curve for PKC $\delta$ -depleted PC3 cell lines. Western blots showing the depletion of either PKC isozyme are shown. Two additional experiments show similar results.

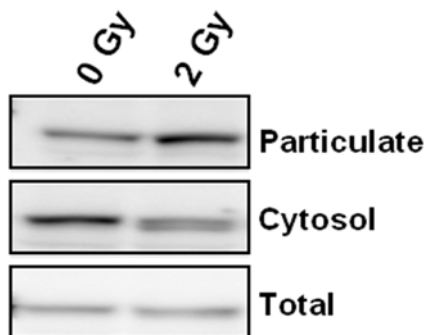
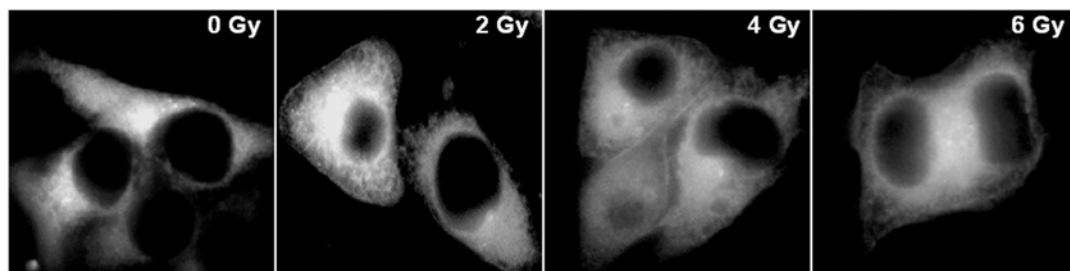
In addition, de-regulation of the PKC $\epsilon$  gene has been reported in other cancer types, such as in lung, breast and thyroid cancer (6, 92, 115). Whether PKC $\epsilon$  is implicated in prostate cancer cell survival in response to  $\gamma$ -irradiation is not known. We irradiated the PKC $\epsilon$ -depleted cell lines and examined their survival. We found that depletion of PKC $\epsilon$  significantly radiosensitizes PC3 prostate cancer cells, suggesting that PKC $\epsilon$  plays a pro-survival role in response to  $\gamma$ -irradiation (Figure 4.5).

#### **$\gamma$ -irradiation promotes PKC $\epsilon$ translocation to the plasma membrane**

Early studies by Nakajima *et al.* reported that ionizing radiation can generate DAG and translocate PKCs to plasma membrane in rat hepatocytes (129, 130). We decided to investigate whether PKC $\epsilon$  can be redistributed to membranes in response to  $\gamma$ -irradiation in PC3 cells. Using a subcellular fractionation approach we found that  $\gamma$ -irradiation (2 Gy) could induce translocation of PKC $\epsilon$  from cytosol to the particulate fraction (Figure 4.6A). As a second approach we expressed GFP-PKC $\epsilon$  in PC3 cells and assessed its localization in response to  $\gamma$ -irradiation. Confocal images revealed that GFP-PKC $\epsilon$  significantly translocates to the plasma membrane 5 min after  $\gamma$ -irradiation (2, 4, 6 Gy) (Figure 4.6B). As PKCs become activated when translocated to the plasma membrane, these results strongly suggest that  $\gamma$ -irradiation activates PKC $\epsilon$ .



**Figure 4.5** *PKCε* depletion enhances radiosensitivity of PC3 cells. Left panel, survival curve for PKCε-depleted cell lines. Right panel, Western blot showing depletion of PKCε in PC3 prostate cancer cells.

**A****B**

**Figure 4.6** *Translocation of PKC $\epsilon$  after  $\gamma$ -irradiation.* **A.** Subcellular fractionation of PKC $\epsilon$  after  $\gamma$ -irradiation. After serum starvation for 72 h, PC3 cells were subjected to  $\gamma$ -irradiation. After 2 h, cell lysates were fractionated into cytosolic and particulate fractions by centrifugation. PKC $\epsilon$  levels were determined by Western blot using a specific anti-PKC $\epsilon$  antibody. Similar results were obtained in two experiments. **B.** PC3 prostate cancer cells were transfected with pEGFP-PKC $\epsilon$ , serum-starved for 72 h, and then irradiated with different doses of  $\gamma$ -irradiation. Cells were fixed in cold ethanol ( $-20^{\circ}\text{C}$ ) 5 min after irradiation and images were captured by fluorescence microscopy. Representative pictures are shown. Two additional experiments gave similar results.

### **Reactive oxygen species (ROS) mediate PKC $\epsilon$ translocation by $\gamma$ -irradiation**

The active hydroxyl radical (OH $\cdot$ ) is the primary species of ROS produced by ionizing radiation (150). It can produce other highly reactive species, such as superoxide (O $_2^{\cdot-}$ ) and hydrogen peroxide (H $_2$ O $_2$ ). Hydrogen peroxide (H $_2$ O $_2$ ) has been reported to stimulate DAG production in vascular endothelial cells (170). UV radiation also has been reported to generate DAG in human melanocytes and keratinocytes (31). We hypothesize that subcellular translocation of PKC $\epsilon$  in PC3 cells by  $\gamma$ -irradiation is mediated by ROS. To address this issue we used the ROS scavenger N-acetyl-L-cysteine (NAC). As shown in Figure 4.7,  $\gamma$ -irradiation alone induced PKC $\epsilon$  translocation to the cell periphery (*middle panel*). In contrast, pretreatment of NAC (5 mM) abolished plasma membrane translocation of PKC $\epsilon$  (*low panel*), arguing that ionizing radiation-induced ROS are implicated in PKC $\epsilon$  plasma membrane relocalization. Interestingly, perinuclear localization of PKC $\epsilon$  remained unaffected in the presence of NAC.

### **The EGFR inhibitor AG1478 impairs peripheral PKC $\epsilon$ translocation by $\gamma$ -irradiation**

It has been reported that EGFR is activated by ionizing radiation in human cancer cells, and that it mediates cytoprotective responses and radioresistance. Amorino *et al.* reported that ionizing radiation (1-5 Gy) activates EGFR and ERK in human breast carcinoma cells. ERK and its downstream effector p90Rsk could phosphorylate downstream transcription factors involved in cell proliferation, such as CREB, Egr, Est, Stat3, C/EBP and Stat1 (2).



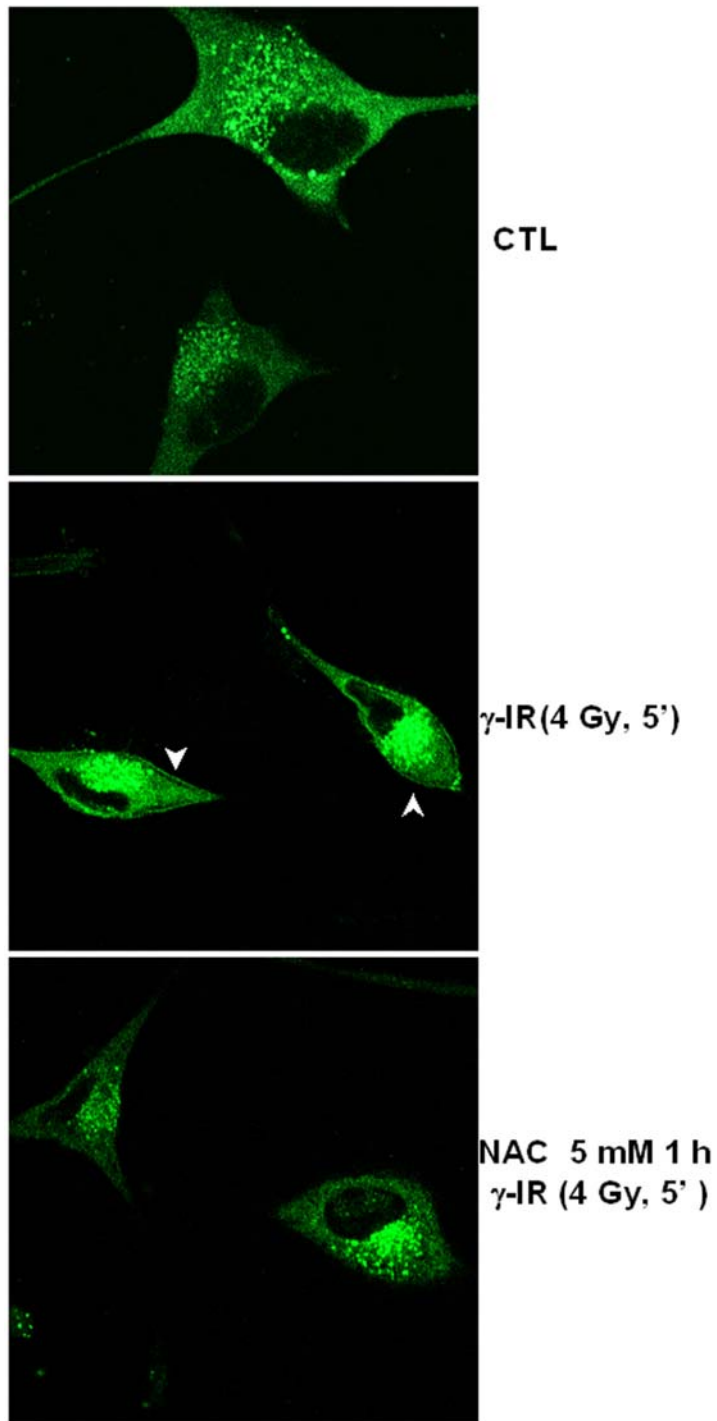


**Figure 4.7** *NAC prevents  $\gamma$ irradiation-mediated PKC $\epsilon$  translocation.* PC3 prostate cancer cells expressing GFP-PKC $\epsilon$  were serum-starved for 72 h and then treated with N-acetyl-L-cysteine (NAC, 5 mM) for 1 h. Cells were then subjected to  $\gamma$ -irradiation (4 Gy) for 5 min and then fixed in cold ethanol (-20°C). Images were captured by confocal microscopy. Two additional experiments showed similar results.

It has been reported that  $\gamma$ -irradiation promotes EGFR phosphorylation at Tyr992 even at higher levels than those induced by EGF. Tyr992 in EGFR couples to PLC $\gamma$  and DAG generation (167), arguing that irradiation-induced EGFR activation may activate PKC $\epsilon$  via DAG binding to their C1 domains. We therefore tested the hypothesis that PKC $\epsilon$  translocation to the plasma membrane by irradiation is mediated by the EGFR-PLC $\gamma$  pathway. PC3 prostate cancer cells were transfected with pEGFP-PKC $\epsilon$ , serum-starved for 72 h, treated with the EGFR inhibitor AG1478 (10  $\mu$ M, 1 h), and then  $\gamma$ -irradiated (4 Gy, 5 min). Cells were fixed and the images were captured by confocal microscopy. As shown in Figure 4.8A, AG1478 impaired the peripheral translocation of PKC $\epsilon$ . To determine a potential involvement of PLC in PKC $\epsilon$  translocation, we used the PLC inhibitor U73122. Its inactive analogue U73433 was used as a negative control. As shown in Figure 4.8B, the PLC $\gamma$  inhibitor impaired  $\gamma$ -irradiation-induced PKC $\epsilon$  membrane translocation. Neither vehicle nor U73433 impaired the peripheral relocalization of GFP-PKC $\epsilon$ . Altogether, these results suggest that PKC $\epsilon$  plasma membrane translocation by  $\gamma$ -irradiation is mediated through the activation of the EGFR-PLC $\gamma$ -DAG signaling pathway. Binding of DAG to the C1 domain in PKC $\epsilon$  may represent the key event in the translocation of this kinase and its consequent activation.

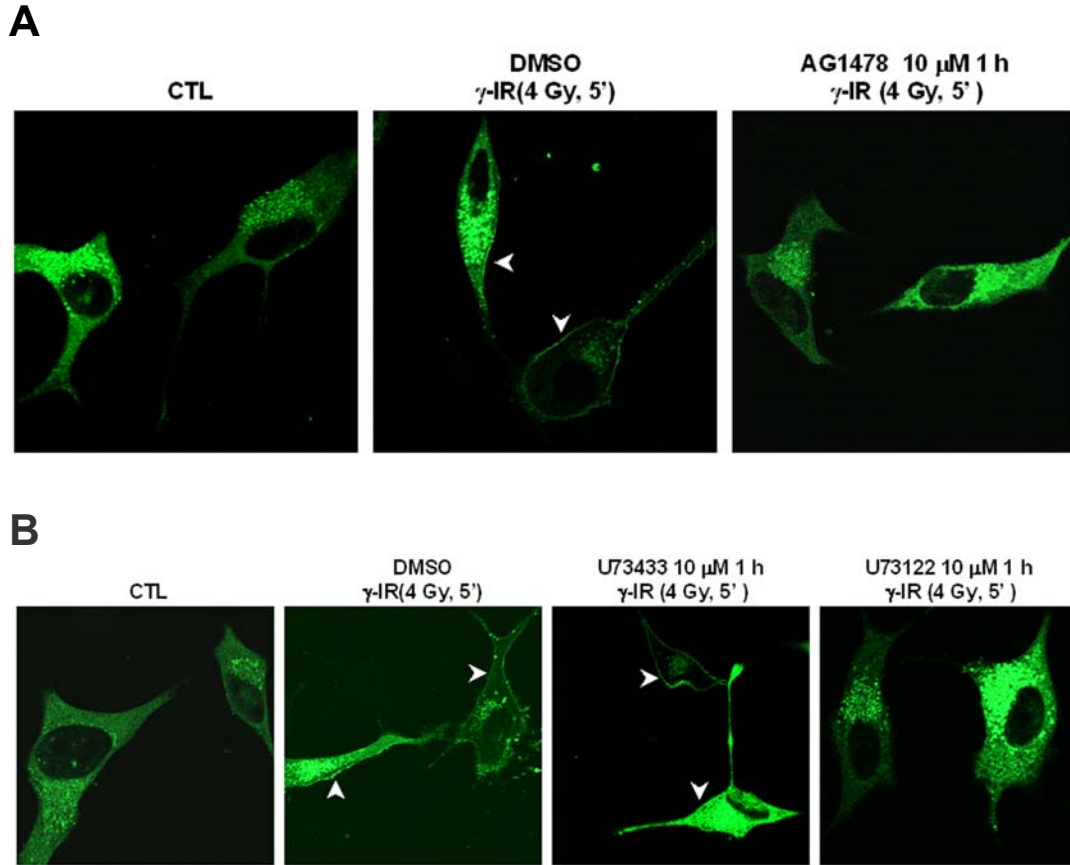


**Figure 4.8** *PKC $\epsilon$  translocation to the plasma membrane by  $\gamma$ irradiation is mediated by EGFR and PLC.* PC3 prostate cancer cells expressing GFP-PKC $\epsilon$  were serum-starved for 72 h and then treated with: **A.** AG1478, or **B.** U73122 or its inactive analogue U73433. Cells were then irradiated (4 Gy, 5 min), and fixed in cold ethanol (-20°C). Images were captured by confocal microscopy. Two additional experiments showed similar results.

## **DISCUSSION**

Prostate cancer is the most commonly diagnosed male non-skin cancer malignancy and second only to lung cancer in human male cancer-related mortality. Although radiotherapy has been widely used in prostate cancer treatment, locally-advanced stages of prostate cancer (LAPC) will relapse after treatment. The underlying mechanisms for LAPC radioresistance are not fully understood. One of the clinical goals in radiotherapy is to achieve the eradication of cancer cells through the combination of radiotherapy and other radiosensitizing regimes. PKC isozymes are implicated in the regulation of cell proliferation, transformation, differentiation, apoptosis, and the metastatic cascade (70). Some studies demonstrated that PKC isozymes are involved in stress-mediated cell death. Oxidative stress such as H<sub>2</sub>O<sub>2</sub> treatment increases intracellular ceramide and decreases DAG levels (63). PKC $\delta$  has been reported to be involved in apoptosis after irradiation of U937, MCF7, and NIH 3T3 cells (54, 59, 97, 200). More recently, PKC $\epsilon$  was reported to sensitize skin to UV radiation (5). However, the relevance of individual PKC isozymes in prostate cancer cell radiosensitivity remains elusive. The purpose of this study was to assess the function of individual PKC isozymes in  $\gamma$ -irradiation-mediated prostate cancer cell death. We demonstrated that inhibition of PKC activity by GF109203X radiosensitizes PC3 prostate cancer cells and significantly enhances  $\gamma$ -irradiation-mediated apoptosis. However, the fact that PKC isozymes exert different cellular functions required an analysis using specific inhibition or depletion of each PKC isozyme. As pharmacological inhibitors of PKC isozymes may not be very specific, we

decided to use shRNA lentiviruses to stably deplete PKC $\alpha$ , PKC $\delta$  or PKC $\epsilon$  from PC3 cells. Clonogenic survival assays revealed that depletion of PKC $\epsilon$  significantly radiosensitizes PC3 prostate cancer cells. In contrast, neither PKC $\alpha$  nor PKC $\delta$  depletion has any significant effect. These results revealed differential roles for discrete PKC isozymes in radiosensitivity of PC3 prostate cancer cells. Our analysis also supports the notion that membrane-activated signaling pathways play important roles in the regulation of radiation-mediated cell death/survival.

Irradiation could induce PKC activation, and several studies suggested potential roles for PKC in radiosensitization (73, 76, 77, 90, 129, 130, 164).  $\gamma$ -irradiation induces DAG production and activates PKC in cultured rat hepatocytes (129, 130). Our present study demonstrates that PKC $\epsilon$  translocates from the cytosol to the plasma membrane upon  $\gamma$ -irradiation. This effect is mediated by EGFR, as determined with EGFR inhibitor AG1478. Ionizing radiation causes a strong phosphorylation of Tyr992 in EGFR, a residue responsible for PLC $\gamma$  docking. Therefore, it may be possible that DAG generated in response to  $\gamma$ -irradiation via PLC $\gamma$  binds to the C1 domain in PKC $\epsilon$ , and that this represents the key event that causes PKC $\epsilon$  activation, ultimately resulting in radioresistance. Not surprisingly, a PLC inhibitor impairs PKC $\epsilon$  translocation by  $\gamma$ -irradiation.

There is extensive evidence that PKC $\epsilon$  mediates survival responses. Studies in the myocardium demonstrated a cardio-protective and anti-apoptotic role for PKC $\epsilon$  in ischemic preconditioning (37, 68, 106, 146). Association of an active PKC $\epsilon$  mutant with Src and Lck has been demonstrated to activate each of these

soluble tyrosine-kinases, and these interactions can be enhanced by ischemic preconditioning (145, 180). PKC $\epsilon$  associates with Akt, Bax and Bcl-2 in prostate cancer cells to modulate cellular apoptosis (121, 192). When overexpressed in LNCaP androgen-dependent prostate cancer cells, PKC $\epsilon$  confers androgen independence, accelerates G1/S transition, and enhances tumorigenic potential of these cells when inoculated into nude mice (190). More recently, Akt has been shown to be an effector of PKC $\epsilon$  that is implicated in the protection from ionizing radiation- and TNF $\alpha$ -induced breast cancer cell death (108). In our laboratory we generated a prostate-specific PKC $\epsilon$  transgenic mice that show prostatic hyperplasia and low-grade PINs (prostate intraepithelial neoplasia). These lesions present elevated levels of phospho-Akt, phospho-S6 and phospho-mTOR, suggesting enhanced survival signaling driven by PKC $\epsilon$  (unpublished data). As PKC $\epsilon$  is overexpressed in human prostate cancer, our results suggest that this kinase may represent an important mediator of prostate cancer progression. We speculate that PKC $\epsilon$ -specific inhibitors may be useful not only for the therapeutics of prostate cancer but also for sensitizing prostate cancer cells to chemotherapy and radiotherapy. From a mechanistic standpoint, our results support the concept that DAG-induced activation of PKC $\epsilon$  is an essential step in radioresistance. Translocation of PKC $\epsilon$  to the plasma membrane via PLC $\gamma$ -DAG is required for the pro-survival effect. On the other hand, PKC $\epsilon$  located in the perinuclear region (possibly bound to p23/Tmp21) is dispensable for survival. Thus, C1 domain-mediated translocation of PKC $\epsilon$  to the plasma membrane is a key event in radioresistance.

## **MATERIALS AND METHODS**

*Materials, cell culture and transfections*-Described in Chapter 2.

*Generation of PKC $\alpha$ , PKC $\delta$  and PKC $\epsilon$ -depleted cell lines using shRNA lentiviruses*- PC3 cells were infected with MISSION<sup>®</sup> lentiviral transduction particles encoding PKC $\alpha$ , PKC $\delta$ , or PKC $\epsilon$  shRNAs. PKC $\alpha$ , PKC $\delta$ , or PKC $\epsilon$  shRNA target sequences are shown in **Table 4.1**. Stable cell lines (pools) were generated by selection with puromycin (1  $\mu$ g/ml).

*Apoptosis assays*- Determination of apoptosis was carried out essentially as described in Chapter 2.

*Irradiation protocol*- PC3 cells were serum-starved for 72 h and then irradiated at different doses once using a Nordian GammaCell 40 irradiator.

*Clonogenic assay*- PC3 cells were trypsinized under sterile condition and plated into 60 mm tissue culture Petri dishes in triplicates at 100 cells/well (0, 2 Gy); 400 cells/well (4 Gy); 1,000 cells/well (6 Gy) and 2,000 cells/well (8 Gy). After 2 weeks, cells were fixed and stained with methylene blue. The number of colonies consisting of 50 or more cells was scored.

*Fluorescence microscopy*- pEGFP-PKC $\epsilon$  was transfected into PC3 cells using Lipofectamine 2000. After 24 h, cells were serum-starved for 72 h, subjected to  $\gamma$ -

irradiation for 5 min and fixed with cold ethanol (-20 °C) for 10 min. Slides were mounted using Fluoromount-G (SouthernBiotech, Birmingham, AL) and viewed with a Carl Zeiss LSM 710 laser-scanning microscope. The confocal images were processed with LSM Image Browser. Images represent individual middle sections of projected Z-series mounting.

*Western blot-* Experiments were carried out essentially as described in Chapter 2.

*Subcellular fractionation-* PC3 cells were harvested 2 h after  $\gamma$ -irradiation into lysis buffer (50 mM Tris-HCl, pH 7.4, 5 mM EGTA, 5  $\mu$ g/ml 4-(2-aminoethyl)-benzenesulfonyl fluoride, 5  $\mu$ g/ml leupeptin, 5  $\mu$ g/ml aprotinin, and 1  $\mu$ g/ml pepstatin A) and lysed by sonication. Separation of cytosolic (soluble) and particulate fractions was performed by ultracentrifugation as described previously (181). Equal amounts of protein (10  $\mu$ g) for each fraction were subjected to SDS-polyacrylamide gel electrophoresis, transferred to PVDF membranes, and immunostained with an anti-PKC $\epsilon$  antibody.



**Table 4.1** Sequences of MISSION<sup>®</sup> shRNA lentiviral transduction particles used to generate PKC $\alpha$ , PKC $\delta$ , or PKC $\epsilon$  stably-depleted PC3 cell lines.

---

**PKC $\alpha$  shRNA:**

TRCN0000001690 (PKC $\alpha$  #1)  
**CCGGCTTTGGAGTTTCGGAGCTGATCTCGAGATCAGCTCCGAAACTCCAAAGTTTTT**

TRCN0000001691 (PKC $\alpha$  #2)  
**CCGGCGAGCTATTTCACTATCATCTCGAGATGATAGACTGAAATAGCTCGTTTTT**

TRCN0000001692 (PKC $\alpha$  #3)  
**CCGGCATGGAAGCTCAGGCAGAAATTCTCGAGAATTTCTGCCTGAGTTCCATGTTTTT**

TRCN0000001693 (PKC $\alpha$  #4)  
**CCGGCCCGTCTTAACACCACCTGATCTCGAGATCAGGTGGTGTAAAGACGGGTTTTT**

TRCN0000001694 (PKC $\alpha$  #5)  
**CCGGACGGCTTGTGTCTGATTCCATCTCGAGATGGAATCAGACACAAGCCGTTTTT**

**PKC $\epsilon$  shRNA:**

TRCN0000000844 (PKC $\epsilon$  #1)  
**CCGGGCAGAAGCTCAAGGGCAAAGATCTCGAGATCTTTGCCCTTGAGTTCTGTTTTT**

TRCN0000000845 (PKC $\epsilon$  #2)  
**CCGGCCCTTCAAACCACGCATTAAACTCGAGTTAATGCGTGGTTTGAAGGGTTTTT**

TRCN0000000846 (PKC $\epsilon$  #3)  
**CCGGCCACAAGTTCCGTATCCACAACCTCGAGTTGTGGATACCGAACTTGTGGTTTTT**

TRCN0000000848 (PKC $\epsilon$  #4)  
**CCGGGCCAGAAGGAAGAGTGTATGTCTCGAGACATACACTCTTCCTTCTGGCTTTTTT**

**PKC $\delta$  shRNA:**

TRCN0000010193 (PKC $\delta$  #1)  
**CCGGGGCCGCTTTGAACTCTACCGTCTCGAGACGGTAGAGTTCAAAGCGGCCTTTTTT**

TRCN0000010194 (PKC $\delta$  #2)  
**CCGGCAAGGCTACAAATGCAGGCAACTCGAGTTGCCTGCATTTGTAGCCTTGTTTTT**

TRCN0000010202 (PKC $\delta$  #3)  
**CCGGGCAAGACAACAGTGGGACCTACTCGAGTAGGTCCCACTGTTGTCTTGCTTTTTT**

TRCN0000010203 (PKC $\delta$  #4)  
**CCGGGCAGGGATTAAAGTGTGAAGACTCGAGTCTTCACACTTTAATCCCTGCTTTTTT**

---

## **CHAPTER 5**

### **Final Remarks**

The second messenger DAG signaling pathway has gained great attention as a crucial regulatory mechanism in the control of cell proliferation, differentiation, apoptosis, cancer initiation and progression. Cysteine-rich (C1) domains were first identified in PKC isozymes as the motifs that bind DAG and phorbol esters. Now it is recognized that C1 domains are also present in chimaerins, RasGRPs, MRCKs, PKDs, DGKs, and Munc-13s (21, 86). Upon binding DAG or phorbol esters, C1 domain-containing proteins translocate to the plasma membrane and other intracellular compartments, including the nuclear membrane, the perinuclear region, the nucleus, and mitochondria. Remarkably, redistribution of C1 domain-containing proteins to distinctive compartments has a significant degree of isozyme-selectivity and ligand-dependence. In addition to their plasma membrane targeting, specificity of PKC isozymes function is also controlled by their association with interacting proteins. In this thesis research, I have studied the regulations and functions of proteins regulated via their C1 domains, including  $\beta$ 2-chimaerin, PKC $\delta$  and PKC $\epsilon$ , in different paradigms in which protein-protein interactions and C1 domain targeting are involved.

In Chapter 2 of this thesis, I present evidence that p23/Tmp21 acts as a C1 domain-docking protein that mediates perinuclear translocation of  $\beta$ 2-chimaerin. Glu227 and Leu248 in the  $\beta$ 2-chimaerin C1 domain are crucial for binding p23/Tmp21 and perinuclear targeting.  $\beta$ 2-chimaerin (Glu227/Leu248) mutant is more active as a Rac-GAP than wild-type  $\beta$ 2-chimaerin. Our previous finding that overexpression of p23/Tmp21 significantly inhibits  $\beta$ 2-chimaerin Rac-GAP activity in COS cells (180), suggests that association of  $\beta$ 2-chimaerin with

p23/Tmp21 limits activation. Recently, a unique phosphorylation site, Ser169, on the  $\beta$ 2-chimaerin Rac-GAP was identified. Phosphorylation at this site by another DAG/phorbol esters receptor (PKC $\delta$ ) negatively regulates  $\beta$ 2-chimaerin plasma membrane translocation, association with V12Rac1, and Rac-GAP activity (Griner *et al.*, submitted for publication). Thus, both Ser169 phosphorylation by PKC $\delta$  and association with p23/Tmp21 represent mechanisms that modulate Rac-GAP activity of  $\beta$ 2-chimaerin (**Figure 1.9**), suggesting a crosstalk between DAG receptors. Importantly we also found that PKC $\delta$  interacts with p23/Tmp21 in the perinuclear region (Chapters 2 and 3). Furthermore, unpublished data revealed that PMA-induced phosphorylation of  $\beta$ 2-chimaerin is significantly decreased in HeLa cells in which p23/Tmp21 has been depleted using shRNA. Collectively, these results imply that p23/Tmp21 plays a role in regulating PKC $\delta$ -mediated  $\beta$ 2-chimaerin phosphorylation. One speculation is that p23/Tmp21 may act as a scaffold protein or a platform for PKC $\delta$ -mediated phosphorylation of  $\beta$ 2-chimaerin. Another possibility might be that phosphorylated  $\beta$ 2-chimaerin preferentially associates with p23/Tmp21 in the perinuclear ER/Golgi region. Future experiments are needed to dissect the role of p23/Tmp21 in the phosphorylation of  $\beta$ 2-chimaerin and determine if Ser169 phosphorylation of  $\beta$ 2-chimaerin affects its association with p23/Tmp21. It still remains unclear what is the physiological function of the p23/Tmp21- $\beta$ 2-chimaerin interaction in perinuclear/Golgi region upon stimulation by DAG/phorbol esters. We previously demonstrated that p23/Tmp21 overexpression counteracts the  $\beta$ 2-chimaerin Rac-GAP activity. Our present study revealed that disruption of p23/Tmp21- $\beta$ 2-

chimaerin complex enhances chimaerin Rac-GAP activity. Therefore, we propose that p23/Tmp21 might act as an anchoring protein for  $\beta$ 2-chimaerin. This may serve various purposes. One is a potential involvement of this Rac-GAP in maintaining a pool of inactive Rac in the perinucleus that can mobilize to the plasma membrane in response to different stimuli (see below). Another possible scenario could be that p23/Tmp21 participates in the intracellular trafficking and sorting. We do not have any experimental results to support this hypothesis, and therefore further studies are needed to dissect this possible process. Time-lapse images demonstrated that upon EGF or PMA treatment,  $\beta$ 2-chimaerin translocates to plasma membrane within 5 min. and then relocalize to the perinuclear region. We thought this dual translocation of  $\beta$ 2-chimaerin might be involved in two steps. In the first step,  $\beta$ 2-chimaerin translocates to plasma membrane to interact with Rac-GTP and down-regulate Rac signals. Subsequently,  $\beta$ 2-chimaerin, after an unknown modification (may be phosphorylation by PKC $\delta$ ), might preferably bind to p23/Tmp21 and translocate from plasma membrane to perinuclear region. Rac is generally thought to cycle between a cytosolic inactive form and an active plasma membrane form. Because a pool of  $\beta$ 2-chimaerin localizes to the plasma membrane upon activation, it is possible that this pool of  $\beta$ 2-chimaerin deactivates Rac at that location. Recent studies have shown that a large pool of Rac is located in the perinuclear region and that this pool of Rac is in its GDP-bound form (95). We speculate that  $\beta$ 2-chimaerin might play a role in the maintenance of this perinuclear pool of Rac in an inactive state before this Rac-GTPase moves to the plasma membrane. Another speculation is that  $\beta$ 2-chimaerin

might be very important for maintaining Golgi structure or functions. Indeed, a previous study revealed that  $\alpha$ 1-chimaerin regulates Golgi stability during interphase (Alonso, M., *et al.* Eur J Cell Biol **76**:93-101.). Further studies are needed to investigate the role of  $\beta$ 2-chimaerin in Golgi functions.

Interestingly, isolated C1 domains from individual PKC isozymes or RasGRP1 differentially interact with p23/Tmp21. In Chapter 3 of this thesis, we demonstrated using a yeast two-hybrid assay that the PKC $\delta$  C1a-b domain interacts with p23/Tmp21. Co-localization analysis by confocal microscopy demonstrated that the C1b domain in PKC $\delta$  is the motif that interacts with p23/Tmp21 in the perinuclear region. In addition, immunoprecipitation analysis and confocal images demonstrated that PKC $\delta$  and p23/Tmp21 form a complex in LNCaP cells. Future experiments are needed to address whether PKC $\delta$  C1b domain interacts with p23/Tmp21 in the same way as PKC $\epsilon$  C1b and  $\beta$ 2-chimaerin C1 domains. Mutations in the corresponding amino acids in PKC $\delta$  should abolish its association with p23/Tmp21 and promote its activity.

Our laboratory and others have established that androgen-dependent prostate cancer cells undergo apoptosis upon phorbol ester treatment, and that the effect was primarily mediated by PKC $\delta$ . By using this paradigm, I now demonstrated that depletion of p23/Tmp21 significantly potentiates PMA-induced apoptosis in LNCaP cells, and notably the effect was rescued by PKC $\delta$  RNAi depletion or treatment with a PKC inhibitor, suggesting that the potentiating apoptotic effect of p23/Tmp21 depletion was mediated by PKC $\delta$ . Interestingly, disruption of PKC $\delta$ -p23/Tmp21 association by depletion of p23/Tmp21 enhances PMA-induced

PKC $\delta$  plasma membrane translocation and activation of the PKC $\delta$  downstream effectors ROCK and JNK, indicating p23/Tmp21 acts as an anchoring protein that limits PKC $\delta$  activation and negatively regulates PMA-induced apoptosis in LNCaP cells. Furthermore, our experiments also demonstrated that depletion of p23/Tmp21 potentiates doxorubicin-mediated apoptosis, a PKC $\delta$ -dependent effect (143). Thus p23/Tmp21 is a negative modulator of PKC $\delta$ -mediated responses. Based on the results presented here, it would be also important to determine if p23/Tmp21 modulates response by RasGRP1 or PKC $\epsilon$ . One speculation is that depletion or down-regulation of p23/Tmp21 might lead to more availability of RasGRP1 or PKC $\epsilon$ . Since these two proteins play important roles in cell transformation, p23/Tmp21 may be also implicated in cancer progression. It would be interesting to analyze the p23/Tmp21 expression profile in different cancer cell lines and tumor samples to determine any potential relationship between p23/Tmp21 expression and tumor progression.

In Chapter 4 of this thesis, I demonstrated that PKC inhibition radiosensitizes PC3 prostate cancer cells. Using a lentiviral-based shRNA delivery approach, I demonstrated that depletion of PKC $\epsilon$  but not PKC $\alpha$  or PKC $\delta$  radiosensitizes PC3 cell. In addition, our experiments revealed that clinically relevant doses of  $\gamma$ -irradiation significantly enhanced PKC $\epsilon$  translocation from the cytosol to the particulate fraction. Moreover, confocal images demonstrated that the EGFR inhibitor AG1478, PLC inhibitor U73122, as well as the reactive oxygen species (ROS) scavenger NAC significantly impair  $\gamma$ -irradiation-induced translocation of PKC $\epsilon$  to the plasma membrane, suggesting that PKC $\epsilon$  is a downstream effector of

the ROS-EGFR-PLC $\gamma$ -DAG signaling pathway and may confer cytoprotective effects upon ionizing radiation. It would be important to determine how activated PKC $\epsilon$  relays signals to downstream effectors that generate the cytoprotective effects. PKC $\epsilon$  can activate MAPKs and lead to the expression of transcription factors, such as CREB, Egr, Est, Stat3, C/EBP and Stat1. PKC $\epsilon$  may also activate Akt or Bcl-2 family members to generate pro-survival effects. In any case, a detailed analysis would be needed to investigate the mechanisms involved in PKC $\epsilon$ -mediated radioresistant effects. It will be also worthwhile to examine the radiosensitizing effect of PKC $\epsilon$  specific inhibitors. Conceivably, specific inhibition of PKC $\epsilon$  may be a useful therapeutic approach to sensitize prostate cancer cells or other cancer cells to  $\gamma$ -irradiation. Not surprisingly, PKC $\epsilon$  also modulates the sensitivity of cancer cells to chemotherapeutic agents (10). Our study highlights the relevance of membrane-related signal cascades other than irradiation-induced DNA damage/repair pathways in controlling ionizing irradiation-induced cell death.

In summary, our studies suggest that the C1 domain plays important roles in modulating the activation of signaling molecules via dual mechanism (**Figure 5.1**). Both lipid binding and protein-protein interactions determine the localization of C1 domain-containing proteins, and these represent essential steps in the activation of these proteins.



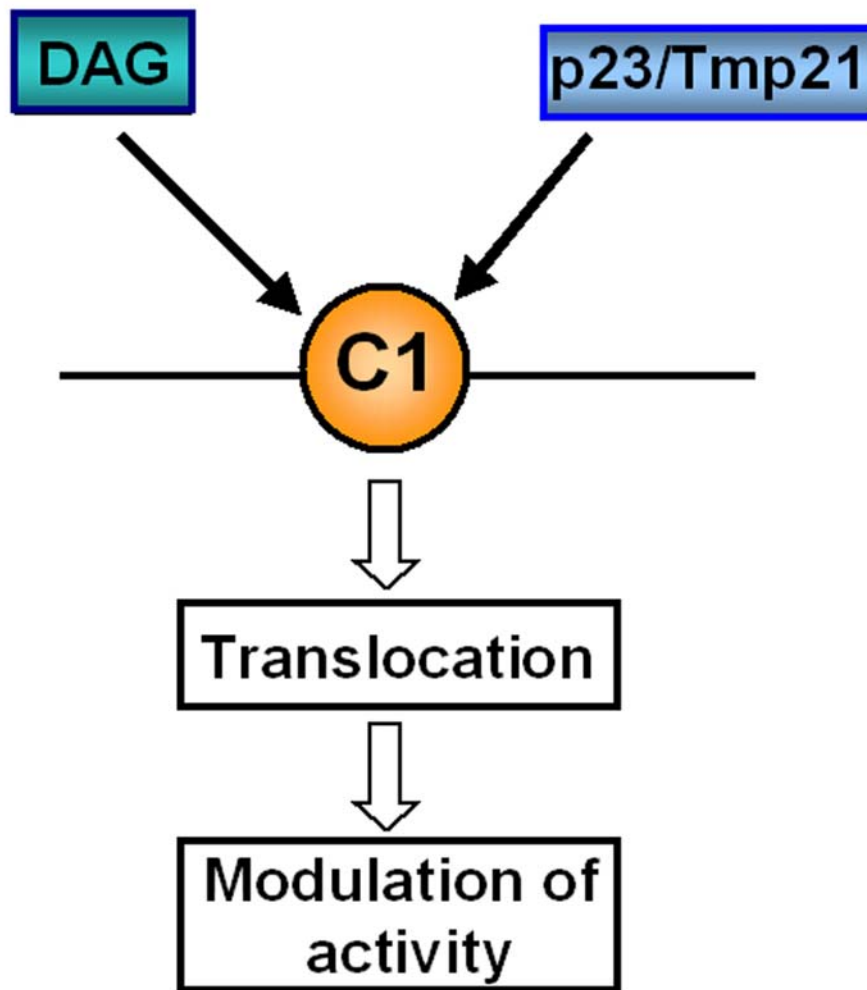


**Figure 5.1** Proposed model of regulation of the C1 domain-containing proteins.

## **BIBLIOGRAPHY**

1. **Ahmed, S., R. Kozma, J. Lee, C. Monfries, N. Harden, and L. Lim.** 1991. The cysteine-rich domain of human proteins, neuronal chimaerin, protein kinase C and diacylglycerol kinase binds zinc. Evidence for the involvement of a zinc-dependent structure in phorbol ester binding. *Biochem J* **280 ( Pt 1)**:233-41.
2. **Amorino, G. P., V. M. Hamilton, K. Valerie, P. Dent, G. Lammering, and R. K. Schmidt-Ullrich.** 2002. Epidermal growth factor receptor dependence of radiation-induced transcription factor activation in human breast carcinoma cells. *Mol Biol Cell* **13**:2233-44.
3. **Anantharam, V., M. Kitazawa, J. Wagner, S. Kaul, and A. G. Kanthasamy.** 2002. Caspase-3-dependent proteolytic cleavage of protein kinase Cdelta is essential for oxidative stress-mediated dopaminergic cell death after exposure to methylcyclopentadienyl manganese tricarbonyl. *J Neurosci* **22**:1738-51.
4. **Anilkumar, N., M. Parsons, R. Monk, T. Ng, and J. C. Adams.** 2003. Interaction of fascin and protein kinase Calpha: a novel intersection in cell adhesion and motility. *EMBO J* **22**:5390-402.
5. **Aziz, M. H., H. T. Manoharan, D. R. Church, N. E. Dreckschmidt, W. Zhong, T. D. Oberley, G. Wilding, and A. K. Verma.** 2007. Protein kinase Cepsilon interacts with signal transducers and activators of transcription 3 (Stat3), phosphorylates Stat3Ser727, and regulates its constitutive activation in prostate cancer. *Cancer Res* **67**:8828-38.
6. **Bae, K. M., H. Wang, G. Jiang, M. G. Chen, L. Lu, and L. Xiao.** 2007. Protein kinase C epsilon is overexpressed in primary human non-small cell lung cancers and functionally required for proliferation of non-small cell lung cancer cells in a p21/Cip1-dependent manner. *Cancer Res* **67**:6053-63.
7. **Barthel, A., K. Nakatani, A. A. Dandekar, and R. A. Roth.** 1998. Protein kinase C modulates the insulin-stimulated increase in Akt1 and Akt3 activity in 3T3-L1 adipocytes. *Biochem Biophys Res Commun* **243**:509-13.
8. **Basu, A., and J. S. Cline.** 1995. Oncogenic transformation alters cisplatin-induced apoptosis in rat embryo fibroblasts. *Int J Cancer* **63**:597-603.
9. **Basu, A., D. Lu, B. Sun, A. N. Moor, G. R. Akkaraju, and J. Huang.** 2002. Proteolytic activation of protein kinase C-epsilon by caspase-mediated processing and transduction of antiapoptotic signals. *J Biol Chem* **277**:41850-6.
10. **Basu, A., and U. Sivaprasad.** 2007. Protein kinase Cepsilon makes the life and death decision. *Cell Signal* **19**:1633-42.
11. **Basu, A., and K. M. Weixel.** 1995. Comparison of protein kinase C activity and isoform expression in cisplatin-sensitive and -resistant ovarian carcinoma cells. *Int J Cancer* **62**:457-60.
12. **Beg, A. A., J. E. Sommer, J. H. Martin, and P. Scheiffele.** 2007. alpha2-Chimaerin is an essential EphA4 effector in the assembly of neuronal locomotor circuits. *Neuron* **55**:768-78.

13. **Betz, A., U. Ashery, M. Rickmann, I. Augustin, E. Neher, T. C. Sudhof, J. Rettig, and N. Brose.** 1998. Munc13-1 is a presynaptic phorbol ester receptor that enhances neurotransmitter release. *Neuron* **21**:123-36.
14. **Bharti, A., S. K. Kraeft, M. Gounder, P. Pandey, S. Jin, Z. M. Yuan, S. P. Lees-Miller, R. Weichselbaum, D. Weaver, L. B. Chen, D. Kufe, and S. Kharbanda.** 1998. Inactivation of DNA-dependent protein kinase by protein kinase Cdelta: implications for apoptosis. *Mol Cell Biol* **18**:6719-28.
15. **Blass, M., I. Kronfeld, G. Kazimirsky, P. M. Blumberg, and C. Brodie.** 2002. Tyrosine phosphorylation of protein kinase Cdelta is essential for its apoptotic effect in response to etoposide. *Mol Cell Biol* **22**:182-95.
16. **Blum, R., P. Feick, M. Puype, J. Vandekerckhove, R. Klengel, W. Nastainczyk, and I. Schulz.** 1996. Tmp21 and p24A, two type I proteins enriched in pancreatic microsomal membranes, are members of a protein family involved in vesicular trafficking. *J Biol Chem* **271**:17183-9.
17. **Blum, R., and A. Lepier.** 2008. The luminal domain of p23 (Tmp21) plays a critical role in p23 cell surface trafficking. *Traffic* **9**:1530-50.
18. **Blum, R., F. Pfeiffer, P. Feick, W. Nastainczyk, B. Kohler, K. H. Schafer, and I. Schulz.** 1999. Intracellular localization and in vivo trafficking of p24A and p23. *J Cell Sci* **112 ( Pt 4)**:537-48.
19. **Blumberg, P. M.** 1991. Complexities of the protein kinase C pathway. *Mol Carcinog* **4**:339-44.
20. **Brodie, C., and P. M. Blumberg.** 2003. Regulation of cell apoptosis by protein kinase c delta. *Apoptosis* **8**:19-27.
21. **Brose, N., and C. Rosenmund.** 2002. Move over protein kinase C, you've got company: alternative cellular effectors of diacylglycerol and phorbol esters. *J Cell Sci* **115**:4399-411.
22. **Bruinsma, S. P., R. L. Cagan, and T. J. Baranski.** 2007. Chimaerin and Rac regulate cell number, adherens junctions, and ERK MAP kinase signaling in the *Drosophila* eye. *Proc Natl Acad Sci U S A* **104**:7098-103.
23. **Buccione, R., S. Bannykh, I. Santone, M. Baldassarre, F. Facchiano, Y. Bozzi, G. Di Tullio, A. Mironov, A. Luini, and M. A. De Matteis.** 1996. Regulation of constitutive exocytic transport by membrane receptors. A biochemical and morphometric study. *J Biol Chem* **271**:3523-33.
24. **Cacace, A. M., S. N. Guadagno, R. S. Krauss, D. Fabbro, and I. B. Weinstein.** 1993. The epsilon isoform of protein kinase C is an oncogene when overexpressed in rat fibroblasts. *Oncogene* **8**:2095-104.
25. **Caloca, M. J., N. Fernandez, N. E. Lewin, D. Ching, R. Modali, P. M. Blumberg, and M. G. Kazanietz.** 1997. Beta2-chimaerin is a high affinity receptor for the phorbol ester tumor promoters. *J Biol Chem* **272**:26488-96.
26. **Caloca, M. J., M. L. Garcia-Bermejo, P. M. Blumberg, N. E. Lewin, E. Kremmer, H. Mischak, S. Wang, K. Nacro, B. Bienfait, V. E. Marquez, and M. G. Kazanietz.** 1999. beta2-chimaerin is a novel target for diacylglycerol: binding properties and changes in subcellular localization mediated by ligand binding to its C1 domain. *Proc Natl Acad Sci U S A* **96**:11854-9.
27. **Caloca, M. J., H. Wang, A. Delemos, S. Wang, and M. G. Kazanietz.** 2001. Phorbol esters and related analogs regulate the subcellular localization of beta 2-

- chimaerin, a non-protein kinase C phorbol ester receptor. *J Biol Chem* **276**:18303-12.
28. **Caloca, M. J., H. Wang, and M. G. Kazanietz.** 2003. Characterization of the Rac-GAP (Rac-GTPase-activating protein) activity of beta2-chimaerin, a 'non-protein kinase C' phorbol ester receptor. *Biochem J* **375**:313-21.
  29. **Canagarajah, B., F. C. Leskow, J. Y. Ho, H. Mischak, L. F. Saidi, M. G. Kazanietz, and J. H. Hurley.** 2004. Structural mechanism for lipid activation of the Rac-specific GAP, beta2-chimaerin. *Cell* **119**:407-18.
  30. **Cardone, M. H., B. L. Smith, W. Song, D. Mochly-Rosen, and K. E. Mostov.** 1994. Phorbol myristate acetate-mediated stimulation of transcytosis and apical recycling in MDCK cells. *J Cell Biol* **124**:717-27.
  31. **Carsberg, C. J., J. Ohanian, and P. S. Friedmann.** 1995. Ultraviolet radiation stimulates a biphasic pattern of 1,2-diacylglycerol formation in cultured human melanocytes and keratinocytes by activation of phospholipases C and D. *Biochem J* **305 ( Pt 2)**:471-7.
  32. **Castagna, M., Y. Takai, K. Kaibuchi, K. Sano, U. Kikkawa, and Y. Nishizuka.** 1982. Direct activation of calcium-activated, phospholipid-dependent protein kinase by tumor-promoting phorbol esters. *J Biol Chem* **257**:7847-51.
  33. **Chen, D., C. Gould, R. Garza, T. Gao, R. Y. Hampton, and A. C. Newton.** 2007. Amplitude control of protein kinase C by RINCK, a novel E3 ubiquitin ligase. *J Biol Chem* **282**:33776-87.
  34. **Chen, D., A. Purohit, E. Halilovic, S. J. Doxsey, and A. C. Newton.** 2004. Centrosomal anchoring of protein kinase C betaII by pericentrin controls microtubule organization, spindle function, and cytokinesis. *J Biol Chem* **279**:4829-39.
  35. **Chen, F., H. Hasegawa, G. Schmitt-Ulms, T. Kawarai, C. Bohm, T. Katayama, Y. Gu, N. Sanjo, M. Glista, E. Rogaeva, Y. Wakutani, R. Pardossi-Piquard, X. Ruan, A. Tandon, F. Checler, P. Marambaud, K. Hansen, D. Westaway, P. St George-Hyslop, and P. Fraser.** 2006. TMP21 is a presenilin complex component that modulates gamma-secretase but not epsilon-secretase activity. *Nature* **440**:1208-12.
  36. **Chen, J., F. Deng, J. Li, and Q. J. Wang.** 2008. Selective binding of phorbol esters and diacylglycerol by individual C1 domains of the PKD family. *Biochem J* **411**:333-42.
  37. **Chen, L., H. Hahn, G. Wu, C. H. Chen, T. Liron, D. Schechtman, G. Cavallaro, L. Banci, Y. Guo, R. Bolli, G. W. Dorn, 2nd, and D. Mochly-Rosen.** 2001. Opposing cardioprotective actions and parallel hypertrophic effects of delta PKC and epsilon PKC. *Proc Natl Acad Sci U S A* **98**:11114-9.
  38. **Chmura, S. J., E. Nodzenski, M. A. Beckett, D. W. Kufe, J. Quintans, and R. R. Weichselbaum.** 1997. Loss of ceramide production confers resistance to radiation-induced apoptosis. *Cancer Res* **57**:1270-5.
  39. **Choi, S. H., G. Czifra, N. Kedei, N. E. Lewin, J. Lazar, Y. Pu, V. E. Marquez, and P. M. Blumberg.** 2008. Characterization of the interaction of phorbol esters with the C1 domain of MRCK (myotonic dystrophy kinase-related Cdc42 binding kinase) alpha/beta. *J Biol Chem* **283**:10543-9.

40. **Clark, A. S., K. A. West, P. M. Blumberg, and P. A. Dennis.** 2003. Altered protein kinase C (PKC) isoforms in non-small cell lung cancer cells: PKCdelta promotes cellular survival and chemotherapeutic resistance. *Cancer Res* **63**:780-6.
41. **Collart, F. R., M. Horio, and E. Huberman.** 1995. Heterogeneity in c-jun gene expression in normal and malignant cells exposed to either ionizing radiation or hydrogen peroxide. *Radiat Res* **142**:188-96.
42. **Colon-Gonzalez, F., and M. G. Kazanietz.** 2006. C1 domains exposed: from diacylglycerol binding to protein-protein interactions. *Biochim Biophys Acta* **1761**:827-37.
43. **Colon-Gonzalez, F., F. C. Leskow, and M. G. Kazanietz.** 2008. Identification of an autoinhibitory mechanism that restricts C1 domain-mediated activation of the Rac-GAP alpha2-chimaerin. *J Biol Chem* **283**:35247-57.
44. **Cornford, P., J. Evans, A. Dodson, K. Parsons, A. Woolfenden, J. Neoptolemos, and C. S. Foster.** 1999. Protein kinase C isoenzyme patterns characteristically modulated in early prostate cancer. *Am J Pathol* **154**:137-44.
45. **Csukai, M., C. H. Chen, M. A. De Matteis, and D. Mochly-Rosen.** 1997. The coatomer protein beta'-COP, a selective binding protein (RACK) for protein kinase Cepsilon. *J Biol Chem* **272**:29200-6.
46. **Csukai, M., and D. Mochly-Rosen.** 1999. Pharmacologic modulation of protein kinase C isozymes: the role of RACKs and subcellular localisation. *Pharmacol Res* **39**:253-9.
47. **Dbaiibo, G. S., L. M. Obeid, and Y. A. Hannun.** 1993. Tumor necrosis factor-alpha (TNF-alpha) signal transduction through ceramide. Dissociation of growth inhibitory effects of TNF-alpha from activation of nuclear factor-kappa B. *J Biol Chem* **268**:17762-6.
48. **De Matteis, M. A., G. Santini, R. A. Kahn, G. Di Tullio, and A. Luini.** 1993. Receptor and protein kinase C-mediated regulation of ARF binding to the Golgi complex. *Nature* **364**:818-21.
49. **DeVries, T. A., M. C. Neville, and M. E. Reyland.** 2002. Nuclear import of PKCdelta is required for apoptosis: identification of a novel nuclear import sequence. *EMBO J* **21**:6050-60.
50. **Ding, L., H. Wang, W. Lang, and L. Xiao.** 2002. Protein kinase C-epsilon promotes survival of lung cancer cells by suppressing apoptosis through dysregulation of the mitochondrial caspase pathway. *J Biol Chem* **277**:35305-13.
51. **Diouf, B., A. Collazos, G. Labesse, F. Macari, A. Choquet, P. Clair, C. Gauthier-Rouviere, N. C. Guerineau, P. Jay, F. Hollande, and D. Joubert.** 2009. A 20-amino acid module of protein kinase C{epsilon} involved in translocation and selective targeting at cell-cell contacts. *J Biol Chem* **284**:18808-15.
52. **Ebinu, J. O., D. A. Bottorff, E. Y. Chan, S. L. Stang, R. J. Dunn, and J. C. Stone.** 1998. RasGRP, a Ras guanyl nucleotide- releasing protein with calcium- and diacylglycerol-binding motifs. *Science* **280**:1082-6.
53. **Elrod-Erickson, M. J., and C. A. Kaiser.** 1996. Genes that control the fidelity of endoplasmic reticulum to Golgi transport identified as suppressors of vesicle budding mutations. *Mol Biol Cell* **7**:1043-58.

54. **Emoto, Y., Y. Manome, G. Meinhardt, H. Kisaki, S. Kharbanda, M. Robertson, T. Ghayur, W. W. Wong, R. Kamen, R. Weichselbaum, and et al.** 1995. Proteolytic activation of protein kinase C delta by an ICE-like protease in apoptotic cells. *Embo J* **14**:6148-56.
55. **Fawcett, J. P., J. Georgiou, J. Ruston, F. Bladt, A. Sherman, N. Warner, B. J. Saab, R. Scott, J. C. Roder, and T. Pawson.** 2007. Nck adaptor proteins control the organization of neuronal circuits important for walking. *Proc Natl Acad Sci U S A* **104**:20973-8.
56. **Flescher, E., and R. Rotem.** 2002. Protein kinase C epsilon mediates the induction of P-glycoprotein in LNCaP prostate carcinoma cells. *Cell Signal* **14**:37-43.
57. **Fucini, R. V., J. L. Chen, C. Sharma, M. M. Kessels, and M. Starnes.** 2002. Golgi vesicle proteins are linked to the assembly of an actin complex defined by mAbp1. *Mol Biol Cell* **13**:621-31.
58. **Fujii, T., M. L. Garcia-Bermejo, J. L. Bernabo, J. Caamano, M. Ohba, T. Kuroki, L. Li, S. H. Yuspa, and M. G. Kazanietz.** 2000. Involvement of protein kinase C delta (PKCdelta) in phorbol ester-induced apoptosis in LNCaP prostate cancer cells. Lack of proteolytic cleavage of PKCdelta. *J Biol Chem* **275**:7574-82.
59. **Fukunaga, M., M. Oka, M. Ichihashi, T. Yamamoto, H. Matsuzaki, and U. Kikkawa.** 2001. UV-induced tyrosine phosphorylation of PKC delta and promotion of apoptosis in the HaCaT cell line. *Biochem Biophys Res Commun* **289**:573-9.
60. **Gavrielides, M. V., A. F. Frijhoff, C. J. Conti, and M. G. Kazanietz.** 2004. Protein kinase C and prostate carcinogenesis: targeting the cell cycle and apoptotic mechanisms. *Curr Drug Targets* **5**:431-43.
61. **Ghayur, T., M. Hugunin, R. V. Talanian, S. Ratnofsky, C. Quinlan, Y. Emoto, P. Pandey, R. Datta, Y. Huang, S. Kharbanda, H. Allen, R. Kamen, W. Wong, and D. Kufe.** 1996. Proteolytic activation of protein kinase C delta by an ICE/CED 3-like protease induces characteristics of apoptosis. *J Exp Med* **184**:2399-404.
62. **Gillespie, S., X. D. Zhang, and P. Hersey.** 2005. Variable expression of protein kinase C epsilon in human melanoma cells regulates sensitivity to TRAIL-induced apoptosis. *Mol Cancer Ther* **4**:668-76.
63. **Goldkorn, T., N. Balaban, M. Shannon, V. Chea, K. Matsukuma, D. Gilchrist, H. Wang, and C. Chan.** 1998. H<sub>2</sub>O<sub>2</sub> acts on cellular membranes to generate ceramide signaling and initiate apoptosis in tracheobronchial epithelial cells. *J Cell Sci* **111 ( Pt 21)**:3209-20.
64. **Gomez, D. E., G. Skilton, D. F. Alonso, and M. G. Kazanietz.** 1999. The role of protein kinase C and novel phorbol ester receptors in tumor cell invasion and metastasis (Review). *Oncol Rep* **6**:1363-70.
65. **Gommel, D. U., A. R. Memon, A. Heiss, F. Lottspeich, J. Pfannstiel, J. Lechner, C. Reinhard, J. B. Helms, W. Nickel, and F. T. Wieland.** 2001. Recruitment to Golgi membranes of ADP-ribosylation factor 1 is mediated by the cytoplasmic domain of p23. *Embo J* **20**:6751-60.
66. **Gonzalez-Guerrico, A. M., and M. G. Kazanietz.** 2005. Phorbol ester-induced apoptosis in prostate cancer cells via autocrine activation of the extrinsic

- apoptotic cascade: a key role for protein kinase C delta. *J Biol Chem* **280**:38982-91.
67. **Grant, S., W. D. Jarvis, P. S. Swerdlow, A. J. Turner, R. S. Traylor, H. J. Wallace, P. S. Lin, G. R. Pettit, and D. A. Gewirtz.** 1992. Potentiation of the activity of 1-beta-D-arabinofuranosylcytosine by the protein kinase C activator bryostatin 1 in HL-60 cells: association with enhanced fragmentation of mature DNA. *Cancer Res* **52**:6270-8.
  68. **Gray, M. O., J. S. Karliner, and D. Mochly-Rosen.** 1997. A selective epsilon-protein kinase C antagonist inhibits protection of cardiac myocytes from hypoxia-induced cell death. *J Biol Chem* **272**:30945-51.
  69. **Greene, N. M., D. S. Williams, and A. C. Newton.** 1995. Kinetics and localization of the phosphorylation of rhodopsin by protein kinase C. *J Biol Chem* **270**:6710-7.
  70. **Griner, E. M., and M. G. Kazanietz.** 2007. Protein kinase C and other diacylglycerol effectors in cancer. *Nat Rev Cancer* **7**:281-94.
  71. **Guan, L., K. Song, M. A. Pysz, K. J. Curry, A. A. Hizli, D. Danielpour, A. R. Black, and J. D. Black.** 2007. Protein kinase C-mediated down-regulation of cyclin D1 involves activation of the translational repressor 4E-BP1 via a phosphoinositide 3-kinase/Akt-independent, protein phosphatase 2A-dependent mechanism in intestinal epithelial cells. *J Biol Chem* **282**:14213-25.
  72. **Gudkov, A. V., and E. A. Komarova.** 2003. The role of p53 in determining sensitivity to radiotherapy. *Nat Rev Cancer* **3**:117-29.
  73. **Haimovitz-Friedman, A., N. Balaban, M. McLoughlin, D. Ehleiter, J. Michaeli, I. Vlodaysky, and Z. Fuks.** 1994. Protein kinase C mediates basic fibroblast growth factor protection of endothelial cells against radiation-induced apoptosis. *Cancer Res* **54**:2591-7.
  74. **Hall, C., G. J. Michael, N. Cann, G. Ferrari, M. Teo, T. Jacobs, C. Monfries, and L. Lim.** 2001. alpha2-chimaerin, a Cdc42/Rac1 regulator, is selectively expressed in the rat embryonic nervous system and is involved in neuritogenesis in N1E-115 neuroblastoma cells. *J Neurosci* **21**:5191-202.
  75. **Hall, C., C. Monfries, P. Smith, H. H. Lim, R. Kozma, S. Ahmed, V. Vanniasingham, T. Leung, and L. Lim.** 1990. Novel human brain cDNA encoding a 34,000 Mr protein n-chimaerin, related to both the regulatory domain of protein kinase C and BCR, the product of the breakpoint cluster region gene. *J Mol Biol* **211**:11-6.
  76. **Hallahan, D. E., S. Virudachalam, J. L. Schwartz, N. Panje, R. Mustafi, and R. R. Weichselbaum.** 1992. Inhibition of protein kinases sensitizes human tumor cells to ionizing radiation. *Radiat Res* **129**:345-50.
  77. **Hallahan, D. E., S. Virudachalam, M. L. Sherman, E. Huberman, D. W. Kufe, and R. R. Weichselbaum.** 1991. Tumor necrosis factor gene expression is mediated by protein kinase C following activation by ionizing radiation. *Cancer Res* **51**:4565-9.
  78. **Hausser, A., P. Storz, G. Link, H. Stoll, Y. C. Liu, A. Altman, K. Pfizenmaier, and F. J. Johannes.** 1999. Protein kinase C mu is negatively regulated by 14-3-3 signal transduction proteins. *J Biol Chem* **274**:9258-64.

79. **Heasman, S. J., and A. J. Ridley.** 2008. Mammalian Rho GTPases: new insights into their functions from in vivo studies. *Nat Rev Mol Cell Biol* **9**:690-701.
80. **Hu, T., and J. H. Exton.** 2004. Protein kinase C $\alpha$  translocates to the perinuclear region to activate phospholipase D1. *J Biol Chem* **279**:35702-8.
81. **Hwang, S. O., S. A. Boswell, J. S. Seo, and S. W. Lee.** 2008. Novel oxidative stress-responsive gene ERS25 functions as a regulator of the heat-shock and cell death response. *J Biol Chem* **283**:13063-9.
82. **Inoue, M., A. Kishimoto, Y. Takai, and Y. Nishizuka.** 1977. Studies on a cyclic nucleotide-independent protein kinase and its proenzyme in mammalian tissues. II. Proenzyme and its activation by calcium-dependent protease from rat brain. *J Biol Chem* **252**:7610-6.
83. **Iwasato, T., H. Katoh, H. Nishimaru, Y. Ishikawa, H. Inoue, Y. M. Saito, R. Ando, M. Iwama, R. Takahashi, M. Negishi, and S. Itohara.** 2007. Rac-GAP alpha-chimerin regulates motor-circuit formation as a key mediator of EphrinB3/EphA4 forward signaling. *Cell* **130**:742-53.
84. **Kazanietz, M. G.** 2000. Eyes wide shut: protein kinase C isozymes are not the only receptors for the phorbol ester tumor promoters. *Mol Carcinog* **28**:5-11.
85. **Kazanietz, M. G., L. B. Areces, A. Bahador, H. Mischak, J. Goodnight, J. F. Mushinski, and P. M. Blumberg.** 1993. Characterization of ligand and substrate specificity for the calcium-dependent and calcium-independent protein kinase C isozymes. *Mol Pharmacol* **44**:298-307.
86. **Kazanietz, M. G., M. J. Caloca, P. Eroles, T. Fujii, M. L. Garcia-Bermejo, M. Reilly, and H. Wang.** 2000. Pharmacology of the receptors for the phorbol ester tumor promoters: multiple receptors with different biochemical properties. *Biochem Pharmacol* **60**:1417-24.
87. **Kearns, B. G., T. P. McGee, P. Mayinger, A. Gedvilaite, S. E. Phillips, S. Kagiwada, and V. A. Bankaitis.** 1997. Essential role for diacylglycerol in protein transport from the yeast Golgi complex. *Nature* **387**:101-5.
88. **Keshamouni, V. G., R. R. Mattingly, and K. B. Reddy.** 2002. Mechanism of 17-beta-estradiol-induced Erk1/2 activation in breast cancer cells. A role for HER2 AND PKC-delta. *J Biol Chem* **277**:22558-65.
89. **Kiley, S. C., K. J. Clark, S. K. Duddy, D. R. Welch, and S. Jaken.** 1999. Increased protein kinase C delta in mammary tumor cells: relationship to transformation and metastatic progression. *Oncogene* **18**:6748-57.
90. **Kim, C. Y., A. J. Giaccia, B. Strulovici, and J. M. Brown.** 1992. Differential expression of protein kinase C epsilon protein in lung cancer cell lines by ionising radiation. *Br J Cancer* **66**:844-9.
91. **Kishimoto, A., Y. Takai, T. Mori, U. Kikkawa, and Y. Nishizuka.** 1980. Activation of calcium and phospholipid-dependent protein kinase by diacylglycerol, its possible relation to phosphatidylinositol turnover. *J Biol Chem* **255**:2273-6.
92. **Knauf, J. A., L. S. Ward, Y. E. Nikiforov, M. Nikiforova, E. Puxeddu, M. Medvedovic, T. Liron, D. Mochly-Rosen, and J. A. Fagin.** 2002. Isozyme-specific abnormalities of PKC in thyroid cancer: evidence for post-transcriptional changes in PKC epsilon. *J Clin Endocrinol Metab* **87**:2150-9.



93. **Konishi, H., H. Matsuzaki, H. Takaishi, T. Yamamoto, M. Fukunaga, Y. Ono, and U. Kikkawa.** 1999. Opposing effects of protein kinase C delta and protein kinase B alpha on H<sub>2</sub>O<sub>2</sub>-induced apoptosis in CHO cells. *Biochem Biophys Res Commun* **264**:840-6.
94. **Koren, R., D. Ben Meir, L. Langzam, Y. Dekel, M. Konichezky, J. Baniel, P. M. Livne, R. Gal, and S. R. Sampson.** 2004. Expression of protein kinase C isoenzymes in benign hyperplasia and carcinoma of prostate. *Oncol Rep* **11**:321-6.
95. **Kraynov, V. S., C. Chamberlain, G. M. Bokoch, M. A. Schwartz, S. Slabaugh, and K. M. Hahn.** 2000. Localized Rac activation dynamics visualized in living cells. *Science* **290**:333-7.
96. **Lammering, G.** 2003. Anti-epidermal growth factor receptor strategies to enhance radiation action. *Curr Med Chem Anticancer Agents* **3**:327-33.
97. **Lee, Y. J., J. W. Soh, N. M. Dean, C. K. Cho, T. H. Kim, S. J. Lee, and Y. S. Lee.** 2002. Protein kinase Cdelta overexpression enhances radiation sensitivity via extracellular regulated protein kinase 1/2 activation, abolishing the radiation-induced G<sub>2</sub>-M arrest. *Cell Growth Differ* **13**:237-46.
98. **Lehel, C., Z. Olah, G. Jakab, and W. B. Anderson.** 1995. Protein kinase C epsilon is localized to the Golgi via its zinc-finger domain and modulates Golgi function. *Proc Natl Acad Sci U S A* **92**:1406-10.
99. **Lehel, C., Z. Olah, G. Jakab, Z. Szallasi, G. Petrovics, G. Harta, P. M. Blumberg, and W. B. Anderson.** 1995. Protein kinase C epsilon subcellular localization domains and proteolytic degradation sites. A model for protein kinase C conformational changes. *J Biol Chem* **270**:19651-8.
100. **Lehel, C., Z. Olah, H. Mischak, J. F. Mushinski, and W. B. Anderson.** 1994. Overexpressed protein kinase C-delta and -epsilon subtypes in NIH 3T3 cells exhibit differential subcellular localization and differential regulation of sodium-dependent phosphate uptake. *J Biol Chem* **269**:4761-6.
101. **Leskow, F. C., B. A. Holloway, H. Wang, M. C. Mullins, and M. G. Kazanietz.** 2006. The zebrafish homologue of mammalian chimerin Rac-GAPs is implicated in epiboly progression during development. *Proc Natl Acad Sci U S A* **103**:5373-8.
102. **Leung, T., B. E. How, E. Manser, and L. Lim.** 1994. Cerebellar beta 2-chimaerin, a GTPase-activating protein for p21 ras-related rac is specifically expressed in granule cells and has a unique N-terminal SH2 domain. *J Biol Chem* **269**:12888-92.
103. **Leung, T., B. E. How, E. Manser, and L. Lim.** 1993. Germ cell beta-chimaerin, a new GTPase-activating protein for p21rac, is specifically expressed during the acrosomal assembly stage in rat testis. *J Biol Chem* **268**:3813-6.
104. **Li, L., P. S. Lorenzo, K. Bogi, P. M. Blumberg, and S. H. Yuspa.** 1999. Protein kinase Cdelta targets mitochondria, alters mitochondrial membrane potential, and induces apoptosis in normal and neoplastic keratinocytes when overexpressed by an adenoviral vector. *Mol Cell Biol* **19**:8547-58.
105. **Li, L., K. Sampat, N. Hu, J. Zakari, and S. H. Yuspa.** 2006. Protein kinase C negatively regulates Akt activity and modifies UVC-induced apoptosis in mouse keratinocytes. *J Biol Chem* **281**:3237-43.

106. **Liu, G. S., M. V. Cohen, D. Mochly-Rosen, and J. M. Downey.** 1999. Protein kinase C-epsilon is responsible for the protection of preconditioning in rabbit cardiomyocytes. *J Mol Cell Cardiol* **31**:1937-48.
107. **Liu, H., Y. Qiu, L. Xiao, and F. Dong.** 2006. Involvement of protein kinase Cepsilon in the negative regulation of Akt activation stimulated by granulocyte colony-stimulating factor. *J Immunol* **176**:2407-13.
108. **Lu, D., J. Huang, and A. Basu.** 2006. Protein kinase Cepsilon activates protein kinase B/Akt via DNA-PK to protect against tumor necrosis factor-alpha-induced cell death. *J Biol Chem* **281**:22799-807.
109. **Maeda, Y., G. V. Beznoussenko, J. Van Lint, A. A. Mironov, and V. Malhotra.** 2001. Recruitment of protein kinase D to the trans-Golgi network via the first cysteine-rich domain. *Embo J* **20**:5982-90.
110. **Magnon, C., P. Opolon, M. Ricard, E. Connault, P. Ardouin, A. Galaup, D. Metivier, J. M. Bidart, S. Germain, M. Perricaudet, and M. Schlumberger.** 2007. Radiation and inhibition of angiogenesis by canstatin synergize to induce HIF-1alpha-mediated tumor apoptotic switch. *J Clin Invest* **117**:1844-55.
111. **Maissel, A., M. Marom, M. Shtutman, G. Shahaf, and E. Livneh.** 2006. PKCeta is localized in the Golgi, ER and nuclear envelope and translocates to the nuclear envelope upon PMA activation and serum-starvation: C1b domain and the pseudosubstrate containing fragment target PKCeta to the Golgi and the nuclear envelope. *Cell Signal* **18**:1127-39.
112. **Majoul, I., M. Straub, S. W. Hell, R. Duden, and H. D. Soling.** 2001. KDEL-cargo regulates interactions between proteins involved in COPI vesicle traffic: measurements in living cells using FRET. *Dev Cell* **1**:139-53.
113. **Majumder, P. K., N. C. Mishra, X. Sun, A. Bharti, S. Kharbanda, S. Saxena, and D. Kufe.** 2001. Targeting of protein kinase C delta to mitochondria in the oxidative stress response. *Cell Growth Differ* **12**:465-70.
114. **Majumder, P. K., P. Pandey, X. Sun, K. Cheng, R. Datta, S. Saxena, S. Kharbanda, and D. Kufe.** 2000. Mitochondrial translocation of protein kinase C delta in phorbol ester-induced cytochrome c release and apoptosis. *J Biol Chem* **275**:21793-6.
115. **Mangat, R., T. Singal, N. S. Dhalla, and P. S. Tappia.** 2006. Inhibition of phospholipase C-gamma 1 augments the decrease in cardiomyocyte viability by H2O2. *Am J Physiol Heart Circ Physiol* **291**:H854-60.
116. **Martin, S. J., D. D. Newmeyer, S. Mathias, D. M. Farschon, H. G. Wang, J. C. Reed, R. N. Kolesnick, and D. R. Green.** 1995. Cell-free reconstitution of Fas-, UV radiation- and ceramide-induced apoptosis. *EMBO J* **14**:5191-200.
117. **Maruyama, I. N., and S. Brenner.** 1991. A phorbol ester/diacylglycerol-binding protein encoded by the unc-13 gene of *Caenorhabditis elegans*. *Proc Natl Acad Sci U S A* **88**:5729-33.
118. **Matsumoto, M., W. Ogawa, Y. Hino, K. Furukawa, Y. Ono, M. Takahashi, M. Ohba, T. Kuroki, and M. Kasuga.** 2001. Inhibition of insulin-induced activation of Akt by a kinase-deficient mutant of the epsilon isozyme of protein kinase C. *J Biol Chem* **276**:14400-6.
119. **Mayne, G. C., and A. W. Murray.** 1998. Evidence that protein kinase Cepsilon mediates phorbol ester inhibition of calphostin C- and tumor necrosis factor-

- alpha-induced apoptosis in U937 histiocytic lymphoma cells. *J Biol Chem* **273**:24115-21.
120. **McConkey, D. J., P. Hartzell, M. Jondal, and S. Orrenius.** 1989. Inhibition of DNA fragmentation in thymocytes and isolated thymocyte nuclei by agents that stimulate protein kinase C. *J Biol Chem* **264**:13399-402.
  121. **McJilton, M. A., C. Van Sikes, G. G. Wescott, D. Wu, T. L. Foreman, C. W. Gregory, D. A. Weidner, O. Harris Ford, A. Morgan Lasater, J. L. Mohler, and D. M. Terrian.** 2003. Protein kinase Cepsilon interacts with Bax and promotes survival of human prostate cancer cells. *Oncogene* **22**:7958-68.
  122. **Mellor, H., and P. J. Parker.** 1998. The extended protein kinase C superfamily. *Biochem J* **332** ( Pt 2):281-92.
  123. **Michiels, F., G. G. Habets, J. C. Stam, R. A. van der Kammen, and J. G. Collard.** 1995. A role for Rac in Tiam1-induced membrane ruffling and invasion. *Nature* **375**:338-40.
  124. **Mischak, H., J. H. Pierce, J. Goodnight, M. G. Kazanietz, P. M. Blumberg, and J. F. Mushinski.** 1993. Phorbol ester-induced myeloid differentiation is mediated by protein kinase C-alpha and -delta and not by protein kinase C-beta II, -epsilon, -zeta, and -eta. *J Biol Chem* **268**:20110-5.
  125. **Miyake, N., J. Chilton, M. Psatha, L. Cheng, C. Andrews, W. M. Chan, K. Law, M. Crosier, S. Lindsay, M. Cheung, J. Allen, N. J. Gutowski, S. Ellard, E. Young, A. Iannaccone, B. Appukuttan, J. T. Stout, S. Christiansen, M. L. Ciccarelli, A. Baldi, M. Campioni, J. C. Zenteno, D. Davenport, L. E. Mariani, M. Sahin, S. Guthrie, and E. C. Engle.** 2008. Human CHN1 mutations hyperactivate alpha2-chimaerin and cause Duane's retraction syndrome. *Science* **321**:839-43.
  126. **Mochly-Rosen, D., and A. S. Gordon.** 1998. Anchoring proteins for protein kinase C: a means for isozyme selectivity. *FASEB J* **12**:35-42.
  127. **Mochly-Rosen, D., H. Khaner, and J. Lopez.** 1991. Identification of intracellular receptor proteins for activated protein kinase C. *Proc Natl Acad Sci U S A* **88**:3997-4000.
  128. **Murray, N. R., D. J. Burns, and A. P. Fields.** 1994. Presence of a beta II protein kinase C-selective nuclear membrane activation factor in human leukemia cells. *J Biol Chem* **269**:21385-90.
  129. **Nakajima, T., and O. Yukawa.** 1999. Mechanism of radiation-induced diacylglycerol production in primary cultured rat hepatocytes. *J Radiat Res (Tokyo)* **40**:135-44.
  130. **Nakajima, T., and O. Yukawa.** 1996. Radiation-induced translocation of protein kinase C through membrane lipid peroxidation in primary cultured rat hepatocytes. *Int J Radiat Biol* **70**:473-80.
  131. **Nakajima, T., O. Yukawa, C. Azuma, H. Ohyama, B. Wang, S. Kojima, I. Hayata, and H. Hama-Inaba.** 2004. Involvement of protein kinase C-related anti-apoptosis signaling in radiation-induced apoptosis in murine thymic lymphoma(3SBH5) cells. *Radiat Res* **161**:528-34.
  132. **Nalefski, E. A., and A. C. Newton.** 2001. Membrane binding kinetics of protein kinase C betaII mediated by the C2 domain. *Biochemistry* **40**:13216-29.

133. **Nassar, N., J. Cancelas, J. Zheng, D. A. Williams, and Y. Zheng.** 2006. Structure-function based design of small molecule inhibitors targeting Rho family GTPases. *Curr Top Med Chem* **6**:1109-16.
134. **Newton, A. C.** 1995. Protein kinase C: structure, function, and regulation. *J Biol Chem* **270**:28495-8.
135. **Nguyen, T. A., L. J. Takemoto, and D. J. Takemoto.** 2004. Inhibition of gap junction activity through the release of the C1B domain of protein kinase Cgamma (PKCgamma) from 14-3-3: identification of PKCgamma-binding sites. *J Biol Chem* **279**:52714-25.
136. **Nishizuka, Y.** 1984. Turnover of inositol phospholipids and signal transduction. *Science* **225**:1365-70.
137. **Nunez, G., M. A. Benedict, Y. Hu, and N. Inohara.** 1998. Caspases: the proteases of the apoptotic pathway. *Oncogene* **17**:3237-45.
138. **Oancea, E., and T. Meyer.** 1998. Protein kinase C as a molecular machine for decoding calcium and diacylglycerol signals. *Cell* **95**:307-18.
139. **Obeid, L. M., C. M. Linardic, L. A. Karolak, and Y. A. Hannun.** 1993. Programmed cell death induced by ceramide. *Science* **259**:1769-71.
140. **Okhrimenko, H., W. Lu, C. Xiang, N. Hamburger, G. Kazimirsky, and C. Brodie.** 2005. Protein kinase C-epsilon regulates the apoptosis and survival of glioma cells. *Cancer Res* **65**:7301-9.
141. **Otsuki, Y., M. Tanaka, S. Yoshii, N. Kawazoe, K. Nakaya, and H. Sugimura.** 2001. Tumor metastasis suppressor nm23H1 regulates Rac1 GTPase by interaction with Tiam1. *Proc Natl Acad Sci U S A* **98**:4385-90.
142. **Pan, Q., L. W. Bao, C. G. Kleer, M. S. Sabel, K. A. Griffith, T. N. Teknos, and S. D. Merajver.** 2005. Protein kinase C epsilon is a predictive biomarker of aggressive breast cancer and a validated target for RNA interference anticancer therapy. *Cancer Res* **65**:8366-71.
143. **Panaretakis, T., E. Laane, K. Pokrovskaja, A. C. Bjorklund, A. Moustakas, B. Zhivotovsky, M. Heyman, M. C. Shoshan, and D. Grander.** 2005. Doxorubicin requires the sequential activation of caspase-2, protein kinase Cdelta, and c-Jun NH2-terminal kinase to induce apoptosis. *Mol Biol Cell* **16**:3821-31.
144. **Pears, C. J., G. Kour, C. House, B. E. Kemp, and P. J. Parker.** 1990. Mutagenesis of the pseudosubstrate site of protein kinase C leads to activation. *Eur J Biochem* **194**:89-94.
145. **Ping, P., C. Song, J. Zhang, Y. Guo, X. Cao, R. C. Li, W. Wu, T. M. Vondriska, J. M. Pass, X. L. Tang, W. M. Pierce, and R. Bolli.** 2002. Formation of protein kinase C(epsilon)-Lck signaling modules confers cardioprotection. *J Clin Invest* **109**:499-507.
146. **Ping, P., J. Zhang, W. M. Pierce, Jr., and R. Bolli.** 2001. Functional proteomic analysis of protein kinase C epsilon signaling complexes in the normal heart and during cardioprotection. *Circ Res* **88**:59-62.
147. **Powell, C. T., N. J. Brittis, D. Stec, H. Hug, W. D. Heston, and W. R. Fair.** 1996. Persistent membrane translocation of protein kinase C alpha during 12-O-tetradecanoylphorbol-13-acetate-induced apoptosis of LNCaP human prostate cancer cells. *Cell Growth Differ* **7**:419-28.

148. **Pu, Y., S. H. Garfield, N. Kedei, and P. M. Blumberg.** 2009. Characterization of the differential roles of the twin C1a and C1b domains of protein kinase C-delta. *J Biol Chem* **284**:1302-12.
149. **Reyland, M. E., S. M. Anderson, A. A. Matassa, K. A. Barzen, and D. O. Quissell.** 1999. Protein kinase C delta is essential for etoposide-induced apoptosis in salivary gland acinar cells. *J Biol Chem* **274**:19115-23.
150. **Riley, P. A.** 1994. Free radicals in biology: oxidative stress and the effects of ionizing radiation. *Int J Radiat Biol* **65**:27-33.
151. **Ron, D., and M. G. Kazanietz.** 1999. New insights into the regulation of protein kinase C and novel phorbol ester receptors. *FASEB J* **13**:1658-76.
152. **Scheel-Toellner, D., D. Pilling, A. N. Akbar, D. Hardie, G. Lombardi, M. Salmon, and J. M. Lord.** 1999. Inhibition of T cell apoptosis by IFN-beta rapidly reverses nuclear translocation of protein kinase C-delta. *Eur J Immunol* **29**:2603-12.
153. **Schultz, A., M. Ling, and C. Larsson.** 2004. Identification of an amino acid residue in the protein kinase C C1b domain crucial for its localization to the Golgi network. *J Biol Chem* **279**:31750-60.
154. **Sherman, M. L., R. Datta, D. E. Hallahan, R. R. Weichselbaum, and D. W. Kufe.** 1990. Ionizing radiation regulates expression of the c-jun protooncogene. *Proc Natl Acad Sci U S A* **87**:5663-6.
155. **Shi, L., W. Y. Fu, K. W. Hung, C. Porchetta, C. Hall, A. K. Fu, and N. Y. Ip.** 2007. Alpha2-chimaerin interacts with EphA4 and regulates EphA4-dependent growth cone collapse. *Proc Natl Acad Sci U S A* **104**:16347-52.
156. **Shindo, M., K. Irie, A. Masuda, H. Ohigashi, Y. Shirai, K. Miyasaka, and N. Saito.** 2003. Synthesis and phorbol ester binding of the cysteine-rich domains of diacylglycerol kinase (DGK) isozymes. DGKgamma and DGKbeta are new targets of tumor-promoting phorbol esters. *J Biol Chem* **278**:18448-54.
157. **Shinohara, H., N. Kayagaki, H. Yagita, N. Oyaizu, M. Ohba, T. Kuroki, and Y. Ikawa.** 2001. A protective role of PKCepsilon against TNF-related apoptosis-inducing ligand (TRAIL)-induced apoptosis in glioma cells. *Biochem Biophys Res Commun* **284**:1162-7.
158. **Shizukuda, Y., M. E. Reyland, and P. M. Buttrick.** 2002. Protein kinase C-delta modulates apoptosis induced by hyperglycemia in adult ventricular myocytes. *Am J Physiol Heart Circ Physiol* **282**:H1625-34.
159. **Siliceo, M., D. Garcia-Bernal, S. Carrasco, E. Diaz-Flores, F. Coluccio Leskow, J. Teixido, M. G. Kazanietz, and I. Merida.** 2006. Beta2-chimaerin provides a diacylglycerol-dependent mechanism for regulation of adhesion and chemotaxis of T cells. *J Cell Sci* **119**:141-52.
160. **Simon, J. P., I. E. Ivanov, B. Shopsin, D. Hersh, M. Adesnik, and D. D. Sabatini.** 1996. The in vitro generation of post-Golgi vesicles carrying viral envelope glycoproteins requires an ARF-like GTP-binding protein and a protein kinase C associated with the Golgi apparatus. *J Biol Chem* **271**:16952-61.
161. **Sivaprasad, U., E. Shankar, and A. Basu.** 2007. Downregulation of Bid is associated with PKCepsilon-mediated TRAIL resistance. *Cell Death Differ* **14**:851-60.

162. **Slaga, T. J.** 1983. Overview of tumor promotion in animals. *Environ Health Perspect* **50**:3-14.
163. **Sohn, K., L. Orci, M. Ravazzola, M. Amherdt, M. Bremser, F. Lottspeich, K. Fiedler, J. B. Helms, and F. T. Wieland.** 1996. A major transmembrane protein of Golgi-derived COPI-coated vesicles involved in coatamer binding. *J Cell Biol* **135**:1239-48.
164. **Song, H. J., T. H. Kim, C. K. Cho, S. Y. Yoo, K. S. Park, and Y. S. Lee.** 1998. Increased expression of ornithine decarboxylase by gamma-ray in mouse epidermal cells: relationship with protein kinase C signaling pathway. *J Radiat Res (Tokyo)* **39**:175-84.
165. **Song, Y., M. Ailenberg, and M. Silverman.** 1999. Human munc13 is a diacylglycerol receptor that induces apoptosis and may contribute to renal cell injury in hyperglycemia. *Mol Biol Cell* **10**:1609-19.
166. **Stahelin, R. V., M. A. Digman, M. Medkova, B. Ananthanarayanan, J. D. Rafter, H. R. Melowic, and W. Cho.** 2004. Mechanism of diacylglycerol-induced membrane targeting and activation of protein kinase Cdelta. *J Biol Chem* **279**:29501-12.
167. **Stevenson, M. A., S. S. Pollock, C. N. Coleman, and S. K. Calderwood.** 1994. X-irradiation, phorbol esters, and H<sub>2</sub>O<sub>2</sub> stimulate mitogen-activated protein kinase activity in NIH-3T3 cells through the formation of reactive oxygen intermediates. *Cancer Res* **54**:12-5.
168. **Sturla, L. M., G. Amorino, M. S. Alexander, R. B. Mikkelsen, K. Valerie, and R. K. Schmidt-Ullrich.** 2005. Requirement of Tyr-992 and Tyr-1173 in phosphorylation of the epidermal growth factor receptor by ionizing radiation and modulation by SHP2. *J Biol Chem* **280**:14597-604.
169. **Sunesson, L., U. Hellman, and C. Larsson.** 2008. Protein kinase Cepsilon binds peripherin and induces its aggregation, which is accompanied by apoptosis of neuroblastoma cells. *J Biol Chem* **283**:16653-64.
170. **Taher, M. M., J. G. Garcia, and V. Natarajan.** 1993. Hydroperoxide-induced diacylglycerol formation and protein kinase C activation in vascular endothelial cells. *Arch Biochem Biophys* **303**:260-6.
171. **Takai, Y., A. Kishimoto, M. Inoue, and Y. Nishizuka.** 1977. Studies on a cyclic nucleotide-independent protein kinase and its proenzyme in mammalian tissues. I. Purification and characterization of an active enzyme from bovine cerebellum. *J Biol Chem* **252**:7603-9.
172. **Takai, Y., A. Kishimoto, U. Kikkawa, T. Mori, and Y. Nishizuka.** 1979. Unsaturated diacylglycerol as a possible messenger for the activation of calcium-activated, phospholipid-dependent protein kinase system. *Biochem Biophys Res Commun* **91**:1218-24.
173. **Takai, Y., M. Yamamoto, M. Inoue, A. Kishimoto, and Y. Nishizuka.** 1977. A proenzyme of cyclic nucleotide-independent protein kinase and its activation by calcium-dependent neutral protease from rat liver. *Biochem Biophys Res Commun* **77**:542-50.
174. **Tanaka, Y., M. V. Gavrielides, Y. Mitsuuchi, T. Fujii, and M. G. Kazanietz.** 2003. Protein kinase C promotes apoptosis in LNCaP prostate cancer cells

- through activation of p38 MAPK and inhibition of the Akt survival pathway. *J Biol Chem* **278**:33753-62.
175. **Tomei, L. D., P. Kanter, and C. E. Wenner.** 1988. Inhibition of radiation-induced apoptosis in vitro by tumor promoters. *Biochem Biophys Res Commun* **155**:324-31.
  176. **Uckun, F. M., G. L. Schieven, L. M. Tuel-Ahlgren, I. Dibirdik, D. E. Myers, J. A. Ledbetter, and C. W. Song.** 1993. Tyrosine phosphorylation is a mandatory proximal step in radiation-induced activation of the protein kinase C signaling pathway in human B-lymphocyte precursors. *Proc Natl Acad Sci U S A* **90**:252-6.
  177. **Uckun, F. M., L. Tuel-Ahlgren, C. W. Song, K. Waddick, D. E. Myers, J. Kirihara, J. A. Ledbetter, and G. L. Schieven.** 1992. Ionizing radiation stimulates unidentified tyrosine-specific protein kinases in human B-lymphocyte precursors, triggering apoptosis and clonogenic cell death. *Proc Natl Acad Sci U S A* **89**:9005-9.
  178. **Valverde, A. M., J. Sinnott-Smith, J. Van Lint, and E. Rozengurt.** 1994. Molecular cloning and characterization of protein kinase D: a target for diacylglycerol and phorbol esters with a distinctive catalytic domain. *Proc Natl Acad Sci U S A* **91**:8572-6.
  179. **Venkatesan, B. A., L. Mahimainathan, N. Ghosh-Choudhury, Y. Gorin, B. Bhandari, A. J. Valente, H. E. Abboud, and G. G. Choudhury.** 2006. PI 3 kinase-dependent Akt kinase and PKCepsilon independently regulate interferon-gamma-induced STAT1alpha serine phosphorylation to induce monocyte chemotactic protein-1 expression. *Cell Signal* **18**:508-18.
  180. **Vondriska, T. M., J. Zhang, C. Song, X. L. Tang, X. Cao, C. P. Baines, J. M. Pass, S. Wang, R. Bolli, and P. Ping.** 2001. Protein kinase C epsilon-Src modules direct signal transduction in nitric oxide-induced cardioprotection: complex formation as a means for cardioprotective signaling. *Circ Res* **88**:1306-13.
  181. **Wang, H., and M. G. Kazanietz.** 2002. Chimaerins, novel non-protein kinase C phorbol ester receptors, associate with Tmp21-I (p23): evidence for a novel anchoring mechanism involving the chimaerin C1 domain. *J Biol Chem* **277**:4541-50.
  182. **Wang, H., and M. G. Kazanietz.** 2006. The lipid second messenger diacylglycerol as a negative regulator of Rac signalling. *Biochem Soc Trans* **34**:855-7.
  183. **Wang, H., and M. G. Kazanietz.** p23/Tmp21 Differentially Targets the Rac-GAP {beta}2-Chimaerin and Protein Kinase C via their C1 Domains. *Mol Biol Cell*.
  184. **Wang, H., C. Yang, F. C. Leskow, J. Sun, B. Canagarajah, J. H. Hurley, and M. G. Kazanietz.** 2006. Phospholipase Cgamma/diacylglycerol-dependent activation of beta2-chimaerin restricts EGF-induced Rac signaling. *EMBO J* **25**:2062-74.
  185. **Wegmeyer, H., J. Egea, N. Rabe, H. Gezelius, A. Filosa, A. Enjin, F. Varoqueaux, K. Deininger, F. Schnutgen, N. Brose, R. Klein, K. Kullander,**

- and A. Betz.** 2007. EphA4-dependent axon guidance is mediated by the RacGAP alpha2-chimaerin. *Neuron* **55**:756-67.
186. **Wen, H. C., W. C. Huang, A. Ali, J. R. Woodgett, and W. W. Lin.** 2003. Negative regulation of phosphatidylinositol 3-kinase and Akt signalling pathway by PKC. *Cell Signal* **15**:37-45.
187. **Woloschak, G. E., C. M. Chang-Liu, and P. Shearin-Jones.** 1990. Regulation of protein kinase C by ionizing radiation. *Cancer Res* **50**:3963-7.
188. **Woodgett, J. R.** 2005. Recent advances in the protein kinase B signaling pathway. *Curr Opin Cell Biol* **17**:150-7.
189. **Worthylake, D. K., K. L. Rossman, and J. Sondek.** 2000. Crystal structure of Rac1 in complex with the guanine nucleotide exchange region of Tiam1. *Nature* **408**:682-8.
190. **Wu, D., T. L. Foreman, C. W. Gregory, M. A. McJilton, G. G. Wescott, O. H. Ford, R. F. Alvey, J. L. Mohler, and D. M. Terrian.** 2002. Protein kinase cepsilon has the potential to advance the recurrence of human prostate cancer. *Cancer Res* **62**:2423-9.
191. **Wu, D., and D. M. Terrian.** 2002. Regulation of caveolin-1 expression and secretion by a protein kinase cepsilon signaling pathway in human prostate cancer cells. *J Biol Chem* **277**:40449-55.
192. **Wu, D., C. U. Thakore, G. G. Wescott, J. A. McCubrey, and D. M. Terrian.** 2004. Integrin signaling links protein kinase Cepsilon to the protein kinase B/Akt survival pathway in recurrent prostate cancer cells. *Oncogene* **23**:8659-72.
193. **Xiao, L., M. Eto, and M. G. Kazanietz.** 2009. ROCK mediates phorbol ester-induced apoptosis in prostate cancer cells via p21Cip1 up-regulation and JNK. *J Biol Chem* **284**:29365-75.
194. **Xu, H., P. Greengard, and S. Gandy.** 1995. Regulated formation of Golgi secretory vesicles containing Alzheimer beta-amyloid precursor protein. *J Biol Chem* **270**:23243-5.
195. **Yang, C., Y. Liu, F. C. Leskow, V. M. Weaver, and M. G. Kazanietz.** 2005. Rac-GAP-dependent inhibition of breast cancer cell proliferation by {beta}2-chimerin. *J Biol Chem* **280**:24363-70.
196. **Yao, L., H. Suzuki, K. Ozawa, J. Deng, C. Lehel, H. Fukamachi, W. B. Anderson, Y. Kawakami, and T. Kawakami.** 1997. Interactions between protein kinase C and pleckstrin homology domains. Inhibition by phosphatidylinositol 4,5-bisphosphate and phorbol 12-myristate 13-acetate. *J Biol Chem* **272**:13033-9.
197. **Yasuda, S., M. Kai, S. Imai, H. Kanoh, and F. Sakane.** 2007. Diacylglycerol kinase gamma interacts with and activates beta2-chimaerin, a Rac-specific GAP, in response to epidermal growth factor. *FEBS Lett* **581**:551-7.
198. **Yin, L., N. Bennani-Baiti, and C. T. Powell.** 2005. Phorbol ester-induced apoptosis of C4-2 cells requires both a unique and a redundant protein kinase C signaling pathway. *J Biol Chem* **280**:5533-41.
199. **Yuan, S., D. W. Miller, G. H. Barnett, J. F. Hahn, and B. R. Williams.** 1995. Identification and characterization of human beta 2-chimaerin: association with malignant transformation in astrocytoma. *Cancer Res* **55**:3456-61.



200. **Yuan, Z. M., T. Utsugisawa, T. Ishiko, S. Nakada, Y. Huang, S. Kharbanda, R. Weichselbaum, and D. Kufe.** 1998. Activation of protein kinase C delta by the c-Abl tyrosine kinase in response to ionizing radiation. *Oncogene* **16**:1643-8.
201. **Zhang, G., M. G. Kazanietz, P. M. Blumberg, and J. H. Hurley.** 1995. Crystal structure of the cys2 activator-binding domain of protein kinase C delta in complex with phorbol ester. *Cell* **81**:917-24.
202. **Zhang, X. M., J. Chen, Y. G. Xia, and Q. Xu.** 2005. Apoptosis of murine melanoma B16-BL6 cells induced by quercetin targeting mitochondria, inhibiting expression of PKC-alpha and translocating PKC-delta. *Cancer Chemother Pharmacol* **55**:251-62.
203. **Zhou, H. Z., J. S. Karliner, and M. O. Gray.** 2002. Moderate alcohol consumption induces sustained cardiac protection by activating PKC-epsilon and Akt. *Am J Physiol Heart Circ Physiol* **283**:H165-74.
204. **Zrachia, A., M. Dobroslav, M. Blass, G. Kazimirsky, I. Kronfeld, P. M. Blumberg, D. Kobilier, S. Lustig, and C. Brodie.** 2002. Infection of glioma cells with Sindbis virus induces selective activation and tyrosine phosphorylation of protein kinase C delta. Implications for Sindbis virus-induced apoptosis. *J Biol Chem* **277**:23693-701.